INTERNATIONAL STANDARD

ISO 15900

Second edition
2020-10

Determination of particle size distribution — Differential electrical mobility analysis for aerosol particles

Détermination de la distribution granulométrique — Analyse de mobilité électrique différentielle pour les particules d'aérosol

Reference number
ISO 15900:2020(E)

ISO copyright office
CP 401 • Ch. de Blandonnet 8
CH-1214 Vernier, Geneva
Phone: +41 22 749 01 11
Email: copyright@iso.org
Website: www.iso.org

Published in Switzerland

Contents

Page

Foreword

ISO (the International Organization for Standardization) is a worldwide federation of national standards bodies (ISO member bodies). The work of preparing International Standards is normally carried out through ISO technical committees. Each member body interested in a subject for which a technical committee has been established has the right to be represented on that committee. International organizations, governmental and non-governmental, in liaison with ISO, also take part in the work. ISO collaborates closely with the International Electrotechnical Commission (IEC) on all matters of electrotechnical standardization.

The procedures used to develop this document and those intended for its further maintenance are described in the ISO/IEC Directives, Part 1. In particular, the different approval criteria needed for the different types of ISO documents should be noted. This document was drafted in accordance with the editorial rules of the ISO/IEC Directives, Part 2 (see www.iso.org/directives).

Attention is drawn to the possibility that some of the elements of this document may be the subject of patent rights. ISO shall not be held responsible for identifying any or all such patent rights. Details of any patent rights identified during the development of the document will be in the Introduction and/or on the ISO list of patent declarations received (see www.iso.org/patents).

Any trade name used in this document is information given for the convenience of users and does not constitute an endorsement.

For an explanation of the voluntary nature of standards, the meaning of ISO specific terms and expressions related to conformity assessment, as well as information about ISO's adherence to the World Trade Organization (WTO) principles in the Technical Barriers to Trade (TBT), see www.iso.org/iso/foreword.html.

This document was prepared by Technical Committee ISO/TC 24, *Particle characterization including sieving*, Subcommittee SC 4, *Particle characterization*.

This second edition cancels and replaces the first edition (ISO 15900:2009), which has been technically revised.

The main changes compared to the previous edition are as follows:

— subclauses on particle losses due to Brownian diffusion, effects due to non-spherical particles, and measurement of particles below 10 nm have been added in Clause 5;

— traceability diagrams for DEMC and DMAS have been added in Clause 5;

— calibration for size measurement in Clause 8 has been refined;

— Clause 9 for "Using a DEMC at a fixed voltage to generate particles of a chosen size" has been added;

— Annex D for "Data inversion" has been rewritten completely;

— Annex F for "Example certificate for a DMAS particle size calibration" has been added;

— former Annex G for "Uncertainty" in the previous edition has been deleted;

— new Annex G for "Good practice for measurements at particle sizes below 10 nm" has been added;

— Annex H for "Examples for overall system tests" has been added;

— Annex I for "Comparison of different approaches to calculate diffusion loss in laminar tube flow" has been added;

— Annex J for "Corrections for effects due to non-spherical particles" has been added.

Any feedback or questions on this document should be directed to the user's national standards body. A complete listing of these bodies can be found at www.iso.org/members.html.

Introduction

Differential electrical mobility classification and analysis of airborne particles has been widely used to measure a variety of aerosol particles ranging from nanometre-size to micrometre-size in the gas phase. In addition, the electrical mobility classification of charged particles can be used to generate mono-disperse particles of known size for calibration of other instruments. One notable feature of these techniques is that they are based on simple physical principles. The techniques have become important in many fields of aerosol science and technology, e.g. aerosol instrumentation, production of materials from aerosols, contamination control in the semiconductor industry, atmospheric aerosol science, characterization of engineered nanoparticles, and so on. However, in order to use electrical mobility classification and analysis correctly, several issues, such as the slip correction factor, the ion-aerosol attachment coefficients, the size-dependent charge distribution on aerosol particles and the method used for inversion of the measured mobility distribution to the aerosol particle size distribution, need due caution.

There is, therefore, a need to establish an International Standard for the use of differential electrical mobility analysis for classifying aerosol particles. Its purpose is to provide a methodology for adequate quality control in particle size and number concentration measurement with this method.

Determination of particle size distribution — Differential electrical mobility analysis for aerosol particles

1 Scope

This document provides guidelines and requirements for the determination of aerosol particle number size distribution by means of the analysis of electrical mobility of aerosol particles. This measurement is usually called "differential electrical mobility analysis for aerosol particles". This analytical method is applicable to particle size measurements ranging from approximately 1 nm to 1 µm. This document does not address the specific instrument design or the specific requirements of particle size distribution measurements for different applications but includes the calculation method of uncertainty. In this document, the complete system for carrying out differential electrical mobility analysis is referred to as DMAS (differential mobility analysing system), while the element within this system that classifies the particles according to their electrical mobility is referred to as DEMC (differential electrical mobility classifier).

NOTE This document does not include technical requirements and specifications for the application of DMAS, which are defined in application specific standards or guidelines, e.g. for road vehicle applications (ISO/TC 22), environmental measurements (ISO/TC 146) or nanotechnologies (ISO/TC 229).

2 Normative references

There are no normative references in this document.

3 Terms and definitions

For the purposes of this document, the following terms and definitions apply.

ISO and IEC maintain terminological databases for use in standardization at the following addresses:

— ISO Online browsing platform: available at https://www.iso.org/obp

— IEC Electropedia: available at http://www.electropedia.org/

3.1
aerosol
system of solid and/or liquid particles suspended in gas

3.2
attachment coefficient
attachment probability of ions and aerosol particles

3.3
bipolar charging
process which attains a conditioned charge distribution of both positive and negative charges on aerosol particles

3.4
bipolar charge conditioner
device which attains a conditioned charge distribution of both positive and negative charges on aerosol particles

3.5
charging
processes that leave aerosol particles with size dependent specific distributions of unipolar or bipolar electrical charges

3.6
charge conditioner
device (or component of a DMAS) which establishes a known conditioned size dependent charge distribution on aerosol particles which are passed through it

3.7
charge distribution function
mathematical and/or empirical description of a conditioned particle size dependent charge distribution

3.8
condensation particle counter
CPC
instrument that measures the particle number concentration of an aerosol

Note 1 to entry: The sizes of particles detected are usually smaller than several hundred nanometres and larger than a few nanometres.

Note 2 to entry: A CPC is one possible detector for use with a DEMC.

Note 3 to entry: In some cases, a condensation particle counter may be called a condensation nucleus counter (CNC).

3.9
conditioned charge distribution
distribution of unipolar or bipolar electrical charges on aerosol particles defined by a charge distribution function, which is in a steady state for a sufficiently long period of time in an aerosol instrument downstream of a unipolar or bipolar charge conditioner

3.10
critical mobility
instrument parameter of a *DEMC* (3.11) that defines the electrical mobility of aerosol particles that exit the DEMC in aerosol form, which may be defined by the geometry, sample and sheath flow rates, and electrical field intensity

Note 1 to entry: Particles larger or smaller than the critical mobility migrate to an electrode or exit with the excess flow and do not exit from the DEMC in aerosol form.

3.11
differential electrical mobility classifier
DEMC
classifier able to select aerosol particles according to their electrical mobility and pass them to its exit

Note 1 to entry: A DEMC classifies aerosol particles by balancing the electrical force on each particle with its aerodynamic drag force in an electrical field. Classified particles are in a narrow range of electrical mobility determined by the operating conditions and physical dimensions of the DEMC, while they can have different sizes due to difference in the number of charges that they have.

Note 2 to entry: Another common acronym for the DEMC is DMA.

3.12
differential mobility analysing system
DMAS
system to measure the size distribution of submicrometre aerosol particles consisting of a charge conditioner, a DEMC, flow meters, a particle detector, interconnecting plumbing, a computer and suitable software

Note 1 to entry: Another common acronym for the DMAS is MPSS (mobility particle size spectrometer).

3.13
electrical mobility
ratio of *migration velocity* (3.18) to electrical field for particles and ions in a gas

3.14
equivalent diameter
d
diameter of a sphere with defined characteristics which behaves under defined conditions in exactly the same way as the particle being described

Note 1 to entry: Particle diameter (or simply diameter) used throughout this document always refers to the electrical mobility equivalent diameter, which defines the size of charged particles with the same electrical mobility or the same terminal migration velocity in still air under the influence of a constant electrical field.

3.15
Faraday cup aerosol electrometer
FCAE
electrometer designed for the measurement of electrical charge concentration carried by an aerosol

Note 1 to entry: A Faraday cup aerosol electrometer consists of an electrically conducting and electrically grounded cup as a guard to cover the sensing element that includes aerosol filtering media to capture charged aerosol particles, an electrical connection between the sensing element and an electrometer circuit, and a flow meter. An FCAE measures electrical current ranging from about one femtoampere (fA) to about ten picoamperes (pA).

3.16
Knudsen number
Kn
ratio of gas molecular mean free path to the radius of the particle, which is an indicator of free molecular flow versus continuum gas flow

3.17
laminar flow
gas flow with no temporally or spatially irregular activity or turbulent eddy flow

3.18
migration velocity
steady-state velocity of a charged airborne particle within an externally applied electric field

3.19
particle diameter
electrical mobility equivalent diameter

Note 1 to entry: Also, just called diameter.

3.20
plateau detection efficiency
mean detection efficiency of a CPC in the size range which is not biased by particle size

[SOURCE: ISO 27891:2015, 3.27, modified — term “plateau efficiency” has been changed to "plateau detection efficiency.]

3.21
Reynolds number
Re
dimensionless number expressed as the ratio of the inertial force to the viscous force

Note 1 to entry: For example, applied to an aerosol particle or a tube carrying aerosol particles

3.22
slip correction
S_C
dimensionless factor used to correct the drag force acting on a particle for non-continuum effects that become important when the particle size is comparable to or smaller than the mean free path of the gas molecules

3.23
Stokes's drag
drag force acting on a particle that is moving relative to a continuum fluid in the creeping flow limit (low Reynolds number)

3.24
transfer function
ratio of particle concentration at the outlet of a DEMC to the particle concentration at the inlet of the DEMC

Note 1 to entry: It is normally expressed as a function of electrical mobility.

3.25
unipolar charge conditioner
device which attains a conditioned charge distribution of either positive or negative charges on aerosol particles

3.26
unipolar charging
process which attains a conditioned charge distribution of positive or negative charges on aerosol particles

4 Symbols

For the purposes of this document, the following symbols apply.

Symbol	Quantity	SI Unit
A, B, C	elements of the slip correction factor defined in Formula (2)	dimensionless
c	thermal velocity of an ion or molecule	m s^{-1}
D	diffusion coefficient	m^2 s^{-1}
d	aerosol particle diameter	m
E	electric field strength in a DEMC	V m^{-1}
e	elementary charge = 1,602 176 634 × 10^{-19} C	
Kn	Knudsen number	(dimensionless)
k	Boltzmann constant = 1,380 649 × 10^{-23} J K^{-1}	
L	effective active length of a DEMC, approximated by the axial distance between the midpoint of the aerosol entrance and the midpoint of the exit slit of a cylindrical DEMC	m
L_{Tube}	length of a tube	m
M	molecular mass of air	amu
m	mass of an ion	amu
N	number concentration of aerosol particles, note that C_N is widely used as well.	m^{-3}
N_A	Avogadro constant = 6,022 140 76 × 10^{23} mol^{-1}	
N_I	number concentration of ions	m^{-3}
P	atmospheric pressure	Pa
p	number of elementary charges on a particle	(dimensionless)
q_1, q_2, q_3, q_4	flow rates of air (or gas) and of aerosol entering and exiting a DEMC	m^3 s^{-1}
Q_a	aerosol air flow rate	m^3 s^{-1}

Symbol	Quantity	SI Unit
r_1	outer radius of inner cylinder of a cylindrical DEMC	m
r_2	inner radius of outer cylinder of a cylindrical DEMC	m
Re	Reynolds number	(dimensionless)
S	Sutherland constant (=110,4 K at 23 °C and standard atmospheric pressure)	
S_C	slip correction	(dimensionless)
T	absolute temperature	K
t	residence time of an ion	s
U	DC voltage used to establish an electrical field in a DEMC	V
V	volume	m^3
Z	electrical mobility	$m^2\ V^{-1}\ s^{-1}$
Z_1, Z_2, Z_3, Z_4	critical electrical mobilities that describe the transfer function of a DEMC	$m^2\ V^{-1}\ s^{-1}$
β	attachment coefficient of ions onto aerosol particles	$m^3\ s^{-1}$
γ	recombination coefficient of ions	(dimensionless)
δ	radius of a limiting sphere	m
ε	relative error	
μ_{gas}	coefficient of dynamic viscosity of a gas	$kg\ m^{-1}\ s^{-1}$
λ	mean free path	m
ρ	mass density	$kg\ m^{-3}$

5 General principle

5.1 Particle size classification with the DEMC

The measurement of particle size distributions with a DMAS is based on particle classification by electrical mobility in a DEMC. The DEMC may be designed in many different ways; for example, coaxial cylindrical DEMC, radial DEMC, parallel plate DEMC, etc. The coaxial cylindrical DEMC shown in Figure 1 is an example of a widely used design. It consists of two coaxial, cylindrical electrodes with two inlets. One inlet (marked q_1 in Figure 1) is for filtered clean sheath air. The other inlet (marked q_2) is for the sample aerosol.

The sample aerosol, some of whose particles are electrically charged, enters the DEMC as a thin annular cylinder around a core of filtered, particle-free sheath air. By applying a voltage, an electric field is created between the inner and outer electrodes. A charged particle in the presence of an electric field will migrate within the field and reach a terminal migration velocity when the fluid dynamic drag on the particle balances the driving force of the electric field. Charged particles of the correct polarity within the sample aerosol begin to drift across the sheath air flow towards the inner electrode. At the same time, the clean sheath air flow carries the charged airborne particles downward. A small fraction of the charged particles enters the thin circumferential slit near the bottom of the centre electrode and is carried by the air flow to the detector (in the direction marked q_3). By varying the voltage, particles of different electrical mobility are selected. The remaining (not extracted) air flow leaves the DEMC as excess flow (q_4).

When used within a DMAS, measurements of relevant parameters such as voltage, flow and their timings need to be combined with other measurements such as the output from the particle detector. These parameters are usually controlled using a system controller as shown in Figure 5.

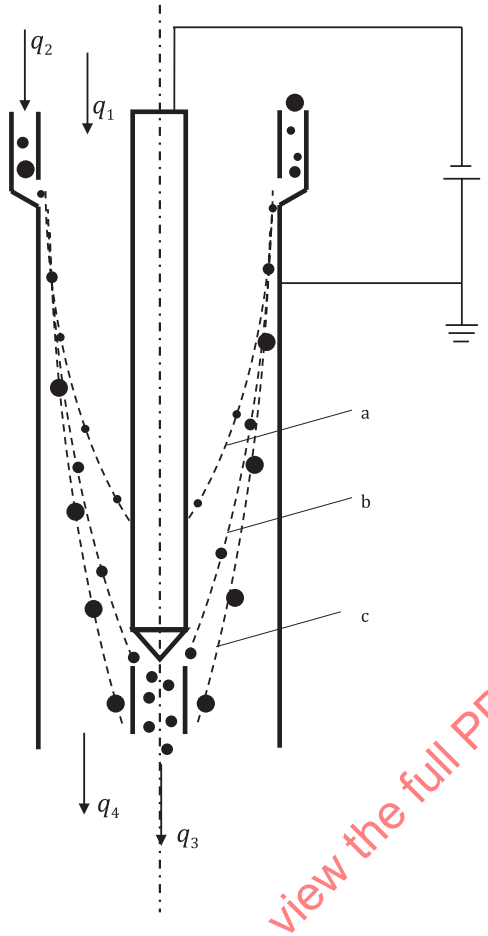

Key

q_1	sheath flow	a	Trajectory of particles trapped in the DEMC due to high electrical mobility.
q_2	sample aerosol flow	b	Trajectory of particles leaving the DEMC with q_3.
q_3	mobility selected aerosol flow	c	Trajectory of particles trapped in the DEMC due to low electrical mobility.
q_4	excess flow		

Figure 1 — Schematic diagram of coaxial cylindrical DEMC

5.2 Relationship between electrical mobility and particle size

The electrical mobility of a particle depends on its size and its electric charge. The relationship between electrical mobility and particle size for spherical particles can be described by Formula (1):

$$Z(d,p)=\frac{pe}{3\pi\mu_{\text{gas}}d}S_{\text{C}} \tag{1}$$

The slip correction, S_{C}, extends the Stokes's drag force on a spherical particle moving with low Reynolds number in a gas phase to nanometre-sized particles. It is approximated by the expression given in Formula (2):

$$S_{\text{C}}=1+Kn\left[A+B\exp\left(-\frac{C}{Kn}\right)\right] \tag{2}$$

For a detailed discussion of the slip correction, see Annex C.

The dynamic viscosity and the mean free path of gas molecules used within Formulae (1) and (2), respectively, depend on both the temperature and the pressure of the carrier gas. Formulae (3) and (4) shall be used to calculate the viscosity and the mean free path for temperatures and pressures different from the reference temperature and pressure, T_0 and P_0, specified in Table 1, respectively.

$$\mu_{\text{gas}} = \mu_{\text{gas},0} \cdot \left(\frac{T}{T_0} \right)^{\frac{3}{2}} \cdot \left(\frac{T_0 + S}{T + S} \right) \tag{3}$$

$$\lambda = \lambda_0 \cdot \left(\frac{T}{T_0} \right)^{2} \cdot \left(\frac{P_0}{P} \right) \cdot \left(\frac{T_0 + S}{T + S} \right) \tag{4}$$

where S, the Sutherland constant, has the value given in Table 1.

Unless explicitly specified differently in the measurement report, Formulae (1) to (4) and the set of parameters given in Table 1 shall be used for the calculation of the relation between electrical mobility and particle size in air.

Table 1 — Values of parameters for the calculation of the electrical mobility from the particle size in dry air at T_0 = 296,15 K and P_0 = 101,3 kPa [33]

Parameter	Value
$\mu_{\text{gas},0}$	1,832 45 × 10^{-5} kg m^{-1} s^{-1}
λ_0	6,730 × 10^{-8} m
S	110,4 K
A	1,165
B	0,483
C	0,997

5.3 Measurement and data inversion

For a given supply voltage, U, the response, $R(U)$, of the particle detector to aerosol particles entering the DEMC is given by Formula (5), which is called the basic equation for the response of the electrical mobility measurement:

$$R(U) = q_2 \sum_{p=1}^{\infty} \int_{d=0}^{\infty} n(d) \cdot P(d) \cdot f_p(d) \cdot \Omega(Z(d,p), \Delta\Phi(U)) \cdot W(d,p) \, \mathrm{d}d \tag{5}$$

For condensation particle counters (CPCs), the response is particle number concentration, while it is charge concentration for Faraday cup aerosol electrometers (FCAEs).

$W(d, p)$ describes the detector response;

For CPCs, $W(d, p) = \eta_{\text{CPC}}(d)\, q_{\text{CPC}-1}$, where $\eta_{\text{CPC}}(d)$ is the size-dependent detection efficiency of the CPC and q_{CPC} is the detection flow of the CPC.

For FCAEs, $W(d, p) = p\, e\, \eta_{\text{FCAE}}(d)\, q_{\text{FCAE}-1}$, where p is the number of elementary charges on a particle, e is the elementary charge, $\eta_{\text{FCAE}}(d)$ is the size-dependent detection efficiency of the FCAE, and q_{FCAE} is the detection flow of the FCAE.

$n(d)\,\mathrm{d}d$ is the number concentration of aerosol particles in the diameter interval dd around d;

$P(d)$ is the penetration which accounts for diffusion losses (see 5.6 and Annex I).

$f_p(d)$ is the charge distribution function (see 5.5 and Annex A);

$\Omega[Z(d,p),\Delta\Phi(U)]$ is the transfer function of the DEMC (see 5.4 and Annex E), which uses the functions $Z(d, p)$ and $\Delta\Phi(U)$ below as arguments;

$Z(d, p)$ is the electrical mobility of a particle with diameter d carrying p elementary charges (see 5.2);

$\Delta\Phi(U)$ is a function of the supply voltage and the geometry of the DEMC (see 5.4 and Annex E). For a cylindrical DEMC, $\Delta\Phi(U)$ is given in Formula (E.2).

If the transfer function, Ω, the charge distribution function, $f_p(d)$, and the maximum particle size (see 6.2.1) are known, the particle size distributions can be calculated based on the measurements with a DEMC. An example calculation is given in Annex D.

NOTE 1 Formula (5) applies to the case when the DEMC classifies positively-charged particles, since the range of the summation is from p = +1 to +∞. For the mode of classifying negatively-charged particles, the range is from p = −1 to -∞.

NOTE 2 A DEMC can be (electrically) described as a capacitor. $\Delta\Phi(U)$ can then be linked to the DEMC's capacitance, C_E, where $\Delta\Phi(U) = U \cdot C_E/(2 \cdot \pi \cdot \varepsilon_0)$, $\varepsilon_0 = 8{,}854 \times 10^{-12}$ F m^{-1}.

5.4 Transfer function of the DEMC

The transfer function, Ω, of a DEMC is defined as the probability that an aerosol particle which enters the DEMC at the aerosol inlet will leave via the detector outlet. It can, mathematically, easily be described in the mobility regime. Therefore, this approach is taken here. The transfer function depends on the particle's electrical mobility, Z, on the four volumetric flow rates, on the geometry of the DEMC and on the electrical field strength. The influence of the geometry and the electrical field strength on the transfer function is expressed by $\Delta\Phi$, which is a function of the geometry and the variable supply voltage, U, of the DEMC. For a given supply voltage, $\Delta\Phi$ is constant.

If particle inertia, gravimetric sedimentation, Brownian motion, space charge and its image forces are neglected, and if the sheath flow in the DEMC is recirculated ($q_1 = q_4$, also resulting in $q_2 = q_3$), the transfer function of a DEMC can be described as an isosceles triangle with the half-width, ΔZ, centred around the electrical mobility, Z^*, as in Figure 2.

When particle diffusion due to Brownian motion is significant, the resolution of the DEMC classification is reduced, which corresponds to a broader and shorter transfer function.

A detailed discussion of the transfer function for the example of a coaxial cylindrical DEMC can be found in Annex E.

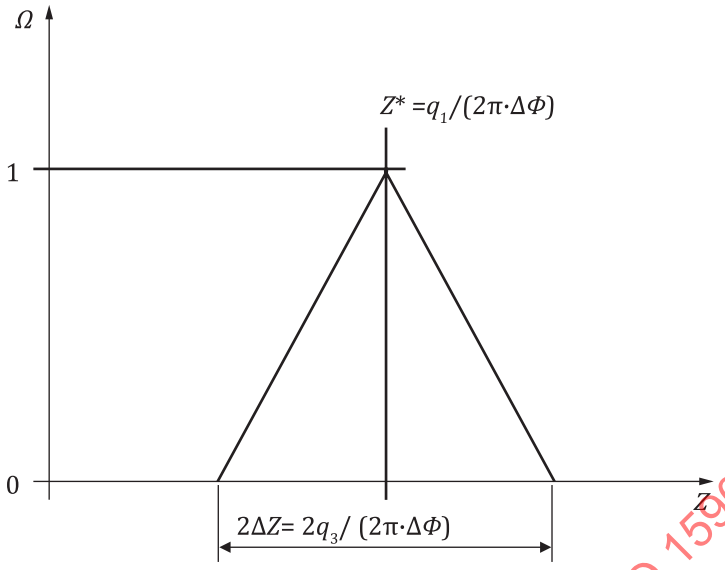

Key

Z	electrical mobility	Z^*	centre electrical mobility of the transfer function
Ω	transfer function	ΔZ	half-width of the transfer function

Figure 2 — Transfer function of a DEMC with sheath flow re-circulation ($q_1 = q_4$ and $q_2 = q_3$)

5.5 Charge distribution function

5.5.1 General

As stated in 5.3, the particle size-dependent charge distribution function, $f_p(d)$, shall be explicitly known to calculate the size distribution of airborne particles classified in a DEMC. A charge conditioner is used at the entrance of a DEMC to achieve a conditioned charge distribution which is independent of the initial charge state of the aerosol particles and which is - at least for typical aerosol residence times in a DEMC - in a steady-state or stable. $f_p(d)$ may then be given by a set of formulae or tabulated data, approximating the size-dependent charge distribution by theoretical models and/or empirical data.

There are several types of bipolar or unipolar charge conditioners which are described in more detail in 5.5.2. Bipolar charge conditioners produce positively and negatively charged particles while unipolar charge conditioners produce particles of one polarity (positive or negative) only.

5.5.2 Charge distribution function for radioactive bipolar charge conditioners

For commercially available radioactive bipolar charge conditioners the charge distribution function under standard conditions (spherical particles in air (293,15 K, 101,3 kPa) is given by Formula (6) in combination with the coefficients given in Table 2 and Formula (7) which are derived from an approximation (Wiedensohler (1988) [50] to theoretical models in combination with a result from Gunn (1956) [24]).

$$\log\left[f_p(d)\right] = \sum_{i=0}^{5} a_i(p)\cdot(\log d)^i \tag{6}$$

NOTE 1 In Formula (6), d is given in nanometres.

Formula (6) is valid for the size range:

1 nm ≤ d ≤ 1 000 nm for p = {-2, –1, 0, +1, +2}

Table 2 — Coefficients $a_i(p)$ for Formula (6) for radioactive ion sources

i	$a_i(p)$				
	$p = -2$	$p = -1$	$p = 0$	$p = +1$	$p = +2$
0	−26,332 8	−2,319 7	−0,000 3	−2,348 4	−44,475 6
1	35,904 4	0,617 5	−0,101 4	0,604 4	79,377 2
2	−21,460 8	0,620 1	0,307 3	0,480 0	−62,890 0
3	7,086 7	−0,110 5	−0,337 2	0,001 3	26,449 2
4	−1,308 8	−0,126 0	0,102 3	−0,155 3	−5,748 0
5	0,105 1	0,029 7	−0,010 5	0,032 0	0,504 9

The charge distribution function, $f_p(d)$, with three or more elementary charge units can be calculated using the following Formula (7), which is based on Gunn's model:

$$f_p(d) = \frac{e}{\sqrt{4\pi^2 \varepsilon_0 dkT}} \cdot \exp \frac{-\left[p - \frac{2\pi\varepsilon_0 dkT}{e^2} \cdot \ln\left(\frac{N_I^+}{N_I^-} \cdot \frac{Z_I^+}{Z_I^-}\right)\right]^2}{2\frac{2\pi\varepsilon_0 dkT}{e^2}} \tag{7}$$

where $N_I^{\pm}$ is the concentration of positive or negative small ions.

For this calculation, the concentration of positive and negative ions is assumed to be equal, and the ratio of ion mobilities Z_I^+ / Z_I^- was taken from Wiedensohler (1988) to be 0,875. Results of this calculation are given in Table 3 and in Figure A.1.

NOTE 2 Two coefficients in Wiedensohler (1988) were later corrected. The coefficients in Table 2 contain this correction.

Table 3 — Bipolar charge distribution function $f_p(d)$ for spherical particles in air (293,15 K, 101,3 kPa), produced by radioactive charge conditioners; see Formulae (6) and (7)

d	Charge distribution function												
(nm)	−6	−5	−4	−3	−2	−1	0	+1	+2	+3	+4	+5	+6
1	0	0	0	0	0	0,004 8	0,999 3	0,004 5	0	0	0	0	0
2	0	0	0	0	0	0,008 3	0,974 2	0,007 5	0	0	0	0	0
5	0	0	0	0	0	0,022 5	0,969 3	0,018 9	0	0	0	0	0
10	0	0	0	0	0	0,051 4	0,912 4	0,041 1	0	0	0	0	0
20	0	0	0	0	0,000 2	0,109 6	0,793 1	0,084 6	0,000 1	0	0	0	0
50	0	0	0	0	0,011 4	0,222 9	0,581 4	0,169 6	0,006 6	0	0	0	0
100	0	0	0,000 1	0,003 7	0,056 1	0,279 3	0,425 9	0,213 8	0,031 7	0,001 7	0	0	0
200	0	0,000 5	0,005 3	0,034 0	0,121 1	0,264 1	0,299 1	0,204 3	0,071 9	0,015 3	0,001 8	0,000 1	0
500	0,006 7	0,020 7	0,050 4	0,098 0	0,149 0	0,181 6	0,181 8	0,140 3	0,089 1	0,044 0	0,017 3	0,005 4	0,001 4
1 000	0,035 7	0,058 4	0,085 4	0,111 3	0,126 1	0,138 5	0,123 5	0,103 9	0,075 4	0,050 0	0,029 3	0,015 4	0,007 2

5.5.3 Charge distribution functions for other bipolar and unipolar charge conditioners

Calculations of the respective charge distribution functions for non-radioactive bipolar and unipolar charge conditioners are complicated and require careful experimental verification before usage in data inversion routines for the analysis of measured data. The theoretical concepts described in Annex A may be helpful for the experienced user to calculate a charge distribution function for a given charge conditioner. Annex A also shows an example for the charge distribution function for a charge conditioner based on an X-ray ionization source.

5.6 Particle losses in the DMAS

When aerosol particles collide with a surface, they adhere due to van der Waals force, electrostatic force and surface tension. Particles transported to any inner surface (e.g. tubing) of the DMAS – besides those transported to the electrodes of the DEMC forced by the electrical field - do not reach the particle detector; they are lost. Such losses can be caused by diffusional and electrostatic effects. Inertial transport and deposition are not significant in a DMAS because of the particle size range. Since the air flow in nearly all parts of the DMAS is laminar and the particles are small, the dominant transport mechanism for the particles is Brownian diffusion. The smaller the particle the more rapid their diffusion (Einstein, 1905) and the higher their losses. Hence, the measured size distribution will under-represent small particles. Diffusion losses in the DMAS should be estimated and corrected.

Three sets of equations for diffusion losses in straight tubes [Gormley and Kennedy (1949) [59], Hinds (1999) [60] and Willeke and Baron (1993) [68]], which give very similar results, can be found in literature; they all quantify the penetration P_{Tube} through a straight tube (i.e. the ratio between the particle concentration leaving the tube and entering the tube) with laminar flow.

The formulae to calculate the diffusion loss can be found in Annex I, which also contains a comparison between the three approaches.

5.7 Effects due to non-spherical particles

In a DEMC, particles are classified according to their electrical mobility. For spherical particles, Formulae (1) and (2) in 5.2 are sufficient to relate a particle's electrical mobility to its diameter. For non-spherical particles, introducing the mobility equivalent diameter overcomes the complex problem of otherwise necessary corrections for Formulae (1) and (2). In addition, the charge distribution for non-spherical particles can differ from the charge distribution for spherical particles (see 5.5).

All published approaches for the correction of the effects of non-spherical particles require knowledge about the particle shape; they can therefore be used only in special cases. An example for a correction is shown in Annex J.

5.8 Measurement of particle sizes below 10 nm

Measurement uncertainties increase as particle sizes decrease from 10 nm towards 1 nm. Good measurement practice given in Annex G should be followed to achieve acceptable quality when measuring in the below 10 nm size range.

5.9 Traceability of measurement results

Figures 3 and 4 illustrate the metrological traceability chains for quantities that are influential to results of measurements by a DMAS.

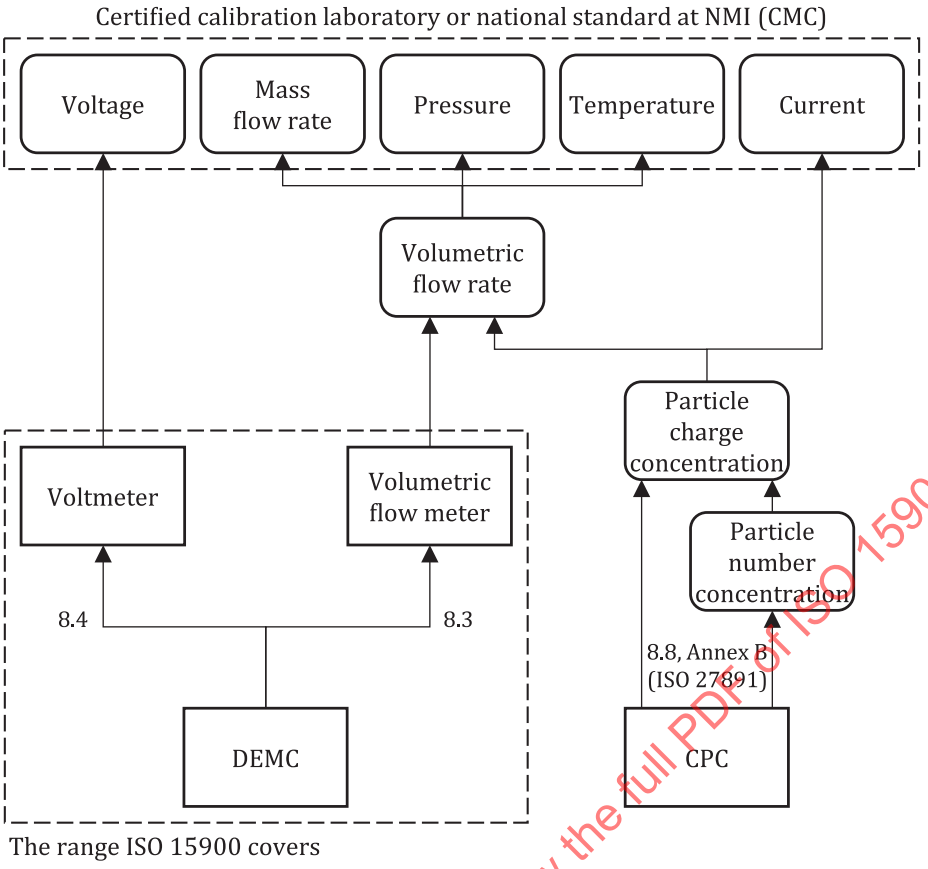

Figure 3 — Traceability diagram for DEMC and CPC with references to subclauses in Clause 8

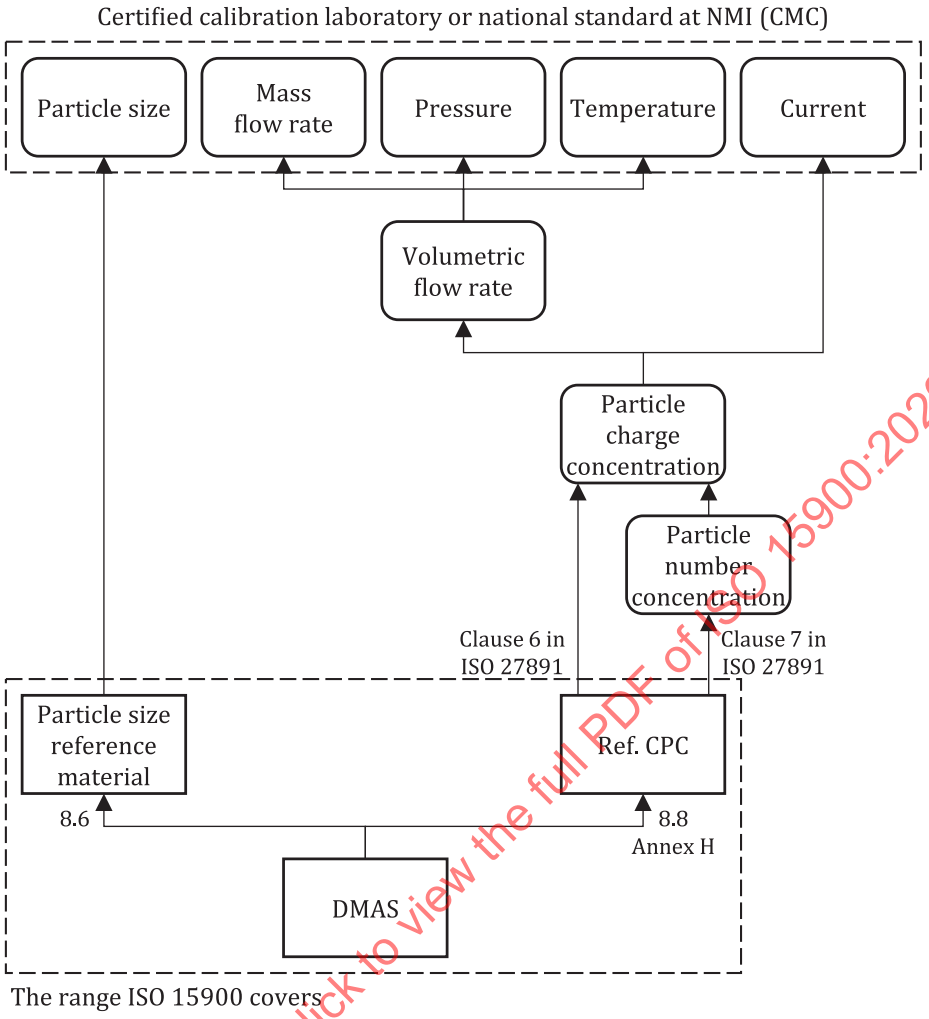

Figure 4 — Traceability diagram for DMAS with references to subclauses in Clause 8

6 System and apparatus

6.1 General configuration

A complete DMAS for the measurement of particle size distributions based on differential electrical mobility analysis typically has the following fundamental components (see Figure 5):

a) pre-conditioner;

b) charge conditioner;

c) DEMC with flow control and high voltage control;

d) aerosol particle detector;

e) system controller with data acquisition and data analysis (typically built-in firmware or dedicated software on a personal computer).

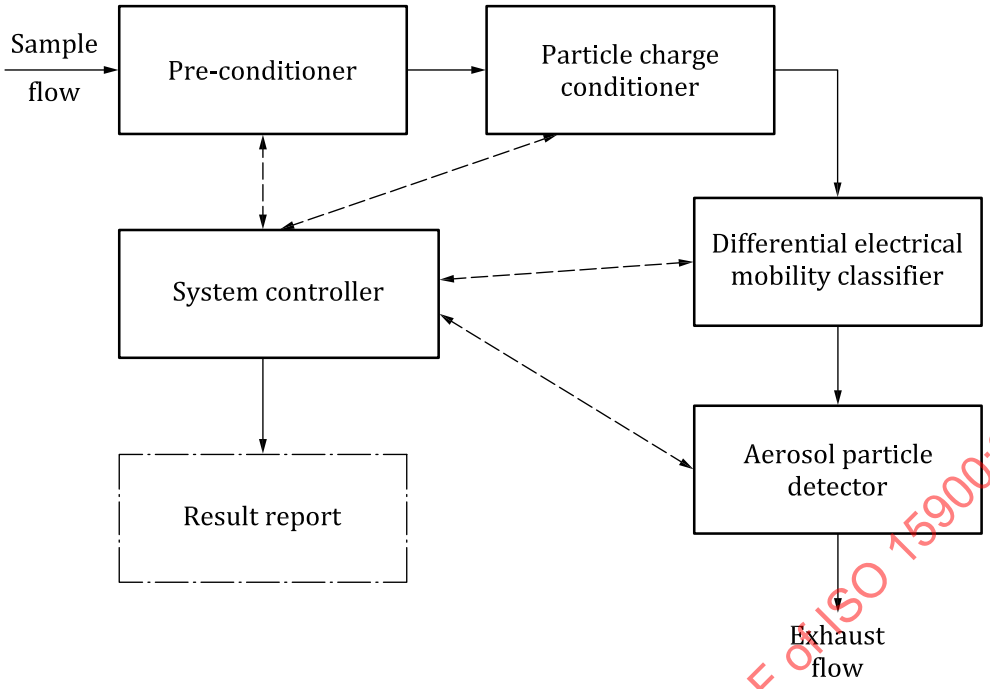

Figure 5 — Fundamental components of the differential mobility analysing system (DMAS)

Differential electrical mobility analysis is typically used for airborne particles ranging from a few nanometres to approximately one micrometre. Aerosol samples can be measured from a variety of sources. The most common sample sources are particles aerosolized from a liquid suspension, particles sampled directly from the atmosphere and particles sampled from a combustion source. The particle pre-conditioner and the charge conditioner are necessary to achieve defined sample conditions.

Most DMASs separate a mono-mobile fraction of the aerosol flow, which is transferred to the aerosol particle detector for particle number concentration measurement. In addition to the basic system configuration shown in Figure 5, other configurations exist, for example, systems with two parallel DEMCs and detectors for extended particle size range, systems with multiple detectors or systems with multiple parallel DEMCs and detectors.

The entire measurement is controlled by the system controller, which also acquires data and performs data inversion. The system control can, for example, reside as software and/or hardware in a personal computer. It can also be integrated into a self-contained particle sizing instrument.

6.2 Components

6.2.1 Pre-conditioner

The pre-conditioner component serves two purposes: removing large particles and, if necessary, reducing the sample humidity. Other pre-conditioning may be required for specific applications.

NOTE Calibrating the differential pressure across the particle pre-conditioner against the flow rate through this device is a helpful sample aerosol flow measurement which does not interfere with the incoming particles.

6.2.2 Charge conditioner

In order to calculate the particle number distribution from the measured electrical mobility number distribution, a known particle size-dependent distribution of electrical charges shall be generated on the aerosol particles. Charge conditioners upstream of a DEMC are used for this purpose. The charge distribution is the result of the random thermal diffusion (Brownian motion) of the ions which leads to frequent collisions with the particles and the attachment of ions on particles. The particle concentration to be charged shall be limited in such a way that the depletion of ions due to ion attachment to the

particles does not lead to significantly reduced charges on the particles. The particle charging depends mainly on the so-called $N_I \cdot t$ product, which is the concentration of either positive or negative ions, N_I, multiplied by the typical interaction time, t, of aerosol particles with the ions. In some charge conditioner designs the ion transport is purposely influenced by AC- or DC-electric fields and sheath air flows.

Unipolar charging can yield a higher $N_I \cdot t$ product than bipolar charging, thus increasing the transmission efficiency of a DMAS by increasing the number of charged particles. The increased $N_I \cdot t$ product, however, leads to both a higher fraction of multiply-charged particles and higher charge levels on these particles. This has the adverse effect of reducing the size resolution of the DEMC. Therefore, unipolar charging is typically used for instruments with lower size resolution or when the size range being measured is limited such that multiple charges remain insignificant.

A.3 gives an overview on charge conditioners.

6.2.3 DEMC

The DEMC is the core component of a DMAS. The basic operating principle is electrical mobility discrimination by particle migration perpendicular to a laminar sheath flow. The migration is determined by an external electrical force and the counteracting particle drag forces in the laminar sheath flow.

DEMC can be designed in a variety of geometries. The classifying characteristic of a DEMC is described by its transfer function. Whatever the geometrical design of the DEMC, the transfer function is defined by the critical mobilities, which are determined by the geometrical dimensions of the device, by the flow rates and by the voltage potential between the electrodes. Details on the transfer function of the DEMC can be found in 5.4. For the example of a coaxial cylindrical DEMC, details on the critical mobilities as well as the transfer function can be found in Annex E.

Measuring a particle size distribution is usually achieved by changing the voltage. For transient measurements, DMASs with multiple particle detectors have been designed. These systems typically operate with fixed voltages.

6.2.4 Aerosol particle detector

The aerosol outlet from the DEMC shall be connected to a well-characterized particle detector. This instrument shall be able to detect particles exiting the DEMC with known efficiency across the entire size range to be reported. The lower end of the size range limits the aerosol particle detector that can be used. In general, either a continuous flow condensation particle counter (CPC) or an aerosol electrometer is used.

In a CPC, aerosol particles are exposed to condensable supersaturated vapour. Vapour condensing on the particles grows them into droplets that can be counted by optical means.

Aerosol electrometers are typically designed as Faraday cup aerosol electrometers (FCAEs). The aerosol particles deposit on a filter inside the Faraday cup. The electrical charge on the deposited particles can be measured as a current by the electrometer amplifier.

These two, most common aerosol particle detectors are discussed further in Annex B.

6.2.5 System controller, data acquisition and analysis

The system controller with data acquisition and data inversion should cover several tasks. Before the measurement, the system control of an automated measuring system should set all operating parameters and flag the operator if any of these parameters cannot be set correctly. During the measurement, the system control should acquire and monitor all critical parameters (for example, the flow rates) and flag a warning to the operator if any of these parameters are outside pre-established tolerances. At the same time, the control system should set the electrode voltage through the variable high voltage supply and read the particle number data from the aerosol particle detector. Either during or after the measurement, data inversion takes place and the measured particle size distribution is presented, stored, exported, etc.

The system control should also create an event log which contains all detected irregularities during a measurement.

7 Measurement procedures

7.1 Setup and preparation of the instrument

7.1.1 General

Proper instrument setup is critical in obtaining the correct particle size distribution. There are many different ways to configure and operate a DMAS instrument and the reader shall refer to the manufacturer's instrument manuals for specific details. This clause addresses only those issues common to all types of DMAS systems.

7.1.2 Aerosol pre-conditioning: Adapting the aerosol to be measured to the requirements of the DMAS

7.1.2.1 Particle concentration

The particle concentration in the aerosol entering the DMAS may not exceed the upper limit of the operating range of the system. If not, dilution is required to reduce the particle concentration. ISO 27891:2015, Annex F contains a description of diluters.

7.1.2.2 Temperature and pressure

Temperature and pressure of the aerosol entering the DMAS shall be within the operating range of the system. If not, temperature conditioning as well as pressure adaption are necessary. Whenever possible, such conditioning should be made with neglectable (or at least minimized) effect on the particle properties.

7.1.2.3 Humidity

A DMAS requires non-condensing conditions for reliable operation. If the risk of condensation within the system exists, drying is required.

For atmospheric sampling, humidity may or may not play a role in obtaining an accurate particle size distribution. However, it shall be considered when making a measurement. Hygroscopic particles (e.g. sulfate particles) can change size depending on the amount of water in the air. Other types of particles (e.g. elemental carbon) will not be appreciably affected by humidity. Since humidity can change over time, the size distribution of the sample aerosol can also change over time. If sampling times are sufficiently long, the aerosol size distribution can change during a single measurement. This can be avoided by pre-drying the incoming aerosol with a membrane or diffusion dryer or by using dry dilution air to lower the relative humidity to less than 40 %. Other humidity control devices can allow measurements to be made at a constant relative humidity. In any case, it is important to consider how humidity may affect atmospheric aerosol measurements and how a dryer may affect particle losses.

Particles obtained through atomization shall be thoroughly dried in order to obtain an accurate particle size distribution. Dilution air is preferable if the aerosol concentration is very high and can tolerate dilution. If that is not the case, a membrane or diffusion dryer is the best choice.

7.1.3 Aerosol pre-conditioning: Separation of large particles

Measuring particle size distributions with a DMAS requires data inversion, as described in 5.3 and Annex D. In order to solve the inversion equations, it is necessary to know the size of the largest particles allowed to enter the DEMC. This will prevent larger multiply-charged particles from entering the DEMC. Large particles carrying multiple charges may have the same electrical mobility as smaller,

singly-charged particles. By removing the larger particles, the true size distribution is more accurately determined.

A pre-separator with known cut-off sizes shall be installed in the sample aerosol flow to fulfil this need. Commonly used pre-separators are impactors or cyclones. The cut-off size and steepness of the cut-off curve should be selected such that

a) the pre-separator does not remove particles from the desired size range of the measurement, and

b) the cut-off size is within the size range for data inversion.

NOTE Impactors are mostly used for sample aerosol flow rates of less than 1,5 l/min; cyclones are applicable for sample aerosol flow rates of 1 l/min and more.

During operation, some particles will deposit in the pre-separator. Therefore, the pre-separator needs to be regularly inspected and cleaned when necessary.

7.1.4 Charge conditioning

All aerosol samples shall be charge conditioned in a defined and reproducible way just before entering the DEMC. See Annex A for an overview on charge conditioners and for more details.

It is important to ensure proper performance of the charge conditioner, especially at a high incoming particle concentration. An improperly working charge conditioner will skew the particle size distribution, giving incorrect results.

7.1.5 DEMC: Flows

The flow control system is an important component with respect to the precision, resolution and repeatability of a DEMC. Both the particle sizing and the particle concentration measurement rely on accurately known flows.

Depending on the type of DEMC used, the sheath flow to sample aerosol flow ratio will vary. A high sheath/sample aerosol flow ratio will result in a narrow transfer function with better resolution of the size distribution. A higher sheath flow rate also reduces diffusion broadening within the DEMC. A low sheath/sample aerosol flow ratio will increase the aerosol concentration, desirable for lower concentration aerosols.

Every DEMC has two flows entering the device (sample aerosol flow and sheath flow) and two flows exiting the device (mobility selected aerosol flow and excess flow). Three out of these four flows shall be controlled for stable operation. The sheath air shall be particle free. In order to avoid interference with the aerosol to be measured, the recommended flows to be controlled are the recirculating excess/sheath flow and the mobility selected aerosol flow. Absolute accuracy on the flow rate measurements is critical since the sample aerosol flow is, in general, determined by the difference between the outgoing flows and the incoming sheath flow.

The inlet and outlet flows are strongly coupled, so upstream or downstream perturbations to any one of the flows may cause other flows to change. To minimize the sensitivity to such perturbations, the flow network should be carefully designed. The volumetric flow rates shall be defined and kept constant during the measurement. It should be periodically ensured that there are no leaks in the system.

The flow control system can be simplified and stabilized by cleaning and recirculation of the excess flow as sheath flow in a closed loop. This recirculation not only guarantees that the sheath flow equals the excess flow, it also eases the constraints on the precision with which the sheath and excess flow rates are measured since, in steady-state operation, the incoming sample aerosol flow exactly equals the outgoing mobility selected aerosol flow, provided there are no leaks in the recirculation system and the temperature of the recycled particle-free gas is the same as that of the incoming aerosol flow into the DEMC. An exception is a measuring setup where the aerosol inlet is pressurized (overpressure sampling mode). In such a case, it might become necessary to use a metered bleed to allow balancing of the flows.

7.1.6 DEMC: Voltage

In most DMAS systems, a variable DC high-voltage supply is used to control the potential difference between the DEMC's electrodes. Fluctuations in the voltage across the DEMC will greatly affect the resulting particle size distribution measurement. On the low voltage range, any uncorrected offset of the power supply influences the sizing accuracy for high mobility particles.

For large, low-mobility particles, the required voltage can be high, reaching up to 10 kV to 12 kV. The maximum voltage should be limited in order to prevent arcing within the instrument. Arcing generates artefact particles and can damage exposed surfaces in the instrument. The stability of the supplied voltage influences the resolution and repeatability of the DEMC.

For safety reasons, the outer DEMC surfaces are normally grounded while the variable, positive or negative voltage supply is connected to an inner electrode.

7.1.7 DEMC: Temperature and pressure

The temperature and pressure inside the DEMC should be monitored during the measurement. Temperature and pressure fluctuations will adversely affect the data inversion unless they are taken into account.

7.1.8 Particle detection: CPC

Typically, a CPC has effectively 100 % detection efficiency over a wide range of particle sizes. Toward the low end of the detectable size range, the detection efficiency decreases to zero with a relatively steep sensitivity curve.

If the measuring range of the differential mobility analysing system extends into the range of the decreasing efficiency curve of the CPC, the measurements shall be corrected accordingly.

A CPC shall be operated within its specified particle concentration range. If the particle concentration is higher than the upper limit of the specified concentration range, particle coincidence will become significant and therefore will cause erroneous measurements.

7.1.9 Particle detection: FCAE

If an FCAE is used as a particle detector, the particle concentration exiting the DEMC shall provide an electrical current well above the noise level of the electrometer. Currently, aerosol electrometers measure electrical currents down to approximately 1 fA (or approximately 6 250 singly-charged particles per second).

7.1.10 Data acquisition

Most commercially available instruments have data acquisition software. It is important to make sure that the software collects all of the necessary data during the measurement. This will include the particle counts (from the particle counter) or electrical current (from the electrometer), the DEMC voltage, all necessary flow rates, temperature, pressure, etc. Some software packages have more options than others. Refer to the instrument manufacturer's manuals for details on setting up the data acquisition system.

7.2 Pre-measurement checks

7.2.1 General

There are several tests that can be made to ensure that the entire system is operating properly. These tests are also helpful in instrument troubleshooting.

7.2.2 Overall DMAS check

Apply clean air (through a HEPA filter) to the DMAS inlet and run a size distribution measurement. There should be no (or only very few) particles detected across the whole particle size distribution. Remove the filter to expose the DMAS to normal, non-filtered air and run another size distribution measurement. Check if a significantly larger number of particles are observed in the size distribution compared to that of filtered air.

7.2.3 Data acquisition check

Ensure that the data acquisition system is connected and operating properly. Verify that the voltages, particle counts, flow rates and other necessary data are recorded.

7.3 Measurement

Once the instrument has been set up and checked, measurement can begin. The parameters of the measurement will depend on the type of DMAS system used and the type of aerosol being measured. In all cases, determination of the particle size distribution requires measuring the number concentration of all particles exiting the DEMC at a given voltage. These have the same electrical mobility but can have different sizes due to possible multiple charges. Repeated measurements of the particle concentration at different voltages will provide a concentration versus electrical mobility curve that is the basis for determining the size distribution.

There are many different ways to run a DMAS. It is up to the operator to decide on the best method based on the measurements to be made, the equipment used and the instrument manufacturer's recommendations.

For the measurement, a few considerations should be noted.

a) A stepping DMAS system changes the voltage between concentration measurements. For a stepping system, it is important to allow enough time for the particle detector to achieve a steady-state concentration. The amount of time needed for each step can be approximated by determining the travel time of the aerosol from the DEMC inlet to the particle detector based on the operating flow rate and tube length. Some commercial software packages can reduce the time needed between voltage steps by the use of proprietary algorithms. However, manual scans and manual adjustments will usually need longer times at each voltage.

b) A scanning DMAS system smoothly changes the voltage (often as an exponential ramp) during a continuous measurement of the particle concentration. The scanning direction “upscan” designates a scan from a low voltage to a high voltage. The inverse is called “downscan”. For a scanning system, the time constants (residence time of the particle in the DEMC, residence time in the tubing between DEMC and particle detector, the response time of the particle detector and the time constant for the voltage ramp) and the scanning direction may cause a shift and a deformation of the transfer function compared with the stepping system (Collins et al., 2004, [12]).

c) It is important to know the stability of the source. Rapid changes of the size distribution, the particle concentration, or both, affect the measurement of the size distribution. Critical conditions of the particle source can be identified by repeating the size distribution measurement and by changing the measuring procedure (number of voltage steps, scan time).

The periodic tests and calibrations required during measurement are set out in Clause 8.

7.4 Maintenance

The maintenance schedule for a DMAS depends highly on the application, including aerosol type and aerosol concentration. The interval for maintenance depends on the sampled aerosol concentration and frequency of use. The following parts of a DMAS should be regularly cleaned:

Pre-separator: Pre-separator (e.g. impactors or cyclones) surfaces which get in contact with sampled aerosol should be cleaned with compressed air or an ultrasonic bath. Particles collected on pre-

separator surfaces should be removed. Impactor plates should be recoated with a thin layer of vacuum grease. The maintenance should be done every six hours of sampling unless experience has proven that longer sampling times between cleanings may be tolerated.

Charge conditioner: Charge conditioners should be checked to ensure operation as expected; e.g. the radiation source of radioactive charge conditioners has not exceeded its useful lifetime. Cleaning charge conditioners can be hazardous and should only be performed by a trained professional. The cleaning or repair of radioactive sources by the end-user is not recommended. Local radiation protection laws, regulations, guidelines etc. can apply when using these devices, (see A.2.2.5).

Electrodes: DEMC electrodes should be cleaned after every few months of continuous sampling. Use a very soft tissue to clean all electrode surfaces. Some particles on the electrodes will have no effect on the performance of the DEMC, but layers of particles could cause flow disturbances and could distort the electrical field. After cleaning, the surfaces of the DEMC electrodes should be checked visually for any damage. Even small scratches could lead to flow disturbances or change the electrical field, causing turbulence and resulting in an inaccurate transfer function for the DEMC.

Other internal components: During operation, many components are exposed to solid or liquid particle deposition. All components that are exposed to such deposition shall be cleaned regularly. Excessive soiling may change the geometry and particle cut-size of the pre-conditioner, may reduce the efficiency of the charge conditioner, may distort the electric field and/or the laminar flow in the DEMC and may affect the accuracy of the particle detector.

Filters for sheath air/excess air: Most of the aerosol particles entering a DEMC will not be classified and will exit with the excess flow and deposit on a clean-air filter. The filter shall be replaced when necessary to avoid creating a large pressure drop within the sheath flow, which is normally obtained from recirculation of the excess flow.

8 Periodic tests and calibrations

8.1 Overview

Following the procedures in 8.2 to 8.8 ensures that a DMAS attains a known, small uncertainty for measurement of particle size and concentration. These procedures shall be performed only by qualified personnel. The procedures shall cover the fundamental components as summarized in the matrix in Table 4. Test and calibration procedures are also described, e.g. in Wiedensohler et al. (2018) [75].

Table 4 — Matrix for sensitive components of a DMAS

	Charge conditioner	DEMC	Aerosol particle detector	System controller	Entire DMAS
Zero tests (8.2)			X		X
Flow rate tests (8.3)		X	X	X	X
Voltage calibration (8.4)		X		X	
Charge conditioner test (8.5)	X			X	X
Calibration for size measurement (8.6)				X	X
Size resolution test (8.7)				X	X
Number concentration calibration (8.8)			X	X	X

NOTE The pre-conditioner is not listed in this table since it requires only the maintenance in 7.4 and does not require periodic tests and calibrations.

8.2 Zero tests

8.2.1 General

Once the flow rates are checked, there are three zero tests that can be performed to ensure that there are no leaks and that the instruments are working properly.

A CPC should be used as particle detector for the zero tests.

If one of these three tests fails, additional leakage test of the components and eventually service to repair a leak in the DMAS may become necessary.

8.2.2 Particle detector zero test

Disconnect the particle detector from the DEMC and keep the tubing exposed to normal office or laboratory room air (not clean-room air). Ensure that the instrument is on and there is air flow into the particle detector at the correct rate. The particle detector should count a high concentration of particles. The particle detector may even saturate while sampling room air. Place a high-efficiency particulate air (HEPA) filter on the inlet and make sure that the particle detector signal drops to a negligible level compared to the concentration to be measured.

8.2.3 Overall DMAS zero test with inlet filter

Reconnect the particle detector to the rest of the DMAS, apply clean air (through a HEPA filter with at least 99,99 % efficiency) to the DMAS inlet and run a particle number size distribution measurement. There should be no (or at most only a few counts in discontinuous, randomly distributed bins) particles across the whole particle number size distribution. If the particle detector detects particles, there are leaks in the DMAS, either in the components or in the interconnecting tubes.

8.2.4 Overall DMAS zero test with DEMC voltage set to 0 V

Make sure the aerosol inlet tube to the DEMC is open to normal room air (not clean-room air). Set up the appropriate sheath flow and sample aerosol flow rates within the DEMC and to the particle detector. Set the voltage applied to the DEMC to 0 V. The particle detector should count no (or at most only a few) particles in 1 min. If the particle detector detects particles:

a) the sheath/sample aerosol flow ratio could be too low and particles are diffusing into the monodisperse outlet of the DEMC. This can be corrected by decreasing the aerosol flow rate or increasing the sheath flow rate.

b) the flow rates within the DEMC are too high and turbulent conditions exist. If this is the case, reduce the flow rates to return to laminar flow.

8.3 Flow rate tests

The flow meters indicating the volumetric flow rates of sheath flow, excess flow, sample aerosol flow and mobility selected aerosol flow shall be tested. Regular calibration of these flow meters shall be made against a flow meter that is traceable to internationally accepted standards.

Volumetric flow rates govern the DEMC transfer function. If mass flow meters are used to measure or control flow rate, transformation from mass flow rate to volumetric flow rate is necessary.

The procedure described in 8.6.5.5 b) is to monitor correct sheath flow, see Wiedensohler et al. (2018) [75].

NOTE When the excess air is circulated and used as the sheath air, one can assume that the sample aerosol flow and the mobility selected aerosol flow are equivalent if the air leakage in the circulation circuit is verified to be negligible. In such cases, the flow meters need only be calibrated for the sheath air, the sample and the mobility selected aerosol flows.

8.4 Voltage calibration

The voltage applied to the DEMC shall be calibrated against a voltmeter that is traceable to internationally accepted standards.

8.5 Charge conditioner test

Aging of ion sources (e.g. radioactive materials) in the charge conditioner may change the charge distribution for particles. If the tests for the entire DMAS (see 8.6, 8.7 and 8.8) fail, the charge conditioner can be one of the reasons.

Testing of the charge conditioners themselves should be done using particle number size distributions and number concentrations similar to those to be measured with the DMAS in which the charge conditioner is applied. Such tests require extensive laboratory equipment like sophisticated test aerosol generators and tandem DEMCs and test protocols that depend on the type of the charge conditioner. These tests are not subject of this document.

Charge conditioner integrity should be checked regularly at least by visual inspection of the device and, if applicable, by tests described in the device's user manual.

8.6 Calibration for size measurement

8.6.1 General

This subclause comprises two procedures for the size calibration of the DMAS. The first procedure describes size calibration for the standard operating mode, i.e. the so-called dynamic scanning mode. The second procedure is on calibration in the static step mode. Particle size standards described in 8.6.3 are used in both procedures.

8.6.2 Purpose of calibration

The tests and calibrations described in 8.2 to 8.5 are necessary to check accuracy and integrity of individual components of the DMAS. However, they are not necessarily sufficient for verification of the accuracy of sizing by a DMAS as an entire system. Therefore, a dynamic particle size calibration procedure for the standard DMAS sizing method is described in 8.6.4 and shall be carried out to test for accuracy and to calculate the dynamic sizing error. It includes the data inversion and correction algorithms given by the manufacturer. Therefore, it is relatively easy to perform and is suitable as a test method for typical users.

A size calibration is also feasible when the DMAS is statically set at fixed voltage(s), respectively fixed particle size(s). This is e.g. required in ISO 27891 for the particle number concentration calibration of CPCs. Here, the static sizing error of the DMAS has a considerable influence on the uncertainty. The static size calibration procedure is described in 8.6.5.

8.6.3 Particle size standards

Only particle size certified reference materials with reputable certificates should be used. A reputable certificate shall mean either one that has been produced by a laboratory accredited to ISO 17034 or an equivalent standard. The standard particles should be monodisperse and should have a certified diameter, d_c, with relative standard uncertainty, $u_{r,cert}$, equal to or less than 5 %.

DMAS calibration with standard monodisperse particles of a certified size requires due attention with respect to

— the method of dispersing these particles in air,

— the concentration of the particle dispersion in the liquid that has to be dispersed, which shall be sufficiently low to substantially avoid aerosol particles other than singlet particles,

— the due removal of any non-volatile dissolved materials from the liquid other than the certified particles (remove surfactants and ionic species, etc.) prior to the aerosolization of the particles.

The coefficient of variation of the test aerosol particle size distribution used for calibration should be equal to or less than 20 %, whenever possible.

8.6.4 Dynamic DMAS particle size calibration procedure

8.6.4.1 Procedure

In this procedure the DMAS is operated with the voltage of the DMAS being swept continuously. The procedure includes the data inversion and correction algorithms given by the manufacturer and uses test aerosol particles with a certified size, d_c. The procedure contains the following steps.

NOTE 1 If the instrument is working properly, the median diameter of monodisperse aerosols measured by following the procedure in this subclause would be accurate even though the data processing is assuming polydisperse aerosols [56].

a) Aerosol generation

Aerosolize particles of a certified size, d_c.

b) Check or determine the correct delay time

The delay time t_d is the time which elapses between a particle leaving the classifying section of the DEMC with q_3 and its detection by the particle detector. An incorrect delay time causes a shift of the measured size distribution on the size axis. The use of the correct delay time is therefore crucial for the calibration procedure described here. There are two ways to check and – if required – adjust the delay time:

1) Sweep the DEMC voltage of the DMAS under test first upwards from the low to the high value of the desired voltage range; next repeat the measurement with a reversed voltage sweep from the high value to the low value. Adjust the DMAS' delay time such that the number median diameters found for d_c in both measurements do not differ by more than 2 %. The lower the voltage scan rate (e.g. 120 s measurement time for each measurement), the better this method will work.

2) If the DMAS allows voltage scans with high scan rates, run a first measurement with a low scan rate (e.g. a size distribution measurement with 120 s measurement time). Repeat the measurement with a high scan rate (e.g. 15 s measurement time). Adjust the DMAS' delay time such that the number median diameters found for d_c in both measurements do not differ by more than 2 %. The higher the difference between the low and the high scan rate, the better this method will work. However, the scan rate limits given by the manufacturer of the DMAS shall not be exceeded.

If the width of the peak which represents d_c in the number size distribution data are only one size channel, the geometric (also known as logarithmic) midpoint diameter of this size channel shall be used as the number median diameter.

If the peak extends over more than one size channel, determine the number median diameter by using either the software given by the manufacturer or statistics tools to fit the peak around d_c in the size distribution data (presented as $\mathrm{d}N/\mathrm{d}\ \log d$ versus d) to a lognormal distribution function. The median diameter of this lognormal fit represents the measured d_c.

NOTE 2 Other statistic number size distribution values like the geometric mean diameter or the mode diameter can be used instead of the number median diameter.

c) Size distribution measurement

Measure the number size distribution of the test aerosol particles with the DMAS under test and determine the number median diameter representing d_c.

d) Determine the arithmetic average diameter $\bar{d}$

Repeat the measurement c) n times and calculate the arithmetic average, $\bar{d}$, of the n number median diameters.

e) Calculate the relative error

Use Formula (8) to calculate the relative error, ε:

$$\varepsilon(d_c) = \frac{|\bar{d} - d_c|}{d_c} \cdot 100 \tag{8}$$

8.6.4.2 Report for dynamic DMAS particle size calibration

The following information shall be included in the report:

a) date of calibration;

b) certified size, d_c, and relative standard uncertainty, $u_{r,cert}(d_c)$;

c) DMAS type and settings, such as flow rates, voltage range, voltage scan rate, etc.;

d) pressure and temperature in the DEMC during test;

e) average of the median diameters, $\bar{d}$;

f) standard deviation of d_i (i = 1 to n);

g) relative error, ε and number of repetitions n.

Information on points b) to g) shall be given for each certified particle size standard used. The tolerance value(s) for ε shall be prescribed based on the purpose or requirements of the measurement in which the DMAS is used, the sizing capability of a specific DMAS and the magnitude of the size uncertainty of the standard particles used in the test. A suggested certificate template for reporting calibration results is given in Annex F.

8.6.5 Static DMAS particle size calibration procedure

8.6.5.1 Procedure

In this procedure the DEMC voltage is changed stepwise during measurements and only errors that arise in the static operation of the DMAS are considered.

It is assumed that flow rates and voltages have been calibrated as described in 8.3 and 8.4, respectively. This calibration reveals deviations due to either errors in the DEMC dimensions or residual errors in the flow rates (or both). These errors can be corrected by including an appropriate correction factor in the formula that calculates electrical mobility from DEMC parameters. For example, where a cylindrical DEMC is involved, Formula (9)

$$Z = \zeta \cdot \frac{(2q_1 + q_2 - q_3) \cdot \ln(r_2 / r_1)}{4\pi L} \tag{9}$$

can be used [see Annex E, Formulae (E.2) and (E.8)], where the correction factor is denoted by ζ.

In the calibration method described here, the value of the correction factor is to be determined through measurement of particle size standards by the DMAS under calibration, so that the measured electrical mobility of the standard particles matches the electrical mobility calculated by Formula (9) for the certified size of the standard particles.

The uncertainty associated to the result of the calibration shall be calculated following the procedure below and reported. This calculation method is in accordance with the guidelines given in ISO/IEC Guide 98-3.

The procedure comprises the following steps.

a) Select a particle size standard with certified size, d_c.

b) Record the temperature and pressure in the DEMC after the DMAS reached thermal equilibrium with its environment.

c) Aerosolize the particles from the standard.

d) Obtain a spectrum of the particle number concentration, N, while the voltage, U, is changed step-wise.

e) Calculate the number-weighted mean electrical mobility, $\bar{Z}$, from the U-N spectrum obtained in Step d) by following the procedure in 8.6.5.2.

f) Repeat Steps d) and e) n times and obtain the average of the mean electrical mobility, $\bar{\bar{Z}}$.

g) Calculate the electrical mobility, Z_c, that corresponds to the certified size, d_c, of the standard particles by using Formulae (1) to (4). Use pressure and temperature obtained in Step b) in the calculations of the slip correction, viscosity and mean free path.

h) Calculate the correction factor, ζ, as:

$$\zeta = \frac{Z_c}{\bar{\bar{Z}}} \tag{10}$$

NOTE It is not required to determine ζ at more than one particle size, since the ζ value is independent of particle size if the assumption on the sources of sizing errors is correct.

8.6.5.2 Calculations of the number-weighted mean electrical mobility,

Based on the work by Knutson and Whitby (1975) [36], the number-weighted mean electrical mobility, , can be calculated from a U-N spectrum as:

$$\bar{Z} = \frac{I_1^*}{N_{in} q_2 \left(\frac{2\pi L}{q_4 \ln(r_2/r_1)} \right)} \tag{11}$$

The terms q_2, q_4, L, r_1 and r_2 are defined in 5.1 and Annex E, and the terms I_1^*, N_{in} and I_1 can be calculated using the following formulae, which replace integrals by sums (trapezoidal rule with non-uniform grid) of k voltage intervals:

$$I_1^* = \frac{1}{2} \sum_{i=1}^{k} \left(\frac{N(U_{i+1})}{U_{i+1}^2} + \frac{N(U_i)}{U_i^2} \right) (U_{i+1} - U_i) \tag{12}$$

$$N_{in} = \frac{I_0^*}{q_2 I_0} \tag{13}$$

where

$$I_0^* = \frac{1}{2} \sum_{i=1}^{k} \left(\frac{N(U_{i+1})}{U_{i+1}} + \frac{N(U_i)}{U_i} \right) (U_{i+1} - U_i)$$

and

$$I_0 = \left[\left(1-q_2^{'}\right)\ln\left(1-q_2^{'}\right)-\left(1+q_3^{'}-q_2^{'}\right)\ln\left(1+q_3^{'}-q_2^{'}\right)+\left(1+q_3^{'}\right)\ln\left(1+q_3^{'}\right)\right]/q_2^{'}$$

$$I_1 = \frac{1}{q_2^{'}}\ln\frac{1+q_3^{'}-q_2^{'}}{\left(1+q_3^{'}\right)\left(1-q_2^{'}\right)}$$

$$q_2^{'} = q_2/q_4$$

$$q_3^{'} = q_3/q_4$$

(q_1, q_2, q_3, q_4. are defined in 5.1.)

8.6.5.3 Uncertainty of the result of the calibration

The standard uncertainty of the calibration result using standard-size particles of the certified size, d_c, denoted by $u_c(d_c)$, can be evaluated by taking two uncertainties into consideration:

a) the standard uncertainty of the certified particle size, $u_{cert}(d_c)$, and

b) the uncertainty due to random dispersion that occurs in the repeated measurement of $\bar{Z}$ in determination of the correction factor, ζ.

In this document, the uncertainty associated with the correction factor, $u(\zeta)$, is not explicitly calculated. Instead, the uncertainty of the calibration result is expressed in terms of particle size, rather than in electrical mobility, although a more direct expression of the uncertainty would be that of ζ, which is a value defined in the mobility domain. The uncertainty $u(\zeta)$ is a combination of the experimental standard deviation of the measured Z, described below, and the uncertainty associated with the electrical mobility calculated for the certified standard particles, Z_c.

The uncertainty expressed in particle size has the advantage that the uncertainty which arises in conversion between particle size and mobility can be omitted in the calculation of the combined uncertainty, based on the argument by Mulholland et al. (2006)[42]. In addition, it is easier for typical users to interpret the value of the uncertainty if it is expressed in terms of particle size.

The uncertainty in the size of the certified spheres is expected to be a significant component of this latter uncertainty. Because the uncertainty in the size of the certified spheres is easily handled as a direct contribution to the uncertainty of the size calibration, in this document the uncertainty associated with Z_c is effectively assumed to be represented by the uncertainty in the size of the certified spheres, as follows.

The random dispersion in determination of ζ is expressed as the experimental standard deviation of Z; that is:

$$s(\bar{Z})=\sqrt{\frac{\sum_{k=1}^{n}\left(\overline{Z_k}-\bar{\bar{Z}}\right)^2}{n-1}} \tag{14}$$

Convert this experimental standard deviation in electrical mobility, $s(\bar{Z})$, to that in particle size, $s(d_{\bar{Z}})$, as:

$$s(d_{\bar{Z}})=s(\bar{Z})\cdot\left|\frac{\mathrm{d}d}{\mathrm{d}Z}\right|_{d=d_{\bar{Z}}} \tag{15}$$

where

$$\left|\frac{\mathrm{d}d}{\mathrm{d}Z}\right|_{d=d_{\bar{Z}}} = \left(\left|\frac{\mathrm{d}Z}{\mathrm{d}d}\right|_{d=d_{\bar{Z}}}\right)^{-1}$$

$$= \left(-\frac{Z}{S_{\mathrm{C}}(d_{\bar{Z}})\cdot d_{\bar{Z}}}\left\{2S_{\mathrm{C}}(d_{\bar{Z}})-1+BC\exp\left[-C/Kn(d_{\bar{Z}})\right]\right\}\right)^{-1}$$

$$\cong \left(-\frac{Z}{S_{\mathrm{C}}(d_{\mathrm{c}})\cdot d_{\mathrm{c}}}\left\{2S_{\mathrm{C}}(d_{\mathrm{c}})-1+BC\exp\left[-C/Kn(d_{\mathrm{c}})\right]\right\}\right)^{-1}$$

(Refer to 5.2 for S_{C}, B, C and Kn.)

It is assumed in the above calculation that $d_{\bar{Z}}\cong d_{\mathrm{c}}$ so that the calculation of $d_{\bar{Z}}$ from $\bar{Z}$ can be omitted.

Using the experimental standard deviation, $s(d_{\bar{Z}})$, the combined standard uncertainty, $u_{\mathrm{c}}(d_{\mathrm{c}})$, is expressed as:

$$u_{\mathrm{c}}(d_{\mathrm{c}})^2=u_{\mathrm{cert}}(d_{\mathrm{c}})^2+\frac{s(d_{\bar{Z}})^2}{n} \tag{16}$$

8.6.5.4 Report for static DMAS particle size calibration

The following information shall be included in the report:

a) date of calibration;

b) certified size, d_{c}, and standard uncertainty, $u_{\mathrm{cert}}(d_{\mathrm{c}})$, and – if applicable – the corresponding electrical mobility, Z_{c};

c) DMAS type and settings, such as flow rates, voltage range, voltage scan rate, etc.;

d) pressure and temperature in the DEMC during test;

e) correction factor ζ;

f) combined standard uncertainty $u_{\mathrm{c}}(d_{\mathrm{c}})$.

NOTE There is no need to include any extra item in the report covering $u(\zeta)$.

A suggested certificate template for reporting calibration results is given in Annex F.

8.6.5.5 Use of calibration data

There are four main options for making use of the size calibration data.

a) Where the calibration data show small errors, or high accuracy data are not a priority, the calibration data can be used to estimate the uncertainties associated with the size values of the size spectra. The uncertainties will be a combination of the correction factor, ζ, and the combined standard uncertainty $u_c(d_c)$.

b) The correction factor, ζ, can be used to adjust the sheath flow of the instrument. The uncertainties will be estimated by the combined standard uncertainty $u_c(d_c)$.

c) The correction factor, ζ, can be used to adjust the electrical mobilities that are used in the calculations leading to size spectra. The uncertainties will be estimated by the combined standard uncertainty $u_c(d_c)$.

d) The correction factor, ζ, can be used to adjust the DEMC voltage to obtain the electrical mobilities that are used in the calculation leading to size spectra. The uncertainties will be estimated by the combined standard uncertainty $u_c(d_c)$.

8.7 Size resolution test

Any disturbance or inhomogeneity of the flow field and/or the electrical field can distort and broaden the transfer function.

When a DMAS measures the size distribution of monodisperse or quasi-monodisperse particles using the approximation method described in D.1, the obtained distribution is broader than the actual distribution. This can be exploited to extract the information about the width (resolution) of the transfer function.

The relative standard deviation of the measured distribution of certified particles, σ_d, at measured particle diameter d, shall be compared with the relative actual standard deviation, σ_c, of the standard particles of certified diameter d_c. This comparison shall consider the theoretical resolution defined by transfer function (see 5.4). Let $\Delta Z/Z^*$ designate the relative width of the transfer function or the inverse resolution of the DEMC. For example, when the DEMC is operated with the sheath and excess flows set equal and hence the transfer function is triangular, Formula (17) should be satisfied to a prescribed tolerance:

$$\frac{\sigma_d}{d} \approx \sqrt{\left(\frac{\sigma_c}{d_c}\right)^2 + \left(\frac{\kappa \cdot \Delta Z}{\sqrt{6} \cdot Z^*}\right)^2} \tag{17}$$

where

$$\kappa = -\frac{Z}{d} \cdot \frac{\mathrm{d}d}{\mathrm{d}Z} = \frac{S_C}{2S_C - 1 + BC\exp[-C/Kn(d)]} \tag{18}$$

S_C, B, C and Kn are as defined in 5.2. Note that this formula is only valid when broadening of the transfer function due to Brownian motion of the particles is expected to be negligible.

8.8 Number concentration calibration

Techniques for calibrating the number concentration measurement of the particle detector are given in Annex B. Approaches to test the overall number concentration measurement of the DMAS are described in Annex H.

9 Using a DEMC at a fixed voltage to generate particles of a chosen size

9.1 General

A DEMC set to a fixed voltage may be used to select particles of a chosen size, for example when calibrating a condensation particle counter (CPC) according to ISO 27891. In this case, it is important to refer to the proper definition of the particle size, e.g. the electrical mobility diameter when a DEMC is used, and to estimate the uncertainty of the size of particles generated. For example, for CPC calibration at sizes below the plateau region of the CPC, an accurate size is needed so that valid comparisons between independent CPC calibrations can be made.

There are several methods that can be used to determine particle size, such as electron microscopy (as used to determine the size of certified spheres), and aerodynamic methods that lead to an aerodynamic diameter (which can be applied to particles of any shape). The sizes obtained with electron microscopy will tend to diverge proportionately more at smaller sizes.

For the purposes of this document, the appropriate metric for particle size shall be the electrical mobility diameter. To generate particles of a chosen mobility diameter and with narrow size distribution a DEMC calibrated according to 8.6.5 shall be used. This describes a size calibration procedure with spheres certified by electron microscopy for sizes at or above 80 nm.

The recommendation of 80 nm as the minimum size of certified reference spheres used to calibrate the DEMC is taken from Reference [86]. The recommendation was made because of deviations between results for different sizing methods for smaller particles, specifically mobility methods compared to Transmission Scanning Electron Microscope and Atomic Force Microscopy. There is an additional problem with using smaller reference spheres, because residue of the liquid in which the spheres are initially suspended will have a larger relative effect on their size, if it forms thin layers around the spheres.

Sizes below 80 nm can be selected using the relationship between electrical mobility and particle size defined in 5.2 (extrapolation), or by using spheres certified specifically for their electrical mobility diameter. A mobility correction factor ζ according to 8.6.5 shall be used to calculate the target mobility and the target particle diameter of particles with the diameter d^* transmitted through the DEMC from the DEMC set diameter d_{DEMC} or set voltage U_{DEMC}.

$$Z^* = \zeta \cdot Z\left(U_{\mathrm{DEMC}}\right) \tag{19}$$

$$d^* = d\left(Z^*, p{=}1\right) = \frac{d_{\mathrm{DEMC}}\left(U_{\mathrm{DEMC}}\right)}{\zeta} \cdot \frac{S_{\mathrm{c}}\left(d^*\right)}{S_{\mathrm{c}}\left(d_{\mathrm{DEMC}}\left(U_{\mathrm{DEMC}}\right)\right)} \tag{20}$$

Since $S_C(d^*)$ is not known, iterations are necessary to solve above formula.

The relative standard uncertainty, $u(d^*)$ associated with this mobility diameter is a combination of several components:

— The effects of larger, multiply-charged particles that have the same electrical mobility as singly-charged particles;

— The uncertainty in the size calibration, referring to 8.6;

— Variations in sheath flow (closed loop system) or in all flows (open system) which affect the transmitted particle size of a DEMC;

Below 80 nm, when using extrapolation, the following components contribute:

— The uncertainty in the supply voltage, U, used to calculate the electrical mobility (relative to the electrical mobility selected at the 80 nm size calibration).

— The uncertainty in the slip correction

These uncertainties (see also Table 5) can be quantified and combined. Following ISO/IEC Guide 98-3, the components are estimated as standard deviations and combined, before a coverage factor is applied. For simplicity, all components are considered to be independent, and standard deviations are expressed as percentage effects on the result.

Table 5 — Uncertainty components for DEMC selected size and how to estimate them

Uncertainty component	Symbol	Subclause	Estimation
Multiply-charged particles	$u_r(MC)$	9.2	Negligible
Size calibration with certified spheres	$u_r(d_c)$	9.3	According to 8.6.5.3
Sheath flow	$u_r(q)$	9.4	Uncertainty associated with the flow control, taken to be 2 %, see Annex E)
Slip correction (if applicable)	$u_r(S_C)$	9.5	Negligible
Voltage (if applicable)	$u_r(U)$	9.6	Taken to be 0,5 % (see Annex E)

9.2 Multiply-charged particles

When a DEMC is used to select monodisperse particles of a chosen size, care shall be taken to avoid any significant number of larger, multiply-charged particles with the same electrical mobility being selected at the same time. This is especially important when small particles are being used to determine the low-size cut-off detection efficiency of a CPC, as the CPC will have a higher detection efficiency for the larger particles.

In general the problem can be avoided by using a primary aerosol source with a narrow size distribution, and by selecting particles from the size region above the mode of the primary aerosol size distribution, or by using a second charge conditioner and DEMC in series with the first one.

If there is any doubt about the fraction of multiply charged particles in the selected particle distribution, the procedure given in Annex D of ISO 27891:2015 can be used to determine this fraction, which shall be less than 10 %. The contribution to the uncertainty of the particle size can then be treated as negligible.

9.3 Size calibration with certified spheres

The uncertainty in the size of particles selected using a DEMC at a fixed voltage will be directly dependent on the uncertainty of the calibration of the DEMC using size-certified spheres. The procedure for determining this uncertainty is described in 8.6, specifically 8.6.5.3. The uncertainty of the DEMC calibration, expressed as a percentage of the particle size used for this calibration, shall be used here.

9.4 Sheath flow

For simplicity, singly-charged particles are assumed in the following relations; sample aerosol flow and mobility selected aerosol flow are assumed to be equal, as are sheath flow and excess flow.

For uncertainty considerations, the simplification that the targeted particle size d^* is inversely proportional to the sheath flow q_1 is appropriate:

[from Formulae (1) and (E.8)],

$$d^* \sim 1/Z^* \sim 1/q_1 \tag{21}$$

and hence, the related uncertainty component $u_r(q)$ is proportional to $(\Delta q_1/q_1)$, where Δq_1 is the expected absolute deviation from a set sheath air flow rate q_1. If Δq_1 is not known, it can - for the purpose of this document - be calculated as the standard error of the mean after repeated measurement of q_1 with a reputable flowmeter.

Unless more accurate measurements of the values of q_1 at the time of the DEMC calibration and at the time of its use to generate particles of a chosen size are available, an uncertainty of 2 % shall be assumed, following Annex E.

NOTE Omitting the slip correction (S_C) in the conversion from d to Z, Formula (21), leads to an overestimation of the actual uncertainty.

9.5 Slip correction (if applicable)

When a DEMC calibration using spheres of 80 nm diameter or larger is extrapolated to lower sizes, the accuracy of the lower size relies on the correctness of the slip correction. However, following 5.2, for the purposes of this document, the slip correction is defined by convention. There is therefore no uncertainty associated with the application of the slip correction, by convention.

9.6 Voltage (if applicable)

When a DEMC calibration using spheres of 80 nm diameter or larger is extrapolated to lower sizes, the accuracy of the lower size relies on the accuracy of the voltage across the DEMC.

For uncertainty considerations, it is assumed that the targeted particle size d^* is proportional to the DEMC voltage $d^* \sim 1/Z^* \sim U$, hence the related uncertainty component $u_r(U)$ is proportional to $(\Delta U/U)$, where ΔU is the expected absolute deviation from a set voltage U. If ΔU is not known it can - for the purpose of this document - be calculated as the standard error of the mean after repeated measurement of U with a reputable voltmeter.

The uncertainty of the voltage is generally found to be small compared to other uncertainties. Following Annex E, a value of 0,5 % can be used.

9.7 Calculation of overall uncertainty

All of these uncertainty components contribute linearly to the reported result. For the purposes of this document, they are assumed to be independent, so that the combined standard uncertainty is given by

$$u_r(d^*) = \sqrt{u_r^2(d_c) + u_r^2(q) + u_r^2(U)} \quad (22)$$

The coverage factor k shall be taken to be 2, so that the expanded uncertainty U_r, in percent, is given by $U_r = 2u_r(d^*)$. For example, when $u_r(d_c)$ is 3 %, Formula (22) with $u_r(q)$ = 2 % and $u_r(U)$ = 0,5 % gives $u_r(d^*) = 3{,}64\%$, and then U_r = 7,3 %.

In practice this will be slightly larger than the uncertainty associated with the calibration of the DEMC with size-certified spheres.

10 Reporting of results

Results will always be reported as a part of the results of the broader experimental system. ISO 9276-1 may be helpful for determining how to present size distribution results.

The DMAS parameters to be recorded for each experiment, or set of experiments, shall include the following:

a) date of analysis;

b) unique identification of the analysis laboratory;

c) operator's name;

d) unique identification of the sample;

e) identification of the type of instrument used, including manufacturer, model number (if any), serial number or other unique identification, and type of charge conditioner.

f) sample aerosol flow rate of the gas containing the aerosol particles;

g) sheath flow rate;

h) excess flow rate;

i) mobility selected aerosol flow rate;

j) pressure inside the DEMC during the experiment;

k) temperature inside the DEMC during the experiment;

l) method of calculation employed, including the formulas (or a reference to the formulas) used;

m) observations of unusual events during the experiment.

Annex A
(informative)

Charge conditioners and charge distributions

A.1 General

The function of the charge conditioner in a DMAS is to establish a known size-dependent steady-state charge distribution on the sampled aerosol prior to the size classification process in the DEMC. The charge distribution on the particles can either be bipolar or unipolar.

All charge conditioners can be regarded as ionization sources because they generate ions of either one polarity or both polarities in the carrier gas. These ions interact with the particles to generate a charge distribution. The characteristics of ionization sources frequently used for charge conditioning are outlined in the following subclause.

Since charge conditioners are used to achieve steady-state charge distribution in the sample aerosol flow of a DMAS, the instrument manufacturer and the user shall, by design or by measurement, ensure that the charge conditioner performs correctly and does not produce artefact particles.

A.2 Ionization sources

A.2.1 General

There are three common types of ionization sources for charge conditioning: radioisotopes, soft X-rays and corona-discharges. Other, less common ionization sources are included in Table A.1 but are not described in detail here.

A.2.2 Sources with radioisotopes

Radioisotope charge conditioners generally contain a sealed radioactive source. This device acts as a bipolar diffusion charge conditioner. It produces both negative and positive ions in the carrier gas. The radiation generates so called primary ions like N_2^+ and O_2^+ and free electrons in the carrier gas. These ions are short-lived. Some of them attach themselves to neutral molecules, which then coagulate into relatively stable ion clusters. Diffusion (Brownian movement) leads to collisions between these ions and the aerosol particles and thus to charge transfer to the particles. The $N_I \cdot t$ product reached in a radioactive charge conditioner depends on the type and energy of the radiation of the isotope, on the activity and geometry of the sealed source, on the geometry of the housing, on the flow rate and concentration of the aerosol through the housing and also on the composition of the carrier gas.

Krypton 85 (^{85}Kr), Americium 241 (^{241}Am), Polonium 210 (^{210}Po) and Nickel 63 (^{63}Ni) are the most commonly used radioactive isotopes. Their properties are explained in the following subclauses.

NOTE Sealed radioactive sources are classified based on ISO 2919, which provides tests and a classification system, e.g. for ranges of temperature, pressure, puncture, impact and vibration.

A.2.2.1 Krypton 85 (^{85}Kr)

^{85}Kr is a beta emitter (with 0,43 % gamma radiation probability of 514 keV) with a half-life of 10,78 years. After approximately 10 years, the replacement of ^{85}Kr sources should be considered. The maximum beta energy is 687 keV. Krypton is a noble gas, substantially reducing the health risk in case of leakage or damage to the source. In nearly all sources, the ^{85}Kr gas is contained in a small-diameter sealed stainless steel tube. This tube is contained inside a larger-diameter stainless steel or aluminium

housing. Aerosol passes axially through the housing that contains the ^{85}Kr tube. Part of the beta radiation is absorbed in the steel or aluminium that makes up the tube and the housing, thus producing Bremsstrahlung that also contributes to ion production.

A.2.2.2 Americium 241 (^{241}Am)

^{241}Am is an alpha emitter (with negligible additional beta and gamma radiation) with a half-life of 433 years. Sealed sources of this metal are available as strips covered with a very thin gold or palladium or gold and palladium alloy film. The alpha energy is 5,5 MeV.

A.2.2.3 Polonium 210 (^{210}Po)

^{210}Po is an alpha emitter with a half-life of 138 days. Due to their short half-life, ^{210}Po sources should be replaced annually or more often. The metalloid ^{210}Po is available in the form of gold-coated strips, typically embedded in a protective housing. Its alpha energy is in the range between 4 MeV and 5,3 MeV.

A.2.2.4 Nickel 63 (^{63}Ni)

^{63}Ni is a beta emitter (100 %) with a half-life of 100,1 years. Its beta energy is 67 keV; the decay product is stable ^{63}Cu. ^{63}Ni foils are also used - for example - as ionization source in GC-MS. Unsealed and sealed (inactive Ni overplating) foils with up to 550 MBq are commercially available.

A.2.2.5 Licensing and precautions for radioisotope sources

The use, transportation and disposal of radioisotopes are regulated by government authorities. Basic international standards and guidelines are, for example, set by commissions of the United Nations like IAEO, ICRP, ADR, etc. The licensing, shipping and disposal regulations that govern radioactive sources vary from nation to nation. Local radiation protection laws, regulations, guidelines etc. can apply when using these devices. The manufacturers' instructions shall be understood and followed as well.

A.2.3 Soft X-ray sources

Soft X-ray sources emit X-rays in the energy range below 10 keV. Soft X-rays are a very efficient source for charge conditioning because they have energies much higher than the ionization threshold of all molecules, thus creating an abundance of active ions. This device acts as a bipolar diffusion charge conditioner, comparable to sources with radioisotopes. A stainless steel or aluminium housing is lighted with X-rays from a source. The aerosol flows through the housing from an inlet to an exit port. A radiation window (e.g. Beryllium) protects the X-ray source from particle impact and also attenuates the radiant flux and radiation energy to adjust the ion concentration. X-ray blockers may prevent X-rays from exiting through the aerosol ports. Similar to radioisotope sources, the $N_I \cdot t$ product reached in a soft X-ray charge conditioner depends on the X-ray energy and the radiant flux, the radiation field geometry, the flow rate and concentration of the aerosol flow through the housing and last but not least on the composition of the carrier gas. While radioisotope sources emit radiation continuously, X-ray sources can be turned on and off.

A.2.3.1 Licensing and precautions for soft X-ray sources

The use of soft X-ray sources may be regulated by national and/or local government authorities. The regulations may vary from nation to nation. Local radiation protection laws, regulations, guidelines etc. can apply when using these devices. The manufacturers' instructions shall be understood and followed as well.

A.2.4 Corona discharge

Corona discharge may function as a source for both negative and positive ions in the carrier gas. Either a single corona electrode operated with DC-high voltage (for ions of one polarity) or with AC-high voltage (for two ion polarities), or two separate corona electrodes (one for each ion polarity) can be used.

If an aerosol electrometer is used as a particle detector immediately downstream of the charge conditioner (without the DEMC), an ion trap may be necessary as an additional element to eliminate any remaining free ions from the charge-conditioned aerosol; otherwise an aerosol electrometer would measure these free ions as an additional current.

A.3 Charge conditioning

A.3.1 General

In order to calculate the particle size distribution from the measured electrical mobility distribution, a known particle size-dependent distribution of electrical charges shall be generated on the aerosol particles, described by the charge distribution function, $f_p(d)$. Charge conditioners upstream of a DEMC are used for this purpose.

In a gaseous medium containing aerosol particles and a sufficient concentration of unipolar ions or ions of both polarities, a charge distribution will develop on the particles. As the dominant driving forces are the random thermal diffusion of the ions and the collision between ions and aerosol particles the terms bipolar or unipolar diffusion charging are frequently used for these types of charge conditioning. The main advantage of diffusion charging over other methods is that it depends only weakly upon aerosol particle material (Davison and Gentry 1985)[77]. The following paragraphs describe the characteristics of bipolar and unipolar diffusion charging.

The particle concentration to be charged shall be limited in such a way that the depletion of ions due to ion attachment to the particles does not lead to significantly reduced charges on the particles. The particle charging efficiency depends mainly on the so-called $N_I \cdot t$ product, which is the concentration of either positive or negative ions, N_I, multiplied by their residence time, t, which is the interaction time of aerosol particles with the ions.

Inside a charge conditioner, spatial ion concentration and flow velocity profiles will develop. Therefore, the geometric design has a strong influence on the charging efficiency. In some charge conditioner designs the ion transport is deliberately influenced by AC- or DC- electric fields and sheath air flows.

Table A.1 gives an overview on charge conditioners.

Table A.1 — Overview on charge conditioners and selected references

Category	Type
Bipolar charge conditioners	Radioactive charge conditioner [a] [50]
	Soft-X-ray charge conditioner [80]
	Bipolar corona ionizer [81, 82]
	Surface-discharge microplasma aerosol charger (SMAC) [a] [83, 84]
Unipolar charge conditioners	Positive unipolar corona discharge charge conditioner
	Negative unipolar corona discharge charge conditioner
[a] Can also be applied for unipolar charge conditioning.	

A.3.2 Bipolar charge conditioners

Bipolar charge conditioners (also traditionally called aerosol neutralizers) produce ions of both polarities (i.e. positive and negative ions); they are most common in DMAS systems. Neutral particles can acquire charge while highly charged particles may discharge themselves by capturing ions of the opposite polarity. Bipolar charge conditioners differ by the way the ions are generated.

— Radioactive bipolar diffusion charge conditioners generate ions in the carrier gas by α- or β-radiation from a radioactive isotope.

— X-ray bipolar diffusion charge conditioners use soft-X-rays (<10 keV) for ion generation in the carrier gas.

In the above charge conditioner types, the ions are produced directly in the carrier gas and diffuse to the aerosol particles by Brownian motion.

— Bipolar corona ionizers (BCI) use an arrangement of two DC-Corona ionizer stages (one for each polarity). Ions of opposite charge are produced in separate sections and are subsequently mixed with the aerosol. In another variant bipolar ions are produced by AC-Corona discharging.

A.3.3 Unipolar charge conditioners

Corona charge conditioners applying field charging – in contrast to diffusion charging - are not considered for measurement purposes here because of their increased particle material dependence. Unipolar diffusion charge conditioners generate ions of only one polarity (i.e. positive or negative ions) by corona discharge. Corona discharge is produced by a strong nonuniform electrostatic field such as that between a needle and plate or a concentric thin wire and a tube. The electric field and space charge effects result in repulsion of ions of polarity opposite to that of the wire which may lead to positively or negatively charged particles. There are two designs for corona discharge charge conditioners:

— Negative corona discharge charge conditioner

  The discharge electrode is held at high negative potential. The free electrons are repelled from the electrode and may attach to air molecules to form negative ions. Ozone is generated as a by-product which makes this design not favourable for aerosol charging.

— Positive corona discharge charge conditioner

  In positive corona discharge charge conditioners, the discharge electrode (wire or tip) is held at high positive potential. In this case the free electrons from the corona discharge are attracted to the electrode and do not need to be absorbed. Most commercially available charge conditioners use positive ions due to the fact that the process is stable by controlling the corona current and the emission of ozone can be avoided.

Among the group of positive corona charge conditioners are indirect corona charge conditioners and turbulent jet charge conditioners. Indirect corona charge conditioners shield the particle charging zone from the corona discharging zone in order to reduce particle losses. A grounded electrode in the aerosol flow can be applied as a trap for excess ions. Turbulent jet charge conditioners completely separate the ion generation from the particle charging zone. This leaves the charging zone free of electrical fields and reduces particle losses to a minimum. Ions are transported into the particle charging zone by an additional flow, which dilutes the aerosol flow at the exit.

Other charge conditioning processes such as static electrification, photoionization, thermionic emission, self-charging of radioactive particles and agglomeration are not considered here because of their very restricted controllability and usability to charge conditioning in measuring devices. However, some of these processes have to be taken into account as disturbances.

All charge conditioners described have individual permissible upper particle concentration limits and particle size dependent charging efficiencies. Their respective charge distribution functions, $f_p(d)$, depend on ion concentrations, ion mass and ion mobility as well as on residence time and concentration of particles. Situational factors such as carrier gas composition, purity, humidity and temperature may also influence the performance. A charge conditioner manufacturer should provide the respective charge distribution function and describe the conditions under which the device performs in a predictable way and does not produce artefacts.

NOTE Unipolar charge conditioning is affected by the pre-charge (a/k/a primary charge) on the particles. Some unipolar chargers minimize this effect by a two-stage design, where the first charge conditioner stage operates at the opposite polarity.

A.4 Implementation of bipolar steady-state charging

A.4.1 General

If the aerosol interacts long enough with a sufficient concentration of bipolar ions in a gaseous medium a steady-state bipolar charge distribution will develop on the particles. By bipolar diffusion charging, particles less than 30 nm acquire at most one charge, which is a major requirement for application to the production of monodisperse nanoparticles; nonetheless, single charging efficiencies are rather low.

A.4.2 Charge distribution function of particles

Under the steady-state conditions in the case of bipolar charging, the charge distribution function $f_p(d)$ can be expressed as:

$$f_p(d) = \frac{N_p}{N} = \frac{\prod_{j=+1}^{p} \left(\frac{\beta_{j-1}^{+}}{\beta_j^{-}} \right)}{\Sigma}, \text{ if } p \geq +1 \tag{A.1}$$

$$f_p(d) = \frac{N_p}{N} = \frac{\prod_{j=-1}^{p} \left(\frac{\beta_{j+1}^{-}}{\beta_j^{+}} \right)}{\Sigma}, \text{ if } p \leq -1 \tag{A.2}$$

$$f_p(d) = \frac{N_0}{N} = \frac{1}{\Sigma}, \text{ if } p = 0 \tag{A.3}$$

where

$$\Sigma = \sum_{p=+1}^{+\infty} \left\{ \prod_{j=+1}^{p} \left(\beta_{j-1}^{+} \Big/ \beta_j^{-} \right) \right\} + \sum_{p=-1}^{-\infty} \left\{ \prod_{j=-1}^{p} \left(\beta_{j+1}^{-} \Big/ \beta_j^{+} \right) \right\} + 1$$

$f_p(d)$ is the charge distribution as a function of particle size d;

N is the number concentration of aerosol particles of size d;

N_p is the number concentration of charged particles of size d;

N_0 is the number concentration of uncharged particles of size d;

β is the ion-aerosol attachment coefficient of particles of size d;

p is the number of elementary units of charge.

From the above Formulae (A.1), (A.2), (A.3), if the ion-aerosol attachment coefficients β (combination charging constants) are known, the charge distribution function $f_p(d)$ can be calculated and may be used in Formula (5).

A.4.2.1 Ion-aerosol attachment coefficient – Fuchs' theory

Under the steady-state charging processes, there is a well-known theory describing the ion-aerosol attachment coefficients, β, which is the so-called Fuchs' attachment theory. β can be expressed as:

$$\beta_p^{\pm} = \frac{\pi \cdot c^{\pm} \cdot \alpha \cdot \delta^{\pm 2} \cdot \exp\left\{-\varphi\left(\delta^{\pm}\right)/kT\right\}}{1+\exp\left\{-\varphi\left(\delta^{\pm}\right)/kT\right\}\dfrac{c^{\pm} \cdot \alpha \cdot \delta^{\pm 2}}{4D^{\pm} \cdot a}\displaystyle\int_0^{a/\delta^{\pm}} \exp\{\varphi(a/x)/kT\}\,\mathrm{d}x} \tag{A.4}$$

where

$$x = a/r$$

$$\varphi(r) = \int_0^{\infty} \Theta(r) \cdot \mathrm{d}r = \frac{p \cdot e^2}{4\pi \cdot \varepsilon_0 \cdot r} - \frac{\varepsilon_1 - 1}{\varepsilon_1 + 1} \cdot \frac{e^2}{8\pi \cdot \varepsilon_0} \cdot \frac{a^3}{r^2\left(r^2 - a^2\right)}$$

$$\delta^{\pm} = \frac{a^3}{\lambda^{\pm 2}}\left\{\frac{1}{5}\left(1+\frac{\lambda^{\pm}}{a}\right)^5 - \frac{1}{3}\left(1+\frac{\lambda^{\pm 2}}{a^2}\right)\left(1+\frac{\lambda^{\pm}}{a}\right)^3 + \frac{2}{15}\left(1+\frac{\lambda^{\pm}}{a}\right)^{5/2}\right\}$$

$$\alpha = \left(\frac{a}{\delta^{\pm}}\right)^2$$

a is the aerosol particle radius ($d = 2a$);

r is the distance between the particle and the ion;

$c^{\pm}$ is the thermal velocity of positive or negative small ions;

α is called Fuchs' α parameter, corresponding to the square of the ratio of the particle radius to the limiting sphere;

$\delta^{\pm}$ is the radius of a sphere that divides the free molecular regime near the particle and the continuum regime far from the particle; this imaginary sphere is often called Fuchs' limiting sphere;

k is the Boltzmann constant;

T is the absolute temperature;

$D^{\pm}$ is the thermal diffusion coefficient of positive or negative small ions;

ε_0 is the dielectric constant;

ε_1 is the specific dielectric constant;

$\lambda^{\pm}$ is the mean free path of positive or negative small ions.

If the values of dynamic properties $c^{\pm}$, $D^{\pm}$, $\lambda^{\pm}$ of the small ion, and aerosol particle diameter $d = 2a$ are known, the ion-aerosol attachment coefficients, β, can be calculated.

NOTE Formula (A.4) for α is only valid when the charge is zero ($p = 0$). When the particle is charged ($p \neq 0$), the formula for α becomes rather complex, see Reference [19].

A.4.2.2 Properties of the ion

The values of dynamic properties $c^{\pm}$, $D^{\pm}$, $\lambda^{\pm}$ of small ions can be defined from fundamental gas kinetic theories.

The relationship between the diffusion coefficient and mobility was given by Einstein (1905)[17]; it can be expressed as:

$$D^{\pm} = kTZ^{\pm} / e \tag{A.5}$$

where $Z^{\pm}$ is the electrical mobility of small ions.

The thermal velocity of small ions was derived by Kennard (1938)[32]; it can be expressed as:

$$c^{\pm} = \sqrt{\frac{8k}{\pi \cdot m^{\pm}}} \tag{A.6}$$

where $m^{\pm}$ is the mass of a small ion.

There are several approximation methods for the mean free path of small ions. The representative example of these can respectively be expressed as:

$$\lambda^{\pm} = \frac{16\sqrt{2}}{3\pi} \cdot \frac{D^{\pm}}{c^{\pm}} \cdot \left(\frac{M}{M+m^{\pm}} \right)^{1/2} \tag{A.7}$$

described by Fuchs and Sutugin (1970) [21],

$$\lambda^{\pm} = \frac{32}{3\pi} \cdot \frac{D^{\pm}}{c^{\pm}} \cdot \left(\frac{M}{M+m^{\pm}} \right)^{1/2} \tag{A.8}$$

a first-order Chapman-Enskog approximation, explained by Bricard (1965) [8],

$$\lambda^{\pm} = \frac{1}{1+\sigma} \cdot \frac{16\sqrt{2}}{3\pi} \cdot \frac{D^{\pm}}{c^{\pm}} \cdot \left(\frac{M}{M+m^{\pm}} \right)^{1/2} \tag{A.9}$$

described by Pui (1976) [44], Pui et al. (1988) [45], and Hoppel et al. (1986) [28],

where

M is the average molecular mass of air;

σ is a correction factor: $\sigma = 0{,}132$.

If the ion properties $Z^{\pm}$ and $m^{\pm}$ are known, the charge distribution function, $f_p(d)$, can be calculated. The values of several ion properties are shown in Table A.2.

Table A.2 — Values of ion properties used by various authors

Mobility of ion		Mass of ion		Author and reference
Z^+ ($\times 10^{-4}$ m^2 V^{-1} s^{-1})	Z^- ($\times 10^{-4}$ m^2 V^{-1} s^{-1})	m^+ (amu)	m^- (amu)	
1,15	1,425	290	140	Reischl et al. (1996)
1,40	1,90	109	50	Adachi et al. (1985)
1,40	1,90	130	100	Adachi et al. (1985)
1,15	1,39	140	101	Porstendörfer et al. (1983)
1,20	1,35	150	90	Hoppel and Frick (1986)
1,15	1,39	140	101	Hussin et al. (1983)
1,35	1,60	148	130	Wiedensohler et al. (1986)
1,33	1,84	200	100	Hoppel and Frick (1990)
1,40	1,60	140	101	Wiedensohler and Fissan (1991)

A.4.2.3 Approximation of the bipolar charge distribution for aerosol particles

As described in above subclauses, an expert user of DMAS should be able to calculate the charge distribution function, $f_p(d)$. However, those calculation methods are long and complicated. Therefore, an empirical expression to approximate the charge distribution function, $f_p(d)$, in the size range from 1 nm to 1 000 nm is presented in this subclause. This approximation permits a useful and rapid calculation of the bipolar charge distribution function.

Situational factors such as carrier gas composition, purity, humidity and temperature may limit the validity of the approximation.

For an aerosol particle carrying up to two elementary charges, in steady-state charge conditions, the charge distribution function, $f_p(d)$ can be expressed using the approximation given in Formula (A.10), derived from the Fuchs model.

$$\log\left[f_p(d)\right] = \sum_{i=0}^{5} a_i(p) \cdot (\log d)^i \tag{A.10}$$

Formula (A.10) is valid for the size range:

1 nm ≤ d ≤ 1 000 nm for p = {-2,-1,0,+1,+2}.

NOTE 1 In Formula (A.10), d is given in nanometres.

To develop this approximation, specific values of ion properties are taken, and their sources are

a) ion mobilities from Wiedensohler et al. (1986, 1988) [52, 50] (see Table A.2).

b) ion masses from Hussin et al. (1983) [30], (see Table A.2).

c) the Fuchs' α parameters from Hoppel and Frick (1986) [28].

The coefficients $a_i(p)$ were derived for a charge conditioner with a radioactive ion source (^{210}Po) and air as carrier gas (at ambient conditions) using a least–square regression analysis; they are listed in Table A.3.

Corrections for other carrier gas conditions are described e.g. in Wiedensohler et al. (1986) [52], data for other gas compositions can be found in Wiedensohler and Fissan (1991) [51].

The charge distribution function, $f_p(d)$, with three or more elementary charge units can be calculated using the following Formula (A.11), which is based on Gunn's model:

$$f_p(d) = \frac{e}{\sqrt{4\pi^2 \varepsilon_0 dkT}} \cdot \exp \frac{-\left[p - \frac{2\pi\varepsilon_0 dkT}{e^2} \cdot \ln\left(\frac{N_1^+}{N_1^-} \cdot \frac{Z^+}{Z^-}\right)\right]^2}{2\frac{2\pi\varepsilon_0 dkT}{e^2}} \tag{A.11}$$

where $N_1^{\pm}$ is the concentration of positive or negative small ions.

For this calculation, the concentration of positive and negative ions is assumed to be equal, and the ratio of ion mobilities Z^+/Z^- was taken from Wiedensohler et al. (1986) to be 0,875. The results of this calculation are given in Figure A.1 and in Table 3.

Table A.3 — Coefficients $a_i(p)$ for Formula (A.10) for radioactive ion sources

i	$a_i(p)$				
	p = −2	p = −1	p = 0	p = +1	p = +2
0	−26,332 8	−2,319 7	−0,000 3	−2,348 4	−44,475 6
1	35,904 4	0,617 5	−0,101 4	0,604 4	79,377 2

Table A.3 *(continued)*

i	$a_i(p)$				
	$p = -2$	$p = -1$	$p = 0$	$p = +1$	$p = +2$
2	−21,460 8	0,620 1	0,307 3	0,480 0	−62,890 0
3	7,086 7	−0,110 5	−0,337 2	0,001 3	26,449 2
4	−1,308 8	−0,126 0	0,102 3	−0,155 3	−5,748 0
5	0,105 1	0,029 7	−0,010 5	0,032 0	0,504 9

NOTE 2 Two coefficients in Wiedensohler (1988) were later corrected. The coefficients in Table A.3 contain this correction.

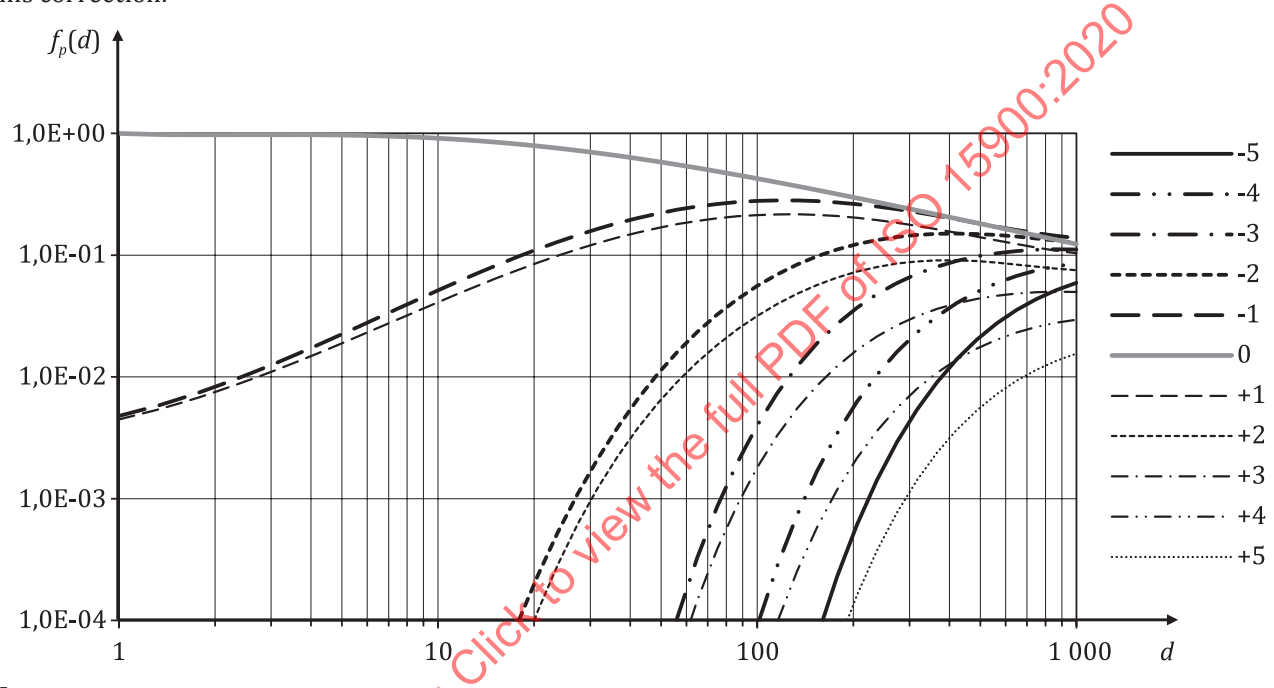

Key

d particle diameter, expressed in nanometres

$f_p(d)$ charge distribution function [-]

Figure A.1 — Charge distribution function for particles in the size range between 1 nm and 1 000 nm calculated from Formulae (A.10) and (A.11) for a bipolar radioactive ion source

While the coefficients in Table A.3 apply for bipolar charge conditioners with radioactive ion sources, they cannot be adapted for other types of bipolar charge conditioners. The empirical coefficients for such other designs of bipolar charge conditioners have to be determined individually for each device design. For example, Tigges et al. (2015) [65] describe a different set of empirical coefficients $a_i(p)$ which apply for two types of charge conditioner with a soft X-ray source with an X-ray tube voltage of 9,5 kV, see Table A.4.

Table A.4 — Coefficients $a_i(p)$ for Formula (A.10) for a bipolar charge conditioner with a 9,5 kV X-ray ion source, Tigges et al. (2015) [65]

i	$a_i(p)$				
	$p = -2$	$p = -1$	$p = 0$	$p = +1$	$p = +2$
0	−30,615 58	−2,335 09	0,001 63	−2,358 89	−27,253 20
1	46,338 85	0,436 35	−0,113 84	0,451 69	38,479 63
2	−31,181 91	1,086 54	0,333 93	0,997 98	−24,271 28

Table A.4 *(continued)*

i	$a_i(p)$				
	$p = -2$	$p = -1$	$p = 0$	$p = +1$	$p = +2$
3	11,390 70	−0,556 79	−0,357 14	−0,481 73	8,441 62
4	−2,220 28	0,049 81	0,107 70	0,026 31	−1,605 89
5	0,179 35	0,005 51	−0,010 82	0,008 04	0,129 17

Analogue to Table 3, Table A.5 shows example data for the approximated charge distribution function. In accordance with the recommendation in Reference [65], ion mobilities used for the calculation of charge levels beyond $p = \pm 2$ [Formula (A.11)] were 1,4 $cm^2/(V{\cdot}s)$ for negative and 1,34 $cm^2/(V{\cdot}s)$ for positive ions, respectively, while the ion concentrations of positive and negative ions were again assumed to be equal.

Table A.5 — Bipolar charge distribution function $f_p(d)$ for spherical particles in air (ambient conditions), produced by an X-ray charge conditioner with a tube voltage of 9,5 kV (from Formulae (A.10) and (A.11) with approximation coefficients from Table A.4)

d **(nm)**	**Charge distribution function**												
	−6	−5	−4	−3	−2	−1	0	+1	+2	+3	+4	+5	+6
1	0	0	0	0	0	0,004 6	1,003 8	0,004 4	0	0	0	0	0
2	0	0	0	0	0	0,007 6	0,974 4	0,007 2	0	0	0	0	0
5	0	0	0	0	0	0,021 1	0,970 8	0,019 4	0	0	0	0	0
10	0	0	0	0	0	0,048 6	0,915 1	0,044 0	0	0	0	0	0
20	0	0	0	0	0,000 2	0,102 1	0,795 2	0,091 7	0,000 2	0	0	0	0
50	0	0	0	0	0,010 2	0,201 8	0,581 9	0,181 9	0,008 1	0	0	0	0
100	0	0	0,000 1	0,002 9	0,047 3	0,252 8	0,426 1	0,229 5	0,039 2	0,002 2	0	0	0
200	0	0,000 3	0,003 7	0,026 4	0,103 3	0,245 6	0,300 5	0,224 7	0,086 9	0,020 3	0,002 6	0,000 2	0
500	0,004 1	0,013 7	0,036 5	0,077 5	0,133 8	0,174 9	0,186 5	0,160 9	0,112 6	0,059 6	0,025 7	0,008 8	0,002 4
1 000	0,022 3	0,040 0	0,063 9	0,091 2	0,112 7	0,123 9	0,131 0	0,113 8	0,095 3	0,070 1	0,045 0	0,025 8	0,013 2

The approximation for the charge conditioner with a 9,5 kV X-ray ion source shows that – compared to the bipolar charge conditioner with a radioactive ion source - a more symmetrical charge distribution is produced, see Figure A.2.

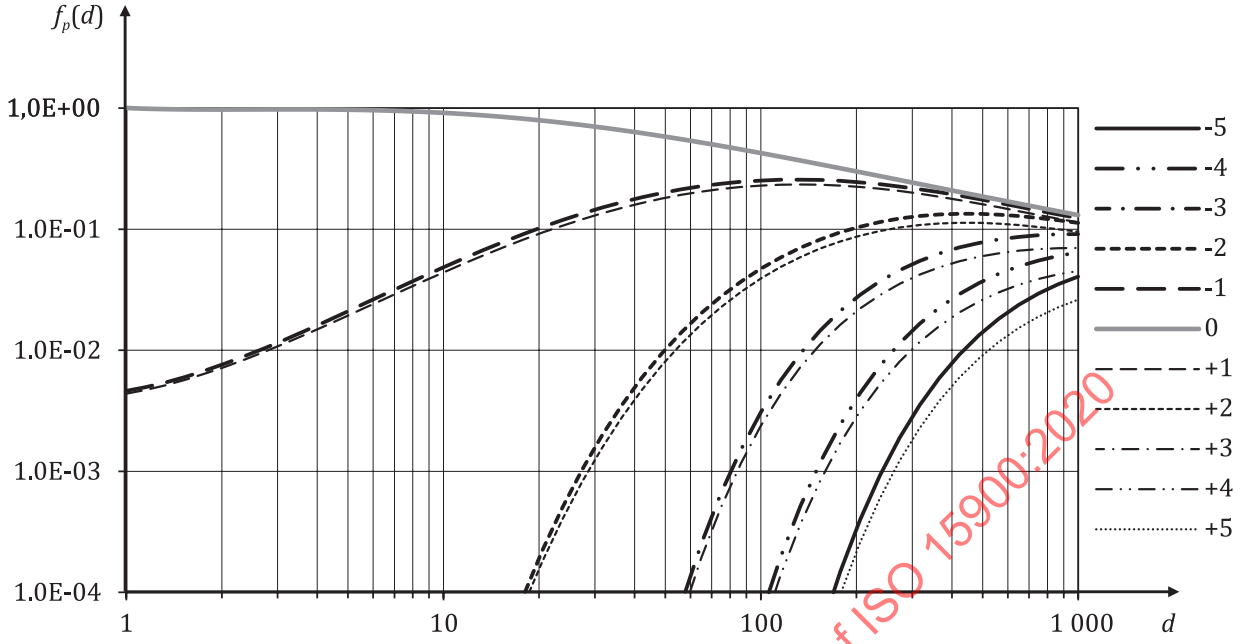

Key

d particle diameter, expressed in nanometres

$f_p(d)$ charge distribution function [-]

Figure A.2 — Charge distribution function for particles in the size range between 1 nm and 1 000 nm calculated from Formulae (A.10) and (A.11) for a bipolar 9,5 kV X-ray ion source

A.5 Implementation of unipolar charge conditioning

Besides the widely used bipolar steady-state charge distribution, unipolar charging can also be used to achieve a defined charge distribution in a DMAS. In a unipolar charge conditioner, ions of either positive or negative polarity are produced by a corona discharge process. Like in bipolar charging, diffusion charging is advantageous because variations caused by the composition of the particles can be neglected for diffusion charging.

Unipolar charging can achieve higher charging probabilities than bipolar charging. This is an advantage if small particles (d < 20 nm) are to be measured. Due to the higher charging probability, more particles are classified by the DEMC and reach the particle detector. This leads to better counting statistics. On the other hand, larger particles (d > 100 nm) carry significantly more multiple charges compared to bipolar charging. This makes the data inversion more complex and reduces the size resolution of large particles. A variety of unipolar charge conditioners for aerosol particles have been described and built; see, for example, Hewitt (1957), Medved et al. (2000), Büscher et al. (1994), Chen and Pui (1999) and Pui et al. (1988).

If corona discharge methods are used to achieve a defined unipolar charge distribution in the sample aerosol flow of a DMAS, the instrument manufacturer and the user shall, by design or by measurement, ensure that the method performs correctly and does not produce artefact particles. The particle concentration to be charged shall be limited in such a way that the depletion of the ion concentration due to ion attachment to the particles does not lead to significantly reduced charges on the particles.

The charging of particles in unipolar corona charge conditioners is very much dependent on individual designs and operating parameters. Therefore, no general approximation for the charge distribution function can be given for the variety of unipolar charge conditioners.

Annex B
(informative)

Particle detectors

B.1 General

It is necessary to select an appropriate particle detector to measure particle concentration downstream of the DEMC. For this purpose, a condensation particle counter (CPC) or a Faraday cup aerosol electrometer (FCAE) is generally used. These detectors are described in this annex.

B.2 Condensation particle counter

B.2.1 General

Aerosol particles entering the CPC are first exposed to an atmosphere containing condensable saturated vapour. Next, a supersaturated condition is generated, causing vapour to condense on the particles, growing the particles into droplets that can be detected by means of light scattered from a light beam.

Typically, a CPC has almost 100 % counting efficiency over a wide range of particle sizes larger than a defined minimum particle size. The counting efficiency decreases to zero at the minimum detectable particle size. To measure the particle size distribution using a CPC, it is necessary to correct the counting efficiency for particles in the size range in which a CPC has less than 100 % counting efficiency.

A CPC usually needs to cover a particle concentration range up to 10^4 or 10^5 particles per cubic centimetre. Because the droplet diameter in the detection zone of a CPC is usually several micrometres and the signal-to-noise ratio for single-droplet-counting is relatively high, a CPC is a reliable method to detect low concentration aerosols. The maximum concentration for single-droplet-counting is limited by the optical design of the instrument and is usually in the range of 10^3 to 10^5 particles per cubic centimetre. If the particle concentration exceeds the upper limit of the specified concentration range of the CPC, particle coincidence becomes significant and the reported concentration will be incorrect.

To measure higher concentrations, some CPCs include a photometric detection method that detects the intensity of the light scattered from all the particles in the sensing zone of the instrument at any given time. A CPC with photometric concentration measurement shall be calibrated periodically to ensure accurate measurements.

Before using the CPC, the user shall confirm that:

a) the flow rate into the CPC is correct. (The flow rate directly influences the particle concentration indicated by a CPC.)

b) there is sufficient working liquid in the CPC reservoir. (If sufficient working liquid is not present or if the working liquid contains too many impurities, condensation of the working liquid on the particle will be inhibited. The result will be an incorrect indication of particle concentration.)

B.2.2 Calibration

For calibration of a CPC, refer to ISO 27891. ISO 27891 describes methods to determine the detection efficiency of a CPC, together with the associated measurement uncertainty, by comparison with a reference instrument which has a reputable calibration certificate, either an FCAE or a reference CPC, under a condition specified by particle number concentration, particle size, and particle composition. Figure B.1 shows the schematic calibration setup.

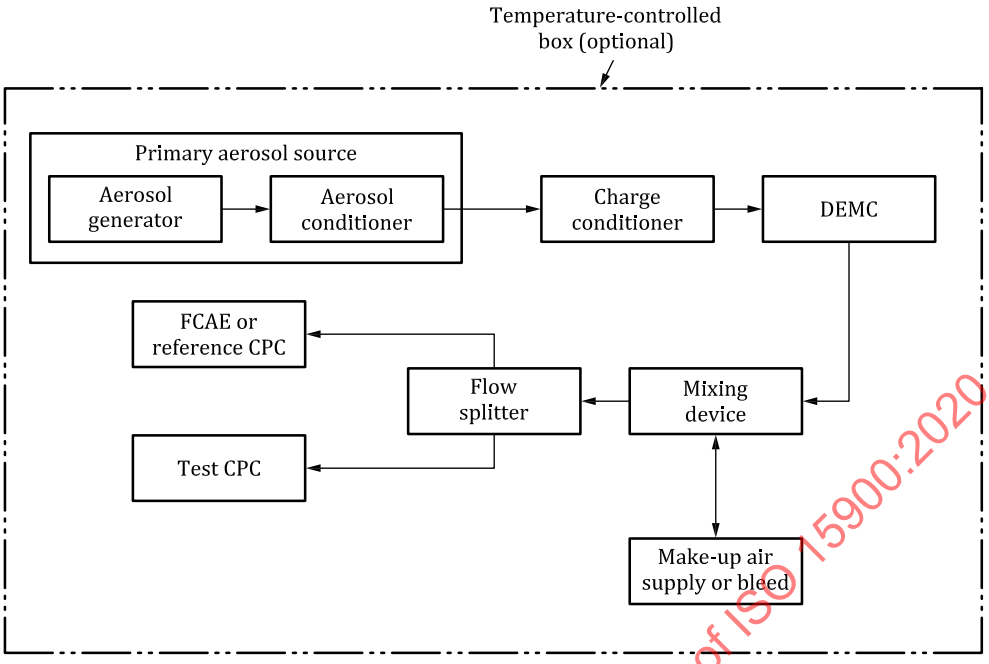

Figure B.1 — Schematic calibration setup (see ISO 27891)

Calibration should be performed for a range of particle sizes and number concentrations, such that the operating range of the DMAS is covered.

B.3 Faraday cup aerosol electrometer

B.3.1 General

An FCAE is a detector of the electrical current resulting from the collection of ions and charged particles in the sample flow. An FCAE is intended to operate in the pressure range between a few atmospheres and high vacuum. An FCAE captures both positive and negative electrical charges and reports the net charge. An FCAE measures the very low electrical current after the charge is released from the particles as they come in contact with conducting parts of the FCAE. When an FCAE is used as an aerosol detector with a DEMC, it shall be designed to allow the gas to permeate through the filter and to fully capture the charged particles. Therefore, it is necessary for an FCAE to have a filter portion inside a cup-shaped housing to efficiently capture the electrical charges. It is not necessary for the filter to be made from conducting material, since space charge on the collected particles will force the electrical current to the conducting surfaces of the Faraday cup that surrounds the filter.

An FCAE is usually suited for the measurement of a charged particle number concentration in the range from 10^4 to 10^8 particles per cubic centimetre. If the electrical charging is based on equilibrium charging, the number concentration of the total (namely, positive, negative and neutral) fine particles in the actual sample gas is typically one to three orders-of-magnitude higher than the number concentration of the (positively or negatively) charged particles measured downstream of a DEMC, depending on the method of charging and the size distribution of the particles. Since the charging efficiency of fine particles depends on particle size, it is necessary to consider in advance whether the relevant sample particle number concentration is within the range of FCAE measurement. If measurements at a lower particle number concentration are necessary, one should consider use of a CPC detector as described in B.2.

While an FCAE being used as a detector with a DEMC is usually operated at or near atmospheric pressure, an FCAE may also be operated at low pressures, in an extreme case, as low as 200 Pa to 930 Pa. For low pressure operation, a special design is needed to reduce aerodynamic resistance.

B.3.2 Structure and detection mechanism of FCAE

Figure B.2 shows a typical FCAE structure. When sample gas containing charged fine particles enters the inlet tube to the FCAE, the gas flows through the filter and the particles are collected on the filter. The filter is normally surrounded by a porous metallic housing, converting the filter into an ion collector. The charge on the fine particles is then released from the particles and forced by space charge within the filter material to the surrounding metal housing.

The electrical current thus formed is very minute, usually measured in units of femtoamperes. The current from the filter passes into an electrometer and is amplified. The amplified current is proportional to the particle number concentration, the average number of electrical charges per particle and the sample flow rate of the charged aerosol entering the FCAE.

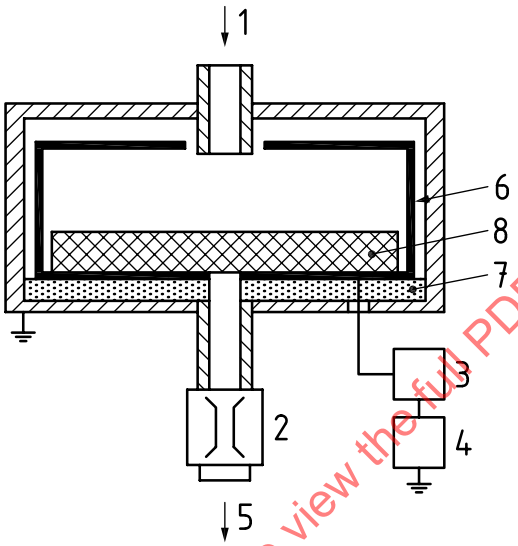

Key

1 charged particles
2 flow meter
3 preamplifier
4 electrometer
5 filtered air
6 faraday cup to collect charge from deposited particles and to reduce externally-induced electro-magnetic noise
7 very high resistance electrical insulator to isolate the filter (8) from electrical ground
8 high-efficiency particulate air (HEPA) filter to trap airborne particles

Figure B.2 — Schematic diagram of Faraday cup aerosol electrometer (FCAE); SOURCE: ISO 27891

B.3.3 Calibration

Both the current measuring device within the FCAE and its flow rate should be calibrated, although this does not provide a check of any losses within the FCAE. The current measurement should be calibrated either with a traceable femtoamp source, or by the relevant traceable calibration of the FCAE feedback resistor and the amplifier gain. The flowmeter used to measure the sample flow rate through the FCAE should be traceably calibrated.

In principle, the FCAE should be calibrated for measurements of electric charge per unit volume (typical units fC/cm^3) over the range of particle size and number concentration that will be used. The method will be very similar to the one for calibrating a CPC against a reference FCAE set out in ISO 27891. The reference FCAE should be one with an up-to-date reputable calibration certificate produced by a laboratory accredited to ISO/IEC 17025 or an equivalent standard, where the type and range of

calibration is within the laboratory's accredited scope, or a metrology institute that offers the relevant calibration service and whose measurements fulfil the requirements of ISO/IEC 17025. In this way the FCAE will be calibrated traceably to international standards.

The FCAE calibration should be carried out at least annually.

Annex C
(informative)

Slip correction factor

C.1 General

The electrical mobility of a particle depends on the particle size and the number of elementary charges. A unique relationship between electrical mobility and particle size is described in 5.2. The theoretical expression for the drag force on a spherical particle moving with low Reynolds number in a gas phase is customarily written by multiplying the Stokes' law expression by a slip correction factor of the form given in Formula (2), repeated here as Formula (C.1), as introduced by Knudsen and Weber (1911).

$$S_C = 1 + Kn\left[A + B\exp\left(-\frac{C}{Kn}\right)\right] \tag{C.1}$$

where

$Kn = \frac{2\lambda}{d}$ is the particle Knudsen number;

λ is the mean free path of gas molecule;

d is the spherical particle diameter;

A, B and C are empirical constants;

S_C is the slip correction.

The goal of this annex is to provide further detail on the source of the recommended parameters for the slip correction factor given in Table C.1.

C.2 Historical investigation of the slip correction factor

First experiments were performed by Millikan between 1909 and 1923 (Millikan 1910 [40], 1923 [41]). His last experiment extended the measurements up to Kn ~134 and visually fitted his data using the form of Formula (C.1). Millikan used the well-known apparatus called "Millikan's oil droplet apparatus" or "Millikan's cell apparatus". He obtained values of A = 0,864 and $A + B$ = 1,154. He found that the value C = 1,25 fitted his data from Kn = 0,25 to 134. The earliest values for A, B and C were determined by Knudsen and Weber (1911) [34] from the damping of torsional oscillation of a pair of glass spheres suspended in a vessel at low pressures; they obtained the values of 0,772, 0,40 and 1,63, respectively. Several authors have used Millikan's values for A, B and C and have modified them using different values of the molecular mean free path, λ. Fuchs recalculated a value of λ = 65,3 nm and modified Millikan's values to A = 1,246, B = 0,42 and C = 0,87 (Fuchs, 1964) [20]. This set of values is probably the most widely used to correct Stokes' law.

Allen and Raabe (1982) [5] reviewed and re-evaluated Millikan's data using up-to-date values of the relevant physical constants and nonlinear least-squares function fitting to make new estimates of the three slip correction parameters: A = 1,155, B = 0,471 and C = 0,596. Also, they made slip correction measurements on solid spherical particles in air using Millikan's cell apparatus, and they obtained A = 1,142, B = 0,558 and C = 0,999 (Allen and Raabe, 1985 [6]). They took the value of the mean free path, λ, of air molecules at T_0 = 296,15 K and P = 760 mmHg to be 6,73 × 10^{-8} m. The mean free path for other temperatures T and pressures P was calculated using Formula (4).

They made a choice for the value $\mu_{gas,0}$ = 1,8324 × 10^{-5} kg m^{-1} s^{-1} for the viscosity of dry air at T_0 = 296,15 K. The values of μ_{gas} for other temperatures were calculated using Formula (3).

The data from Millikan's cell experiments consist of a set of time intervals required for test particles to move vertically between two scale marks as determined visually by the operator. Millikan's cell method requires independent knowledge of the particle mass density, the absence of thermal air currents in the test cell, and detailed knowledge of the electric field in the test cell. For this reason, Hutchins, Harper and Felder (1995)[31] have measured slip correction factors for spherical solid particles in air with an automated apparatus using a new approach which requires none of Millikan's cell conditions. They emphasized that the new method was an application of the modulated dynamic light scattering method, which is fundamentally different from Millikan's cell, and that drag forces on spherical polystyrene latex particles were measured in dry air. In this method, the data are time autocorrelation functions of the intensity of light scattered by single particles from the intersection volume of two coherent laser beams.

This experiment provided detailed information about test particle Brownian motion, including the value of the particle diffusion coefficient. Each test was made on 72 solid spherical particles with diameters ranging from 1,0 µm to 2,2 µm, at air pressures ranging from 760 mmHg to 0,2 mmHg. Collected data provided 1 586 distinct experimental values of the slip correction factor with *Kn* ranging from 0,06 to 500. Analysis of these data gave the values A = 1,231 0 ± 0,002 2, B = 0,469 5 ± 0,003 7 and C = 1,178 3 ± 0,009 1 using the same formulae of Allen and Raabe's analysis, where the mean free path of air molecules and the viscosity of dry air were taken to be 6,73 × 10^{-8} m and 1,832 5 × 10^{-5} kg m^{-1} s^{-1}, respectively, at 760 mmHg and T_0 = 296,15 K. When they compared the results for the drag force ratio of solid and liquid particles, they indicated that the results from kinetic theory and from Allen and Raabe's re-evaluation of Millikan's data agree closely, and the results for solid particles from their work agree closely with Allen and Raabe's results for solid particles, but the kinetic theory and the drag force ratio values of oil droplets fall below those for solid particles over the range *Kn* = 0,09 to 18, with differences as great as 8 %.

The most recent work was published by Kim et al. (2005)[33]. Based on the viscosity and mean free path of air molecules chosen by Allen and Raabe, they measured slip corrections using certified polystyrene latex (PSL) particles of precisely known size and a DEMC. The measurements covered a wide range of sizes (19,9 nm to 269 nm), pressures (98,5 kPa to 8,27 kPa) and Knudsen numbers (0,5 to 83). A detailed uncertainty analysis showed approximation uncertainties (95 % confidence interval) smaller than 3 % for the whole data set.

Table C.1 summarizes three sets of coefficients derived from a choice (see References [6], [31] and [33]) of measurements of slip correction parameters.

Table C.1 — Excerpt from published values of slip correction factors for Stokes' law

Author	Mean free path λ (µm)	A	B	C	$A + B$	Comments
Allen and Raabe (1985)	0,067 3	1,142	0,558	0,999	1,700	for solid particles
Hutchins, et al. (1995)	0,067 3	1,231 0	0,469 5	1,178 3	1,700 5	for solid particles
Kim, Mulholland, Kukuck and Pui (2005)	0,067 3	1,165	0,483	0,997	1,648	Measured with NIST certified PSL particles

C.3 Recommended coefficients for the slip correction factor

In the above description, there is strong evidence that the results of Hutchins, Harper and Felder (1995) [31] of drag force ratio for solid particles closely agree with the results of Allen and Raabe (1985)[6] for solid particles and that the results for the drag force ratio from kinetic theory agree closely with Allen and Raabe's results from re-evaluation of Millikan's oil droplet data. However, the solid particle results differ from the kinetic theory and oil droplet results by up to 8 % in the Knudsen number range of 0,09 to 18.

Considering the traceability of the experiments, this document recommends the use of the coefficients determined by Kim et al. (2005)[33] for particle size distribution measurements (as given in 5.2).

Figure C.1 shows a comparison between the slip correction calculated with the coefficients by Hutchins, Harper and Felder (1995), Allen and Raabe (1985) and Kim et al. (2005). As can be seen, the relative difference of the first two calculations to the calculation with the recommended coefficients is within +3 % and −1 % over a particle diameter range from 1 nm to 10 µm.

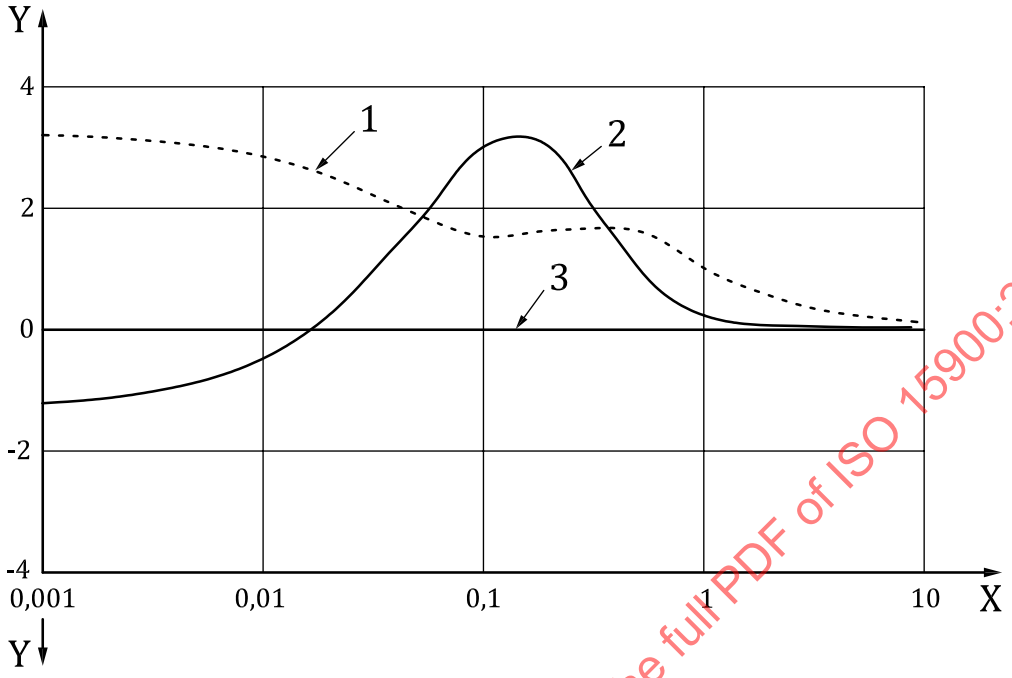

Key

X particle diameter (µm)
Y relative difference (%)
1 Hutchins et al. (1995)
2 Allen and Raabe (1985)
3 Kim et al. (2005)

Figure C.1 — Slip correction and relative difference for coefficients from Hutchins et al. (1995) and Allen and Raabe (1985) compared to Kim et al. (2005)

Annex D
(informative)

Data inversion

D.1 General

When a cylindrical DEMC is operated at high resolution, the following simplifications can be applied to solve Formula (5) for the size distribution function $n(d)$: The basis of the isosceles triangle which covers non-zero values of the DEMC transfer function Ω is small. Hence, for a given central electrical mobility Z^* of the DEMC, which is set by the voltage U^*, the diameters of transmitted particles do not deviate much from d_p^* which is the diameter of particles of charge p with electrical mobility equal to Z^*. Hence, the functions $n(d)$, $f_p(d)$ and $W(d, p)$ can then be replaced by their respective constant values at d_p^* and taken out of the integral as constants:

$$R(U^*)=N_3^*=q_2\sum_{p=1}^{\infty}n(d_p^*)\cdot P(d_p^*)\cdot f_p(d_p^*)\cdot W(d_p^*,p)\int_{d=0}^{\infty}\Omega(Z(d,p),\Delta\Phi(U^*))\mathrm{d}d \tag{D.1}$$

Following the nomenclature in Annex E, N_3^* is the number concentration displayed by the CPC. Further explanation on Z^* is given in 5.4 and Annex E. The detector response W does not depend on the number of elementary charges, p, when a CPC is used as detector.

NOTE 1 When a DMAS measures the size distribution of monodisperse or quasi-monodisperse particles and the above approximation method is used in data inversion, the obtained distribution is broader than the actual distribution [56].

There are several data inversion methods to solve Formula (D.1) while deconvoluting with respect to charge number p. Representative methods were e.g. described by Hoppel (1978) [27] and Knutson (1976) [35].

The integral in Formula (D.1) can be further converted to a function of Z:

$$\int_{d=0}^{\infty}\Omega\left[Z(d,p),\Delta\Phi(U^*)\right]\mathrm{d}d=(\mathrm{d}d/\mathrm{d}Z)_{d_p^*}\int_{Z=\infty}^{0}\Omega(Z,Z^*)\mathrm{d}Z \tag{D.2}$$

For a DMAS with recirculation of the excess flow q_4 into the sheath flow q_1, the differential term in Formula (D.2), $(\mathrm{d}d/\mathrm{d}Z)_{d_p^*}$, can be derived from Figure D.1 which shows the transfer function Ω in the mobility interval around Z^* and the function $d_p(Z)$ describing the corresponding diameters of transmitted particles in this mobility interval, i.e.

$$\left(\frac{dd}{dZ}\right)_{d_p^*}=\left(\frac{d_p(Z^*+\Delta Z^*)-d_p(Z^*-\Delta Z^*)}{Z^*+\Delta Z^*-(Z^*-\Delta Z^*)}\right)=\frac{\Delta d_p^*}{2\Delta Z^*} \tag{D.3}$$

NOTE 2 In Figure D.1, ΔZ^* is the half-width of the transfer function Ω, while Δd_p^* describes the diameter interval that corresponds to the mobility interval of $2\Delta Z^*$.

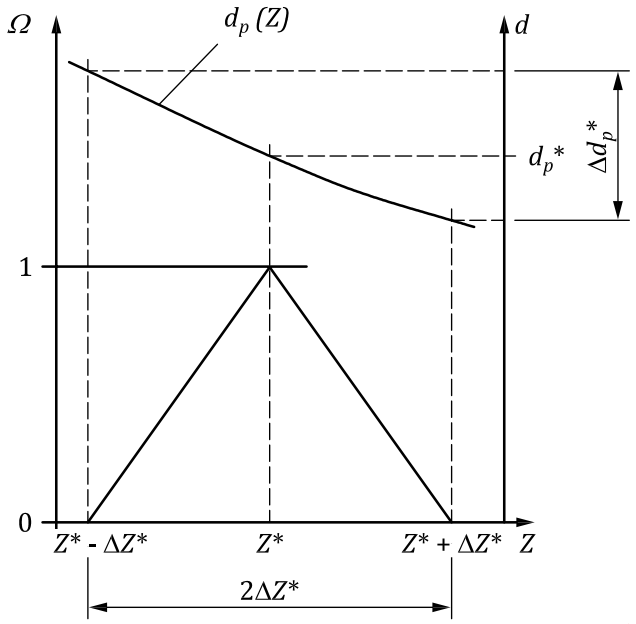

Figure D.1 — Particle diameter, d_p, and transfer function, Ω, in a small mobility interval around Z^*

The integral term in Formula (D.2), $\int_{Z=\infty}^{0} \Omega\left(Z,Z^*\right)\mathrm{d}Z$, corresponds to the area under the transfer function, which has the shape of an isosceles triangle as shown in Figure D.1 when $q_4 = q_1$ is fulfilled. Hence,

$$\int_{Z=\infty}^{0} \Omega\left(Z,Z^*\right)\mathrm{d}Z = \Delta Z^* \tag{D.4}$$

With Formulae (D.3) and (D.4), Formula (D.2) becomes

$$\int_{d=0}^{\infty} \Omega\left[Z(d,p),\Delta\Phi\left(U^*\right)\right]\mathrm{d}d = (\mathrm{d}d/\mathrm{d}Z)_{d_p^*} \int_{Z=\infty}^{0} \Omega\left(Z,Z^*\right)\mathrm{d}Z = \frac{\Delta d_p^*}{2\Delta Z^*}\cdot\Delta Z^* = \frac{\Delta d_p^*}{2} \tag{D.5}$$

The detector response, $W\left(d_p^*,p\right)$, can be converted to

$$W\left(d_p^*,p\right) = \frac{\eta_{\mathrm{CPC}}\left(d_p^*\right)}{q_{\mathrm{CPC}}} = \frac{\eta_{\mathrm{CPC}}\left(d_p^*\right)}{q_3} = \frac{\eta_{\mathrm{CPC}}\left(d_p^*\right)}{q_2} \tag{D.6}$$

assuming that the detection flow of the CPC, q_{CPC}, is equal to the mobility selected aerosol flow of the DEMC, q_3 (i.e. the CPC dilution factor is 1) and that $q_3 = q_2$ since $q_4 = q_1$ for a recirculating DMAS.

With Formulae (D.5) and (D.6), Formula (D.1) can be converted to

$$N_3^* = \frac{1}{2}\sum_{p=1}^{\infty} n\left(d_p^*\right)\cdot P\left(d_p^*\right)\cdot f_p\left(d_p^*\right)\cdot \eta_{\mathrm{CPC}}\left(d_p^*\right)\cdot \Delta d_p^* \tag{D.7}$$

The product of $n\left(d_p^*\right)$ and Δd_p^* gives the number concentration of the particles entering the DEMC in the diameter interval Δd_p^*, i.e.

$$\Delta N_2\left(d_p^*\right) = n\left(d_p^*\right)\cdot \Delta d_p^* \tag{D.8}$$

With $\Delta N_2\left(d_p^*\right)$, Formula (D.7) can be converted to

$$N_3^* = \frac{1}{2}\sum_{p=1}^{\infty} P\left(d_p^*\right)\cdot f_p\left(d_p^*\right)\cdot \eta_{\mathrm{CPC}}\left(d_p^*\right)\cdot \Delta N_2\left(d_p^*\right) \tag{D.9}$$

The term $\frac{1}{2}P\left(d_p^*\right)\cdot f_p\left(d_p^*\right)\cdot \eta_{\mathrm{CPC}}\left(d_p^*\right)\cdot \Delta N_2\left(d_p^*\right)$ for $p > 1$ expresses the contribution of multiply charged particles to N_3^*.

For measurement of polydisperse aerosols in the size range of the DEMC, N_3^* is often dominated by the contribution of singly charged particles. When the contribution of multiply charged particles to N_3^* is negligible, Formula (D.9) is simplified to

$$N_3^* = \frac{1}{2}P\left(d_{p=1}^*\right)\cdot f_{p=+1}\left(d_{p=1}^*\right)\cdot \eta_{\mathrm{CPC}}\left(d_{p=1}^*\right)\cdot \Delta N_2\left(d_{p=1}^*\right) \tag{D.10}$$

From Formula (D.10), the particle concentration in the diameter interval Δd_p^* in the sample inlet flow q_2 assuming only singly charged particles, $\Delta N_{2,\mathrm{OSC}}\left(d_{p=1}^*\right)$, can be derived as

$$\Delta N_{2,\mathrm{OSC}}\left(d_{p=1}^*\right) = \frac{2N_3^*}{P\left(d_{p=1}^*\right)\cdot f_{p=1}\left(d_{p=1}^*\right)\cdot \eta_{\mathrm{CPC}}\left(d_{p=1}^*\right)} \tag{D.11}$$

This approximation with the assumption of only singly charged particles allows simple calculation of particle size distribution function n. An example calculation with the assumption of only singly charged particles using Formula (D.11) is given in D.2.4.

When there are multiply charged particles in, N_3^* however, the number concentration calculated with the assumption of only singly charged particles, $\Delta N_{2,\mathrm{OSC}}\left(d_{p=1}^*\right)$ overestimates the actual concentration, $\Delta N_2\left(d_{p=1}^*\right)$ since the terms $\frac{1}{2}P\left(d_p^*\right)\cdot f_p\left(d_p^*\right)\cdot \eta_{\mathrm{CPC}}\left(d_p^*\right)\cdot \Delta N_2\left(d_p^*\right)$ for $p > 1$ in Formula (D.9) are neglected in Formula (D.11). An example calculation to rectify this overestimation is given in D.2.5.

D.2 Step-by-step DMAS calculation example

D.2.1 General

This subclause demonstrates the data acquisition and inversion for a DMAS with a cylindrical DEMC with closed, recirculating excess and sheath flow system ($q_2 = q_3$ and $q_1 = q_4$) and with a CPC as particle detector. For such a DMAS, it is assumed that the isosceles triangular transfer function with $\Delta Z/Z = q_2/q_1 = \beta_{\mathrm{DEMC}}$ (constant) may be applied [see Formula (E.9)].

The example given in this annex is for a measurement in stepping mode.

For the calculations in the example, the following generalizations are applied to the formulae in D.1.

$$U_i = U^*$$

$$Z_i = Z^*$$

$$\Delta Z_i = \Delta Z^*$$

$$\Delta Z_i / \Delta Z^* = q_2 / q_1 = \beta_{\mathrm{DEMC}}$$

$$d_{i,p} = d_p^*$$

$$N_{3,i} = N_3^*$$

$$\Delta N_2\left(d_{i,p}\right) = \Delta N_2\left(d_p^*\right)$$

where the index i runs from the first to the last stepping data acquisition interval.

D.2.2 Measurement system

The system flows, DEMC geometry, sheath flow temperature and pressure etc. are given in Table D.1. The DEMC-calibration factor ζ as well as the CPC detection efficiency $\eta_{\mathrm{CPC}}(d \geq 30\ \mathrm{nm})$ are assumed to be 1 in this example. There is also no external or internal dilution with respect to the CPC measurement, i.e. $q_{\mathrm{CPC}} = q_3$. An impactor is used as a pre-conditioner of the DMAS.

Table D.1 — Measurement system data

Cylindrical DEMC Data			
q_2 [l/min]	1	q_3 [l/min]	1
q_1 [l/min]	10	q_4 [l/min]	10
L [cm]	44,369	DEMC-calibration factor ζ [-]	1
r_2 [cm]	1,961	Centre polarity	negative
r_1 [cm]	0,937	T-sheath [°C]	21,3
β_{DEMC} [-]	0,1	P-sheath [kPa]	98,2
CPC Data			
CPC detection efficiency η_{CPC} [-]	1	CPC-dilution factor [-]	1
Inlet flow [l/min]	1		

NOTE The polarity of the centre electrode of most commercial DEMCs is limited to only positive or only negative. A recent study described advantages of measuring in both polarities for reducing uncertainties due to charge conditioning in particle size distribution measurement [85].

D.2.3 Data acquisition

For data acquisition in stepping mode in this example, intervals i are chosen such that a gapless measurement in the mobility regime is made. Figure D.2 illustrates the gapless sequence of isosceles triangular transfer functions. First, a starting particle diameter d_{min} is chosen; in this example it is $d_{\mathrm{min}} = 30$ nm.

The largest electrical mobility $Z(d_{\mathrm{min}}, p = 1)$ for singly charged particles is calculated from d_{min} using

$$Z\left(d_{\mathrm{min}}, p=1\right) = \frac{1 \cdot e \cdot S_{\mathrm{C}}\left(d_{\mathrm{min}}\right)}{3 \cdot \pi \cdot \mu_{\mathrm{gas}} \cdot d_{\mathrm{min}}} \tag{D.12}$$

and Formulae (1) to (4); the result is shown in Table D.2

Table D.2 — Calculation of the starting value for the electrical mobility

d_{min} [nm]	T [K]	P [kPa]	μ [kg/(m s)]	λ [nm]	$S_C(d_{min})$ [-]	$Z(d_{min}, p = 1)$ [cm²/(V s)]
30,00	294,45	98,2	$1{,}824\,3 \times 10^{-5}$	68,92	8,139	0,002 528

Next, the centre electrical mobility Z_1 for the first data acquisition interval i = 1 is calculated. Here, like in all data acquisition intervals, isosceles triangular shape of the transfer function according to Formula (D.13) – which holds for the case of recirculated sheath flow – is assumed. For the first data acquisition interval, Formula (D.14) is used to calculate the centre mobility Z_1.

$$Z_i = \Delta Z_i \cdot \beta_{DEMC} \tag{D.13}$$

$$Z_1 = Z(d_{min}, p=1) - \Delta Z_1 = \frac{Z(d_{min}, p=1)}{1+\beta_{DEMC}} \tag{D.14}$$

Considering the DEMC-calibration factor ζ for the electrical mobility, the DEMC voltage for this centre electrical mobility can be derived from Formula (D.15):

$$U_1 = U(Z_1) = \zeta \cdot \frac{q_1 \cdot \ln\left(r_2 / r_1\right)}{2\pi \cdot L \cdot Z_1} \tag{D.15}$$

The result of the calculation of Z_1 and U_1 is shown in Table D.3. The voltage is shown as a negative value to account for the negative polarity at the centre electrode of the DEMC used for the measurements.

Table D.3 — Calculation of the centre electrical mobility and the DEMC voltage for the first data acquisition interval

$Z(d_{min}, p = 1)$ [cm²/(V s)]	q_2/q_1 [-]	Z_1 [cm²/(V s)]	q_1 [cm³/s]	r_1 [cm]	r_2 [cm]	L [cm]	ξ [-]	U_1 [V]
0,002528	0,1	0,002298	166,7	0,937	1,961	44,369	1	−83,44

Since gapless data acquisition is chosen and since the electrical mobility decreases from interval i to interval i + 1, all following data acquisition intervals are defined by

$$Z_i - \Delta Z_i = Z_{i+1} + \Delta Z_{i+1}; \text{ for } i \geq 1 \tag{D.16}$$

$$Z_{i+1} = Z_i \cdot \frac{1-\beta_{DEMC}}{1+\beta_{DEMC}} \tag{D.17}$$

$$U_{i+1} = \zeta \cdot \frac{q_1 \cdot \ln\left(r_2 / r_1\right)}{2\pi \cdot L \cdot Z_{i+1}} \tag{D.18}$$

The number of intervals available for data acquisition is limited by the maximum allowed DEMC voltage, which – in this example – is 10 kV. The data acquisition intervals calculated from above formulae and the DEMC voltage to be set for each interval are also shown in Table D.4.

Table D.4 also contains the results of the example measurement discussed here. An aqueous NaCl solution was aerosolized with a Collison aerosol generator and dried by means of a silica gel diffusion drier. The resulting polydisperse NaCl aerosol (typically used e.g. for filter testing) was then measured with the DMAS in stepping mode. Table D.4 shows the raw concentration $N_{3,i}$ measured by the CPC for each data acquisition interval i.

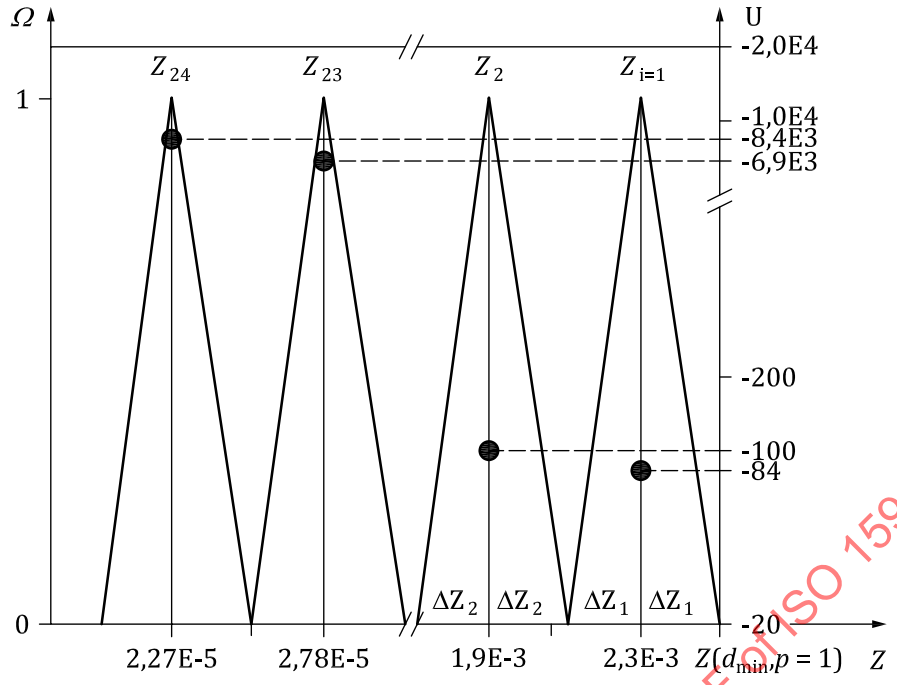

Key

Z electrical mobility [$cm^3/(V\ s)$]

Ω transfer function [-]

U voltage [V]

Figure D.2 — Sequence of gapless isosceles triangular transfer functions Ω and corresponding DEMC voltages U applied for the data acquisition in this example

Table D.4 — Data acquisition interval i, centre electrical mobility Z_i, DEMC-voltage U_i set for each interval, and raw concentration $N_{3,i}$ measured by the CPC

Data acquisition			
i	Z_i [$cm^2/(V\ s)$]	U_i [V]	$N_{3,i}$ [cm^{-3}]
1	2,30E-03	−83,44	2,42E+02
2	1,88E-03	−101,98	3,58E+02
3	1,54E-03	−124,64	5,04E+02
4	1,26E-03	−152,34	6,54E+02
5	1,03E-03	−186,19	8,36E+02
6	8,43E-04	−227,56	1,01E+03
7	6,89E-04	−278,13	1,13E+03
8	5,64E-04	−339,94	1,23E+03
9	4,62E-04	−415,48	1,23E+03
10	3,78E-04	−507,81	1,12E+03
11	3,09E-04	−620,66	1,00E+03
12	2,53E-04	−758,58	8,53E+02
13	2,07E-04	−927,16	6,37E+02
14	1,69E-04	−1133,19	4,74E+02
15	1,38E-04	−1385,01	3,13E+02
16	1,13E-04	−1692,79	1,89E+02
17	9,27E-05	−2068,96	1,06E+02

Table D.4 *(continued)*

Data acquisition			
i	Z_i [cm²/(V s)]	U_i [V]	$N_{3,i}$ [cm⁻³]
18	7,58E-05	−2528,73	5,58E+01
19	6,20E-05	−3090,68	2,52E+01
20	5,08E-05	−3777,49	1,04E+01
21	4,15E-05	−4616,94	3,99E+00
22	3,40E-05	−5642,92	1,26E+00
23	2,78E-05	−6896,90	3,52E-01
24	2,27E-05	−8429,55	8,55E-02

D.2.4 Data inversion assuming only singly charged particles

The first step in data inversion is to calculate $\Delta N_{2,\mathrm{OSC}}\left(d_{i,p=1}\right)$, i.e. the particle concentration in the sample inlet flow q_2 into the DEMC for each data acquisition interval i under the assumption that all particles leaving the DEMC (or reaching the CPC) are singly and positively charged. In analogy to Formula (D.11), the number concentration $\Delta N_{2,\mathrm{OSC}}\left(d_{i,p=1}\right)$ for the data acquisition interval i can be written as:

$$\Delta N_{2,\mathrm{OSC}}\left(d_{i,p=1}\right)=\frac{2N_{3,i}}{P\left(d_{i,p=1}\right)\cdot f_{p=1}\left(d_{i,p=1}\right)\cdot\eta_{\mathrm{CPC}}\left(d_{i,p=1}\right)} \tag{D.19}$$

The mobility diameter $d_{i,p=1}=d_{p=1}\left(Z_i\right)$ in Formula (D.19) is determined by:

$$d_{i,p=1}=\frac{1\cdot e\cdot S_{\mathrm{C}}\left(d_{i,p=1}\right)}{3\cdot\pi\cdot\mu_{\mathrm{gas}}\cdot Z_i} \tag{D.20}$$

Table D.5 shows the results of the iteration for all data acquisition intervals i.

Table D.5 — Centre and boundary electrical mobilities, centre mobility diameter and slip correction factor of each data acquisition interval i

i	Electrical mobility, Z [cm²/(V s)]			Mobility diameter, $d_{i,p=1}$ [nm]	Slip correction, $S_{\mathrm{C}}(d_{i,p=1})$ [-]
	$Z_i+\Delta Z_i$	Z_i	$Z_i-\Delta Z_i$		
1	2,53E-03	2,30E-03	2,07E-03	31,52	7,78
2	2,07E-03	1,88E-03	1,69E-03	35,01	7,06
3	1,69E-03	1,54E-03	1,38E-03	38,89	6,42
4	1,38E-03	1,26E-03	1,13E-03	43,24	5,84
5	1,13E-03	1,03E-03	9,27E-04	48,10	5,32
6	9,27E-04	8,43E-04	7,58E-04	53,55	4,84
7	7,58E-04	6,89E-04	6,20E-04	59,68	4,42
8	6,20E-04	5,64E-04	5,08E-04	66,57	4,03
9	5,08E-04	4,62E-04	4,15E-04	74,35	3,68
10	4,15E-04	3,78E-04	3,40E-04	83,16	3,37
11	3,40E-04	3,09E-04	2,78E-04	93,15	3,09
12	2,78E-04	2,53E-04	2,27E-04	104,52	2,84
13	2,27E-04	2,07E-04	1,86E-04	117,53	2,61
14	1,86E-04	1,69E-04	1,52E-04	132,45	2,41
15	1,52E-04	1,38E-04	1,25E-04	149,66	2,22

Table D.5 *(continued)*

i	Electrical mobility, Z [cm^2/(V s)]			Mobility diameter,	Slip correction,
	$Z_i+\Delta Z_i$	Z_i	$Z_i-\Delta Z_i$	$d_{i,p=1}$ [nm]	$S_C(d_{i,p=1})$ [-]
16	1,25E-04	1,13E-04	1,02E-04	169,61	2,06
17	1,02E-04	9,27E-05	8,34E-05	192,86	1,92
18	8,34E-05	7,58E-05	6,82E-05	220,10	1,79
19	6,82E-05	6,20E-05	5,58E-05	252,21	1,68
20	5,58E-05	5,08E-05	4,57E-05	290,28	1,58
21	4,57E-05	4,15E-05	3,74E-05	335,63	1,50
22	3,74E-05	3,40E-05	3,06E-05	389,94	1,42
23	3,06E-05	2,78E-05	2,50E-05	455,21	1,36
24	2,50E-05	2,27E-05	2,05E-05	533,92	1,30

NOTE Commercial data inversion programs often use a fixed interval scheme in the diameter regime (e.g. logarithmically equal size intervals $\Delta\log(d_{i,p=1})$ = constant). This requires an additional calculation step: mapping the raw CPC concentration data into this set of size intervals. Since this step is not necessary for the step-by-step data inversion demonstrated here, it is omitted.

Since a bipolar charge conditioner with a radioactive ^{85}Kr ion source was used in the measurements, and since the centre electrode polarity of the DEMC was negative, the charging probability $f_{p=1}(d_{i,p=1})$ was calculated using Formulae (A.10) and (A.11) with the coefficients for p = +1 in Table A.3 and an ion mobility ratio of 0,875 (see Annex A).

Size dependent particle penetration through the system $P(d_{i,p=1})$ will be calculated based on the final particle size distribution including multiple charge correction in D.2.5. For the calculation step demonstrated here, $P(d_{i,p=1})$ is set to a value of 1 for all measurement intervals i.

Table D.6 shows the results of the calculation of $f_{p=1}(d_{i,p=1})$ and finally the particle concentration $\Delta N_{2,OSC}\left(d_{i,p=1}\right)$ by Formula (D.19) for each data acquisition interval i in the sample inlet flow q_2 into the DEMC.

Table D.6 — Result of the calculation of the particle number concentration in the inlet flow of the DMAS assuming that all particles in the outlet flow are singly charged. This calculation does not include diffusion losses (i.e. $P(d_{i,p=1})$ = 1 for all intervals i)

i	$d_{i,p=1}$ [nm]	$f_{p=1}(d_{i,p=1})$ [-]	$\eta_{CPC}(d_{i,p=1})$ [-]	$N_{3,i}$ [cm^{-3}]	$\Delta N_{2,OSC}(d_{i,p=1})$ [cm^{-3}]
1	31,52	0,125	1	2,42E+02	3,85E+03
2	35,01	0,136	1	3,58E+02	5,29E+03
3	38,89	0,146	1	5,04E+02	6,91E+03
4	43,24	0,156	1	6,54E+02	8,38E+03
5	48,10	0,166	1	8,36E+02	1,01E+04
6	53,55	0,176	1	1,01E+03	1,15E+04
7	59,68	0,185	1	1,13E+03	1,23E+04
8	66,57	0,193	1	1,23E+03	1,27E+04
9	74,35	0,200	1	1,23E+03	1,23E+04
10	83,16	0,207	1	1,12E+03	1,08E+04
11	93,15	0,212	1	1,00E+03	9,48E+03
12	104,52	0,215	1	8,53E+02	7,94E+03
13	117,53	0,217	1	6,37E+02	5,88E+03
14	132,45	0,217	1	4,74E+02	4,37E+03

Table D.6 *(continued)*

i	$d_{i,p=1}$ [nm]	$f_{p=1}(d_{i,p=1})$ [-]	$\eta_{CPC}(d_{i,p=1})$ [-]	$N_{3,i}$ [cm^{-3}]	$\Delta N_{2,OSC}(d_{i,p=1})$ [cm^{-3}]
15	149,66	0,215	1	3,13E+02	2,91E+03
16	169,61	0,211	1	1,89E+02	1,79E+03
17	192,86	0,206	1	1,06E+02	1,03E+03
18	220,10	0,199	1	5,58E+01	5,60E+02
19	252,21	0,190	1	2,52E+01	2,65E+02
20	290,28	0,181	1	1,04E+01	1,16E+02
21	335,63	0,170	1	3,99E+00	4,70E+01
22	389,94	0,159	1	1,26E+00	1,59E+01
23	455,21	0,147	1	3,52E-01	4,78E+00
24	533,92	0,136	1	8,55E-02	1,26E+00

D.2.5 Multiple charge correction

In this data acquisition and calculation example, the largest data acquisition interval containing particles is $i = 24$. Due to the nature of the aerosol measured in this example (log-normal number size distribution) and due to the cut-off characteristic of the pre-conditioner it can be assumed that the interval $i = 24$ does not contain larger, multiply charged particles. All particles in the interval $i = 24$, i.e. $N_{3,24}$, are therefore considered singly charged; $\Delta N_2(d_{24,p=1})$ for the interval $i = 24$ is correctly calculated by assuming only single charges, i.e. $\Delta N_{2,MCC}\left(d_{24,p=1}\right) = \Delta N_{2,OSC}\left(d_{24,p=1}\right)$, where the subscript MCC in $\Delta N_{2,MCC}$ stands for "with multiple charge correction".

Under steady-state charge conditions there are however, multiply charged particles with a diameter corresponding to $d_{24,p=1}$ which - due to their number of charges - have higher electrical mobilities. These particles are attributed to those data acquisition intervals i with respectively matching mobilities and accordingly, smaller diameters $d_{i,p=1} < d_{24,p=1}$. The purpose of multiple charge correction is to rectify this by subtracting these contributions from the intervals i with matching mobility.

The index k is used in this example to identify the data acquisition interval from which the contributions of multiply charged particles to be corrected in any interval i originate, while the index i describes those data acquisition intervals from which these contributions will be subtracted. Hence $i < k$ always applies.

From the point of view of accuracy, considering up to $p = 6$ charges per particle will suffice in the typical range of most DMASs.

Starting with $k = 24$, there are $\frac{1}{2}\Delta N_2\left(d_{24,p=1}\right)\cdot\sum_{p=2}^{6} f_p\left(d_{24,p}\right)$ particles per unit volume which - due to their higher electrical mobility – are contained in $N_{3,i}$ in data acquisition intervals $i < 24$. Figure D.3 shows the relation between the mobility intervals $[k, p]$ and the data acquisition intervals i for the case of $k = 24$. The boundary mobilities of any mobility interval for singly charged particles $[k, p = 1]$ define the boundaries of the mobility intervals $[k, p > 1]$ containing particles with p charges, which are calculated by multiplying the boundary mobilities of interval $[k, p = 1]$ with the number of charges p as:

$$Z_{k,p} \pm \Delta Z_{k,p} = p\cdot\left(Z_{k,p=1} \pm \Delta Z_{k,p=1}\right) = p\cdot Z_{k,p=1}\left(1 \pm \beta_{DEMC}\right) \quad \text{(D.21)}$$

For $k = 24$, doubly charged particles ($p = 2$) fall into data acquisition intervals $i = 20$ and 21, and triply charged particles ($p = 3$) fall into data acquisition intervals $i = 18$ and 19. The multiply charged particles $\Delta N_2\left(d_{24,p=1}\right)\cdot f_p\left(d_{24,p}\right)$ with $p > 1$ that are contained in the intervals of $[k, p > 1]$ need to be subtracted from $\Delta N_{2,OSC}\left(d_{p=1,i}\right)$, i.e. the particles calculated assuming the only singly charged particles, in the matching data acquisition intervals i. For particles in the interval $k = 24$, the charge correction for

multiply charged particles with p = 2 to p = 6 elementary charges affects data acquisition intervals i = 21 to 15.

The mobility boundaries for [k, p = 1] match the boundaries of the data acquisition interval $i = k$, i.e.

$$Z_{k,p=1} \pm \Delta Z_{k,p=1} = Z_{i=k} \pm \Delta Z_{i=k} \tag{D.22}$$

The boundaries for [k, p > 1] do not match the boundaries of any data acquisition intervals i. However, with the gapless mobility scheme used for data acquisition in this example, each mobility interval [k, p > 1] is always completely covered with a pair of two neighbouring data acquisition intervals i and i - 1. The insert in Figure D.3 shows the example case of k = 24, p = 2, and i = 21 and 20.

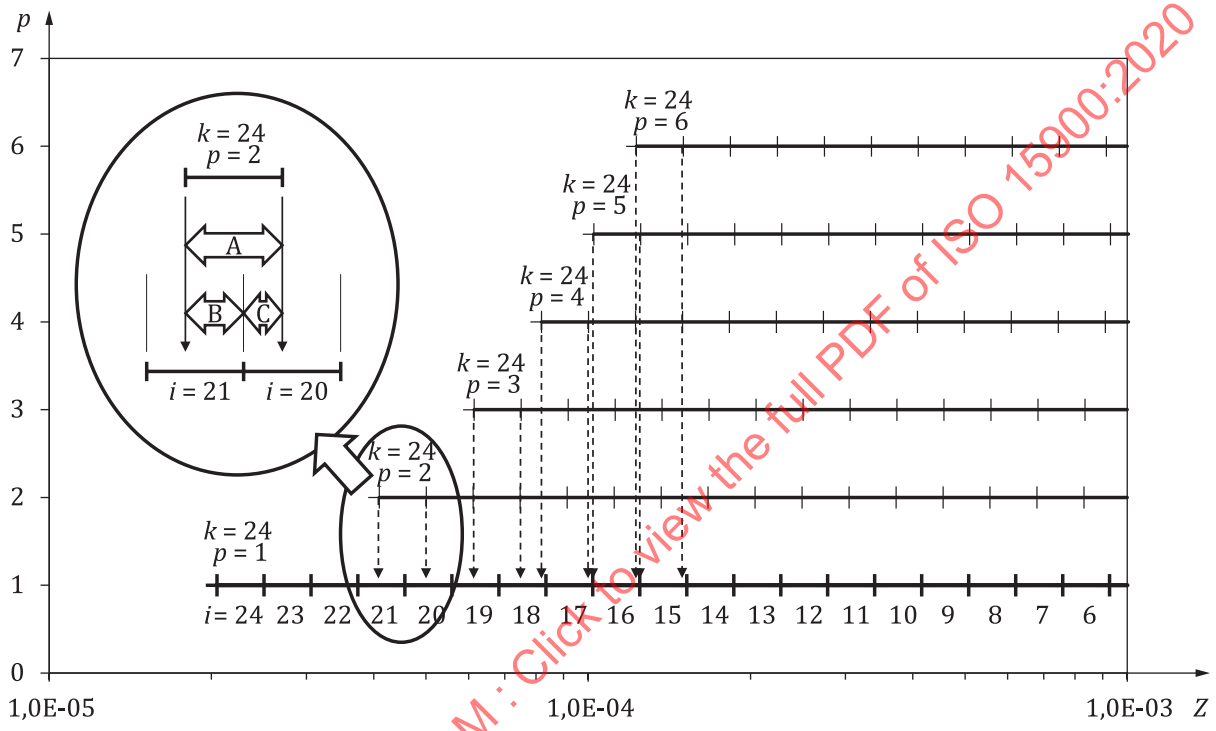

Key

Z electrical mobility [cm^2/(V s)]

p elementary charge per particle

Figure D.3 — Example for the multiple charge correction scheme applied to the particle concentration measured in intervals i = 20 and 21, resulting from multiply charged particles originating from interval k = 24

A simple mobility weight $w_{i,k,p}$ is used to determine the fractions B/A and C/A of the multiply charged particles which are to be subtracted from the neighbouring data acquisition intervals i and $i-1$, respectively (Figure D.3). For example, $w_{i=21,k=24,p=2}$ describes the fraction of the particle concentration of doubly charged particles $\frac{1}{2}\Delta N_2\left(d_{24,p=1}\right)\cdot f_{p=2}\left(d_{24,p=1}\right)/f_{p=1}\left(d_{21,p=1}\right)$ originating from interval k = 24, which is to be subtracted from the particle concentration $\Delta N_{2,\mathrm{OSC}}\left(d_{21,p=1}\right)$ derived for the data acquisition interval i = 21 assuming singly charged particles (see Table D.6).

$$A = \left(Z_{k=24,p=2} + \Delta Z_{k=24,p=2}\right) - \left(Z_{k=24,p=2} - \Delta Z_{k=24,p=2}\right) = 2\Delta Z_{k=24,p=2} = 2\left(2 \cdot Z_{k=24,p=1}\beta_{\mathrm{DEMC}}\right)$$

$$B = \left(Z_{i=21} + \Delta Z_{i=21}\right) - \left(Z_{k=24,p=2} - \Delta Z_{k=24,p=2}\right) = Z_{i=21}\left(1+\beta_{\mathrm{DEMC}}\right) - 2\cdot Z_{k=24,p=1}\left(1-\beta_{\mathrm{DEMC}}\right)$$

$$C=\left(Z_{k=24,p=2}+\Delta Z_{k=24,p=2}\right)-\left(Z_{i=21}+\Delta Z_{i=21}\right)=2\cdot Z_{k=24,p=1}\left(1+\beta_{\mathrm{DEMC}}\right)-Z_{i=21}\left(1+\beta_{\mathrm{DEMC}}\right)$$

$$w_{i=21,k=24,p=2}=\frac{B}{A}=\frac{Z_{i=21}\left(1+\beta_{\mathrm{DEMC}}\right)-2\cdot Z_{k=24,p=1}\left(1-\beta_{\mathrm{DEMC}}\right)}{2\left(2\cdot Z_{k=24,p=1}\beta_{\mathrm{DEMC}}\right)}$$

$$w_{i=20,k=24,p=2}=\frac{C}{A}=1-\frac{B}{A}=\frac{2\cdot Z_{k=24,p=1}\left(1+\beta_{\mathrm{DEMC}}\right)-Z_{i=21}\left(1+\beta_{\mathrm{DEMC}}\right)}{2\left(2\cdot Z_{k=24,p=1}\beta_{\mathrm{DEMC}}\right)}$$

Similarly, for a data acquisition interval i, the weight $w_{i,k,p}$ is calculated with the following formulae:

— For the case: $Z_i\cdot\left(1+\beta_{\mathrm{DEMC}}\right)\geq p\cdot Z_{k,p=1}\cdot\left(1-\beta_{\mathrm{DEMC}}\right)\geq Z_i\cdot\left(1-\beta_{\mathrm{DEMC}}\right)$,

$$w_{i,k,p}=\frac{Z_i\left(1+\beta_{\mathrm{DEMC}}\right)-p\cdot Z_{k,p=1}\left(1-\beta_{\mathrm{DEMC}}\right)}{2\cdot p\cdot Z_{k,p=1}\beta_{\mathrm{DEMC}}} \tag{D.23}$$

— For the case: $Z_i\cdot\left(1+\beta_{\mathrm{DEMC}}\right)\geq p\cdot Z_{k,p=1}\cdot\left(1+\beta_{\mathrm{DEMC}}\right)\geq Z_i\cdot\left(1-\beta_{\mathrm{DEMC}}\right)$

$$w_{i,k,p}=\frac{p\cdot Z_{k,p=1}\left(1+\beta_{\mathrm{DEMC}}\right)-Z_i\left(1+\beta_{\mathrm{DEMC}}\right)}{2\cdot p\cdot Z_{k,p=1}\beta_{\mathrm{DEMC}}} \tag{D.24}$$

NOTE The case in Formula (D.23) corresponds to $w = B/A$ in Figure D.3. The case in Formula (D.24) corresponds to $w = C/A$ in Figure D.3.

Similarly, for each data acquisition interval i, the ratio of the charge distribution function for $p > 1$ at diameter $d_{k,p\,=\,1}$ to the charge distribution function for $p = 1$ at diameter $d_{i,p\,=\,1}$, multiplied by the respective weight $w_{i,k,p}$ needs to be calculated in order to finally correct the number concentration $\Delta N_{2,\mathrm{OSC}}\left(d_{i,p=1}\right)$. The correction factor, $\theta_{i,k}$, is independent of the measured concentrations:

$$\theta_{i,k}=\frac{1}{f_{p=1}\left(d_{i,p=1}\right)}\sum_{p=2}^{6}f_p\left(d_{k,p=1}\right)\cdot w_{i,k,p} \tag{D.25}$$

Table D.7 shows the calculation of $\theta_{i,k}$ for $k = 24$.

Table D.7 — Example calculation of the parameter $\theta_{i,k}$ for multiply charged particles for the interval $k = 24$ with $p \leq 6$

$k = 24$	$\frac{f_p\left(d_{24,p=1}\right)}{f_{p=1}\left(d_{i,p=1}\right)}\cdot w_{i,k,p}$									
	$i = 23$	$i = 22$	$i = 21$	$i = 20$	$i = 19$	$i = 18$	$i = 17$	$i = 16$	$i = 15$	$i = 14$
$p = 2$	0	0	0,269 7	0,233 3	0	0	0	0	0	0
$p = 3$	0	0	0	0	0,119 0	0,113 8	0	0	0	0
$p = 4$	0	0	0	0	0	0,007 9	0,083 5	0	0	0
$p = 5$	0	0	0	0	0	0	0	0,029 1	0,000 7	0
$p = 6$	0	0	0	0	0	0	0	0,000 5	0,007 4	0
$\theta_{i,k=24}$	0	0	0,269 7	0,233 3	0,119 0	0,121 7	0,083 5	0,029 6	0,008 1	0

Since $\theta_{i,k}$ does not depend on the particle number concentration and since the multiple charge correction itself is, concentration wise, only depending on the singly charged ($p = 1$) particles in the intervals k and $i < k$, the multiple charge correction becomes

$$\Delta N_{2,\mathrm{MCC}}\left(d_{i,p=1}\right)=\Delta N_{2,\mathrm{OSC}}\left(d_{i,p=1}\right)-\Delta N_{2,\mathrm{MCC}}\left(d_{k,p=1}\right)\cdot\theta_{i,k} \tag{D.26}$$

Table D.8 shows the results of the multiple charge correction calculation following Formula (D.26) for the initial calculation step at $k = 24$.

Table D.8 — Example for the initial calculation step of the multiple charge correction for multiply charged particles originating from interval $k = 24$ with $p \leq 6$, according to Formula (D.26)

$k = 24$	$i = 23$	$i = 22$	$i = 21$	$i = 20$	$i = 19$	$i = 18$	$i = 17$	$i = 16$	$i = 15$	$i = 14$
$\Delta N_{2,\mathrm{MCC}}\left(d_{k,p=1}\right)$ [cm^{-3}]	1,26	1,26	1,26	1,26	1,26	1,26	1,26	1,26	1,26	1,26
$\theta_{i,k=24}$	0	0	0,269 7	0,233 3	0,119 0	0,121 7	0,083 5	0,029 6	0,008 1	0
$\Delta N_{2,\mathrm{OSC}}\left(d_{i,p=1}\right)$ [cm^{-3}]	4,78	15,9	47,0	116	265	560	1 030	1 790	2 910	4 370
$\Delta N_{2,\mathrm{MCC}}\left(d_{i,p=1}\right)$ [cm^{-3}]	4,78	15,9	46,7	116	265	560	1 030	1 790	2 910	4 370

In the same way, the multiple charge correction calculation based on measurement intervals k is continued downward from $k = 24$ to $k = 1$. While k is stepwise reduced, the correction propagates with every new calculation of $\Delta N_{2,\mathrm{MCC}}\left(d_{i,p=1}\right)$. For every new step, the former value of $\Delta N_{2,\mathrm{MCC}}\left(d_{i,p=1}\right)$ for k becomes the next $\Delta N_{2,\mathrm{OSC}}\left(d_{i,p=1}\right)$ for $k - 1$, i.e. $\left[\Delta N_{2,\mathrm{OSC}}\left(d_{i,p=1}\right)\right]_{k-1}=\left[\Delta N_{2,\mathrm{MCC}}\left(d_{i,p=1}\right)\right]_{k}$. The calculation follows Formula (D.27).

$$\left[\Delta N_{2,\mathrm{MCC}}\left(d_{i,p=1}\right)\right]_{k-1}=\left[\Delta N_{2,\mathrm{MCC}}\left(d_{i,p=1}\right)\right]_{k}-\Delta N_{2,\mathrm{MCC}}\left(d_{k-1,p=1}\right)\cdot\theta_{i,k-1} \tag{D.27}$$

Figure D.4. illustrates the propagation of the correction with decreasing k.

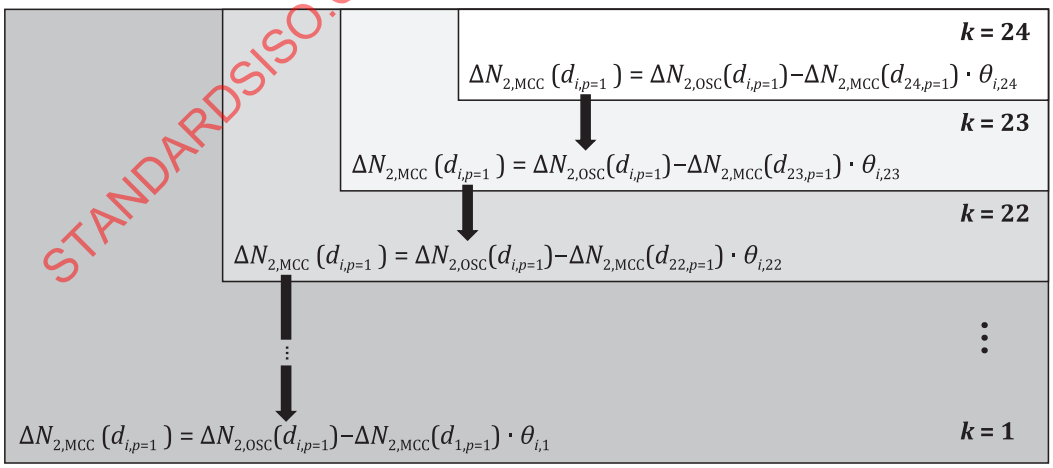

Figure D.4 — Illustration of the step by step calculation of $\Delta N_{2,\mathrm{MCC}}\left(d_{i,p=1}\right)$ for $k = 24$ to $k = 1$ and the correction propagation with decreasing k

The multiple charge corrected particle number concentration $\Delta N_{2,\mathrm{MCC}}\left(d_{i,p=1}\right)$ in this example is calculated for up to 6 particle charges and k = 24 as the largest measurement interval. Table D.9 shows the result of this calculation.

Table D.9 — Result of the calculation of the particle number concentration in the inlet flow of the DMAS including multiple charge correction (MCC)

i	$d_{i,p=1}$ [nm]	$\Delta N_{2,\mathrm{OSC}}\left(d_{i,p=1}\right)$ [cm^{-3}]	$\Delta N_{2,\mathrm{MCC}}\left(d_{i,p=1}\right)$ [cm^{-3}]
1	31,52	3,85E+03	3,80E+03
2	35,01	5,29E+03	4,73E+03
3	38,89	6,91E+03	6,13E+03
4	43,24	8,38E+03	7,36E+03
5	48,10	1,01E+04	8,82E+03
6	53,55	1,15E+04	1,01E+04
7	59,68	1,23E+04	1,08E+04
8	66,57	1,27E+04	1,12E+04
9	74,35	1,23E+04	1,09E+04
10	83,16	1,08E+04	9,63E+03
11	93,15	9,48E+03	8,51E+03
12	104,52	7,94E+03	7,24E+03
13	117,53	5,88E+03	5,41E+03
14	132,45	4,37E+03	4,08E+03
15	149,66	2,91E+03	2,74E+03
16	169,61	1,79E+03	1,71E+03
17	192,86	1,03E+03	9,92E+02
18	220,10	5,60E+02	5,45E+02
19	252,21	2,65E+02	2,59E+02
20	290,28	1,16E+02	1,14E+02
21	335,63	4,70E+01	4,67E+01
22	389,94	1,59E+01	1,59E+01
23	455,21	4,78E+00	4,78E+00
24	533,92	1,26E+00	1,26E+00

NOTE The particle number concentration $\Delta N_{2,\mathrm{MCC}}\left(d_{i,p=1}\right)$ with multiple charge correction can become negative in some intervals. While negative concentrations are physically impossible, this effect can be caused by (a) the simplification by discretization or (b) the inherent measurement uncertainty in $N_{3,i}$ in all measurement intervals.

D.2.6 Diffusion loss correction

This correction follows 5.6 and Annex I. The DMAS is separated into four sections, which are characterized - with respect to the diffusion losses - by their equivalent length and flow rate. Table D.10 shows these sections, their equivalent length and the flow rate.

Table D.10 — Sections of the DMAS for diffusion loss correction

Section	Description	Equivalent L_{Tube} [m]	q [l/min]
1	Pre-separator (Impactor)	2,1	1
2	Tubing to DEMC incl. charge conditioner	1,84	1

Table D.10 *(continued)*

Section	Description	Equivalent L_{Tube} [m]	q [l/min]
3	DEMC	7,1	1
4	Tubing from DEMC to CPC inlet	0,25	1
	Equivalent length for the complete DMAS	**11,29**	**1**

To calculate the penetration through the system, the equivalent lengths of the four section are added to give the total equivalent system length. This is in line with the way that each of equivalent length of the individual sections, were obtained (Wiedensohler et al. 2018 [75]). Formulae (I.1) to (I.4) are used:

$$\mu(d)=\frac{\pi\cdot D(d)\cdot L_{\text{Tube}}}{q} \tag{D.28}$$

$$D(d)=\frac{k\cdot T\cdot S_{\text{c}}(d)}{3\cdot\pi\cdot\mu_{\text{gas}}\cdot d} \tag{D.29}$$

for $\mu(d) \leq 0{,}02$:

$$P_{\text{Tube}}(d)=1-2{,}5638\cdot\mu(d)^{2/3}+1{,}2\cdot\mu(d)+0{,}1767\cdot\mu(d)^{4/3} \tag{D.30}$$

for $\mu(d) > 0{,}02$:

$$P_{\text{Tube}}(d)=0{,}81905\cdot e^{-3{,}6568\mu(d)}+0{,}09753\cdot e^{-22{,}305\mu(d)}+0{,}0325\cdot e^{-56{,}961\mu(d)}+0{,}01544\cdot e^{-107{,}62\mu(d)} \tag{D.31}$$

From the penetration $P(d) = P_{\text{Tube}}(d)$, the diffusion loss corrected particle number concentration $\Delta N_{2,\text{MCC,DLC}}\left(d_{i,p=1}\right)$ at the inlet of the DMAS is calculated following Formula (D.32):

$$\Delta N_{2,\text{MCC,DLC}}\left(d_{i,p=1}\right)=\frac{\Delta N_{2,\text{MCC}}\left(d_{i,p=1}\right)}{P\left(d_{i,p=1}\right)} \tag{D.32}$$

Table D.11 shows diffusion loss parameters $\mu(d_{i,p=1})$ and $D(d_{i,p=1})$, as well as $P(d_{i,p=1})$, the resulting diffusion loss corrected penetration through the DMAS. In addition, $\Delta N_{2,\text{MCC}}\left(d_{i,p=1}\right)$ and $\Delta N_{2,\text{MCC,DLC}}\left(d_{i,p=1}\right)$ are given.

Table D.11 — Calculation of the particle penetration $P(d_{i,p=1})$ through the DMAS and the resulting diffusion loss corrected particle number concentration at the inlet of the DMAS

i	$d_{i,p=1}$ [nm]	$D(d_{i,p=1})$ [m²/s]	$\mu(d_{i,p=1})$ [-]	$P(d_{i,p=1})$ [-]	$\Delta N_{2,\text{MCC}}(d_{i,p=1})$ [cm⁻³]	$\Delta N_{2,\text{MCC,DLC}}(d_{i,p=1})$ [cm⁻³]
1	31,52	5,83E-09	1,24E-02	0,878	3,80E+03	4,33E+03
2	35,01	4,77E-09	1,02E-02	0,892	4,73E+03	5,30E+03
3	38,89	3,90E-09	8,31E-03	0,905	6,13E+03	6,78E+03
4	43,24	3,19E-09	6,80E-03	0,916	7,36E+03	8,03E+03
5	48,10	2,61E-09	5,56E-03	0,926	8,82E+03	9,52E+03
6	53,55	2,14E-09	4,55E-03	0,935	1,01E+04	1,08E+04
7	59,68	1,75E-09	3,72E-03	0,943	1,08E+04	1,14E+04
8	66,57	1,43E-09	3,05E-03	0,950	1,12E+04	1,18E+04
9	74,35	1,17E-09	2,49E-03	0,956	1,09E+04	1,14E+04

Table D.11 *(continued)*

i	$d_{i,p=1}$ [nm]	$D(d_{i,p=1})$ [m^2/s]	$\mu(d_{i,p=1})$ [-]	$P(d_{i,p=1})$ [-]	$\Delta N_{2,MCC}(d_{i,p=1})$ [cm^{-3}]	$\Delta N_{2,MCC,DLC}(d_{i,p=1})$ [cm^{-3}]
10	83,16	9,58E-10	2,04E-03	0,961	9,63E+03	1,00E+04
11	93,15	7,84E-10	1,67E-03	0,966	8,51E+03	8,81E+03
12	104,52	6,41E-10	1,36E-03	0,970	7,24E+03	7,46E+03
13	117,53	5,25E-10	1,12E-03	0,974	5,41E+03	5,56E+03
14	132,45	4,29E-10	9,14E-04	0,977	4,08E+03	4,18E+03
15	149,66	3,51E-10	7,48E-04	0,980	2,74E+03	2,80E+03
16	169,61	2,87E-10	6,12E-04	0,982	1,71E+03	1,74E+03
17	192,86	2,35E-10	5,00E-04	0,984	9,92E+02	1,01E+03
18	220,10	1,92E-10	4,09E-04	0,986	5,45E+02	5,53E+02
19	252,21	1,57E-10	3,35E-04	0,988	2,59E+02	2,63E+02
20	290,28	1,29E-10	2,74E-04	0,990	1,14E+02	1,15E+02
21	335,63	1,05E-10	2,24E-04	0,991	4,67E+01	4,71E+01
22	389,94	8,62E-11	1,83E-04	0,992	1,59E+01	1,60E+01
23	455,21	7,05E-11	1,50E-04	0,993	4,78E+00	4,82E+00
24	533,92	5,77E-11	1,23E-04	0,994	1,26E+00	1,27E+00

D.2.7 Final result

Finally, Table D.12 shows the result of the data inversion including multiple charge correction and diffusion loss correction. The last column in Table D.12 shows the number concentration size distribution function; by convention, normalized to $\Delta\log(d_{i,p=1})$, while the size distribution function n in, for example, Formula (D.8) is normalized to Δd. This normalization is most common in aerosol science because size distribution graphs are generally plotted over a logarithmic size scale. $\Delta\log(d_{i,p=1})$ is calculated following Formula (D.33):

$$\Delta\left(\log\left(d_{i,p=1}\right)\right)=\log\left(d_{i,p=1,\max}\right)-\log\left(d_{i,p=1,\min}\right)=\log\left(\frac{d_{i,p=1,\max}}{d_{i,p=1,\min}}\right) \quad \text{(D.33)}$$

Table D.12 — Final result of the data inversion including multiple charge correction and diffusion loss correction

i	$d_{i,p=1}$ [nm]	$\Delta N_{2,MCC}(d_{i,p=1})$ [cm^{-3}]	$P(d_{i,p=1})$ [-]	$\Delta N_{2,MCC,DLC}(d_{i,p=1})$ [cm^{-3}]	$\Delta\log(d_{i,p=1})$ [-]	$\Delta N_{2,MCC,DLC}(d_{i,p=1})/\Delta\log(d_{i,p=1})$ [cm^{-3}]
1	31,52	3,80E+03	0,878	4,33E+03	4,54E-02	9,55E+04
2	35,01	4,73E+03	0,892	5,30E+03	4,56E-02	1,16E+05
3	38,89	6,13E+03	0,905	6,78E+03	4,59E-02	1,48E+05
4	43,24	7,36E+03	0,916	8,03E+03	4,61E-02	1,74E+05
5	48,10	8,82E+03	0,926	9,52E+03	4,65E-02	2,05E+05
6	53,55	1,01E+04	0,935	1,08E+04	4,68E-02	2,31E+05
7	59,68	1,08E+04	0,943	1,14E+04	4,73E-02	2,42E+05
8	66,57	1,12E+04	0,950	1,18E+04	4,78E-02	2,47E+05
9	74,35	1,09E+04	0,956	1,14E+04	4,83E-02	2,36E+05
10	83,16	9,63E+03	0,961	1,00E+04	4,89E-02	2,05E+05
11	93,15	8,51E+03	0,966	8,81E+03	4,97E-02	1,77E+05
12	104,52	7,24E+03	0,970	7,46E+03	5,05E-02	1,48E+05
13	117,53	5,41E+03	0,974	5,56E+03	5,14E-02	1,08E+05

Table D.12 *(continued)*

i	$d_{i,p=1}$ [nm]	$\Delta N_{2,MCC}(d_{i,p=1})$ [cm^{-3}]	$P(d_{i,p=1})$ [-]	$\Delta N_{2,MCC,DLC}(d_{i,p=1})$ [cm^{-3}]	$\Delta\log(d_{i,p=1})$ [-]	$\Delta N_{2,MCC,DLC}(d_{i,p=1})/\Delta\log(d_{i,p=1})$ [cm^{-3}]
14	132,45	4,08E+03	0,977	4,18E+03	5,25E-02	7,95E+04
15	149,66	2,74E+03	0,980	2,80E+03	5,37E-02	5,22E+04
16	169,61	1,71E+03	0,982	1,74E+03	5,51E-02	3,16E+04
17	192,86	9,92E+02	0,984	1,01E+03	5,66E-02	1,78E+04
18	220,10	5,45E+02	0,986	5,53E+02	5,83E-02	9,48E+03
19	252,21	2,59E+02	0,988	2,63E+02	6,01E-02	4,37E+03
20	290,28	1,14E+02	0,990	1,15E+02	6,21E-02	1,86E+03
21	335,63	4,67E+01	0,991	4,71E+01	6,41E-02	7,34E+02
22	389,94	1,59E+01	0,992	1,60E+01	6,62E-02	2,42E+02
23	455,21	4,78E+00	0,993	4,82E+00	6,83E-02	7,05E+01
24	533,92	1,26E+00	0,994	1,27E+00	7,03E-02	1,80E+01

The resulting particle number size distributions normalized to $\Delta\log(d_{i,p=1})$ are shown in Figure D.5. The three graphs in Figure D.5 show $\Delta N_2(d_{i,p=1})/\Delta\log(d_{i,p=1})$ without corrections (assuming only singly charged particles), with multiple charge correction (MCC), and with both multiple charge correction and diffusion loss correction (MCC and DLC), respectively.

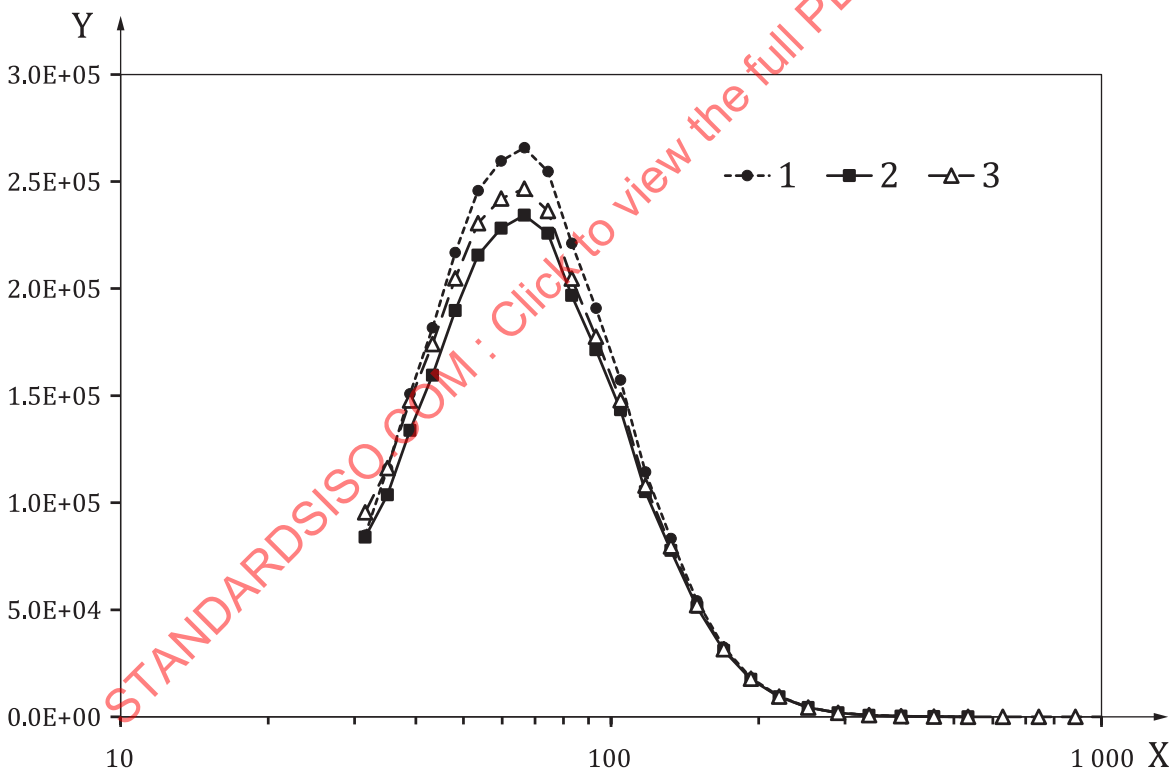

Key

X mobility diameter d [nm]

Y particle number size distribution $\Delta N_2/\Delta\log(d)$ [$1/cm^3$]

1 no MCC or DLC

2 with MCC

3 with MCC and DLC

Figure D.5 — Calculated particle number size distribution $\Delta N_2/\Delta\log(d)$ in the sample aerosol flow q_2 of the DMAS, with and without multiple charge correction (MCC) and diffusion loss correction (DLC)

Annex E
(informative)

Cylindrical DEMC

E.1 Geometry of cylindrical DEMC

A schematic diagram of a cylindrical DEMC is shown in Figure E.1. A clean sheath flow (q_1) surrounds the annular region around the centre rod. The sample aerosol flow (q_2) enters as a thin annular flow adjacent to the outer cylinder. While the majority of the flow exits through holes in the bottom closure of the DEMC as excess flow (q_4), a fraction (q_3) is withdrawn as mobility selected aerosol flow through a circumferential slot located near the bottom of the centre electrode. This flow (q_3) goes to the aerosol detector. The flow in the DEMC from the point where aerosol enters to the point where q_3 is extracted is laminar. The inner or outer electrode is maintained at a voltage (U) while the counter-electrode is grounded. The sample aerosol flow (q_2) enters, and the mobility selected aerosol flow (q_3) leaves through field free regions. Over the effective length (L) between the inlet of q_2 and the outlet of q_3, the particles are exposed to the electric field produced by the voltage (U). The thin lines in Figure E.1 indicate trajectories of charged particles which define the critical mobilities Z_1, Z_2, Z_3 and Z_4 associated with the instrument, described in E.2.

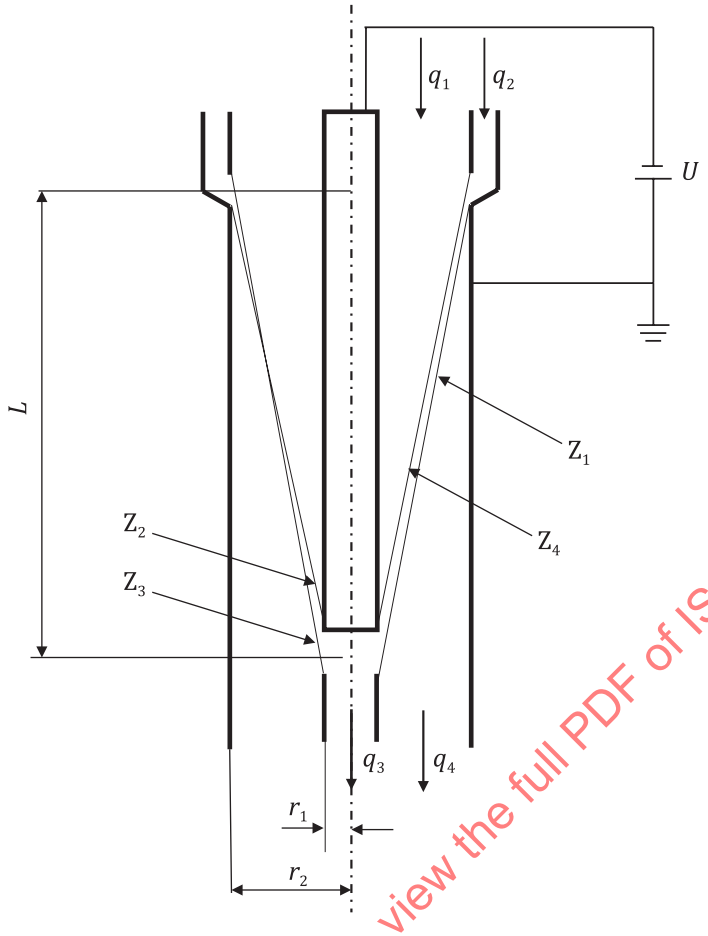

Key

Z_1 - Z_4	critical mobilities	L	effective length
q_1	sheath flow	r_1	radius of the inner electrode
q_2	sample aerosol flow	r_2	radius of the outer electrode
q_3	mobility selected aerosol flow	U	voltage
q_4	excess flow		

Figure E.1 — Schematic diagram of a cylindrical DEMC

E.2 Transfer function

The quantities Z_1, Z_2, Z_3 and Z_4 are the critical mobilities of a charged particle which will follow the critical trajectories shown in Figure E.1. These critical mobilities, determined by the instrument geometry and operating conditions of the DEMC, are given by:

$$Z_1 = \frac{q_1 + q_2 - q_3}{2\pi \cdot \Delta\Phi}, Z_2 = \frac{q_1 + q_2}{2\pi \cdot \Delta\Phi}, Z_3 = \frac{q_1 - q_3}{2\pi \cdot \Delta\Phi}, Z_4 = \frac{q_1}{2\pi \cdot \Delta\Phi} \tag{E.1}$$

where $\Delta\Phi$ is a function of the geometry and the supply voltage of the DEMC.

For a coaxial cylindrical DEMC, $\Delta\Phi$ is defined as:

$$\Delta\Phi = \frac{L \cdot U}{\ln\left(\frac{r_2}{r_1}\right)} \tag{E.2}$$

where

r_1 and r_2 are the radii of the inner and outer electrodes, respectively;

L is the effective electrode length between the aerosol inlet and outlet;

U is the voltage potential between the electrodes of the DEMC.

If particles of a single mobility, Z, enter the DEMC, the transfer function $\Omega(Z)$ is the ratio of the number of particles leaving the DEMC with q_3 to the number of particles with the mobility Z entering the DEMC with q_2, or, in other words, the probability that an aerosol particle which enters the DEMC at the aerosol inlet will leave via the detector outlet:

$$\Omega(Z)=\frac{N_3 \cdot q_3}{N_2(Z) \cdot q_2} \tag{E.3}$$

where N_2 and N_3 are the particle number concentrations entering the DEMC with q_2 and leaving the DEMC with q_3, respectively. If the DEMC is set to the voltage U^*, the transfer function $\Omega(Z)$ can be written as:

$$\Omega(Z)=0 \qquad \text{if } Z < Z_3 \text{ or } Z_2 < Z \tag{E.4}$$

$$\Omega(Z)=\frac{1}{q_2}\left[Z\frac{2\pi \cdot L \cdot U^*}{\ln(r_2/r_1)}-(q_1-q_3)\right] \qquad \text{if } Z_3 < Z < \min(Z_1, Z_4) \tag{E.5}$$

$$\Omega(Z)=\min\left(1,\frac{q_3}{q_2}\right) \qquad \text{if } \min(Z_1, Z_4) < Z < \max(Z_1, Z_4) \tag{E.6}$$

$$\Omega(Z)=\frac{1}{q_2}\left[q_1+q_2-Z\frac{2\pi \cdot L \cdot U^*}{\ln(r_2/r_1)}\right] \qquad \text{if } \max(Z_1, Z_4) < Z < Z_2 \tag{E.7}$$

The transfer function, $\Omega(Z)$ of the DEMC is shown in Figure E.2. The left-hand-side diagram shows the case where $q_3 > q_2$; the centre diagram shows the special case where $q_3 = q_2$; and the right-hand-side diagram shows $\Omega(Z)$ for $q_3 < q_2$.

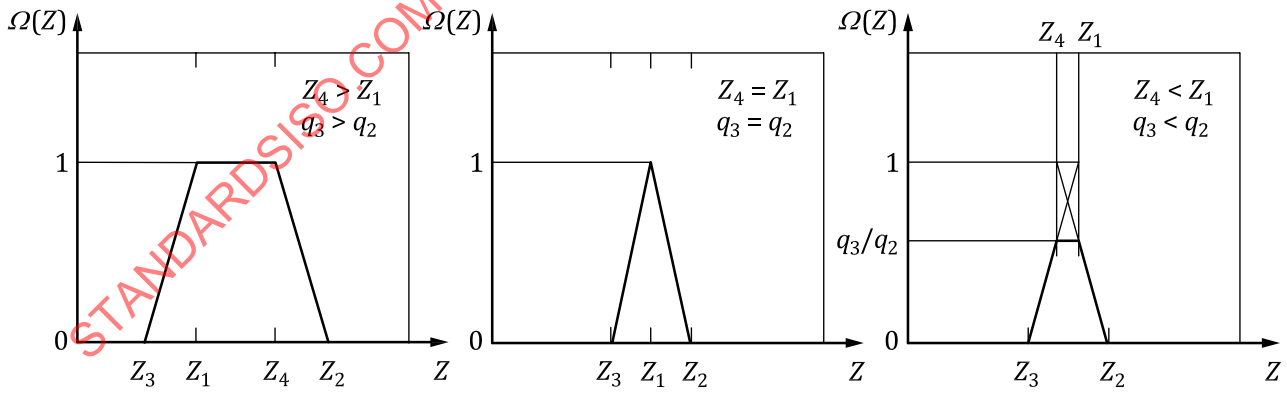

Key

Z electrical mobility

$\Omega(Z)$ transfer function

Figure E.2 — Transfer function for a coaxial cylindrical DEMC

The transfer function has the form of a truncated isosceles triangle centred around:

$$Z^* = Z\left(U^*\right) = \frac{Z_2 + Z_3}{2} = \frac{Z_1 + Z_4}{2} = \frac{2q_1 + q_2 - q_3}{4\pi \cdot \Delta\Phi} = \frac{q_1 + q_4}{4\pi \cdot L \cdot U} \ln\left(r_2 / r_1\right) \tag{E.8}$$

where

Z^* is the electrical mobility of the target particles;

U^* is the voltage potential on the DEMC that corresponds to the mobility Z^*.

From Figure E.2 and Formula (E.1), the mobility resolution $Z^*/\Delta Z$ of the DEMC is defined as:

$$\frac{Z^*}{\Delta Z} = \frac{Z_2 + Z_3}{Z_2 - Z_3} = \frac{2q_1 + q_2 - q_3}{q_2 + q_3} = \frac{q_1 + q_4}{q_2 + q_3} \tag{E.9}$$

In the case of re-circulating the excess flow to the sheath flow ($q_1 = q_4$, which forces $q_2 = q_3$), the mobility resolution simplifies to $Z^*/\Delta Z = q_1/q_2$ with $Z^* = q_1 \cdot \ln\left(r_2 / r_1\right) / \left(2\pi \cdot L \cdot U^*\right)$.

If the DMAS is used to measure a particle size distribution, the particles entering the DEMC will not have a single mobility Z. Instead, a mobility distribution will enter the DEMC. If the mobility distribution function $f(Z)$ of the aerosol particles entering the DEMC is defined as:

$$f(Z) = \frac{\mathrm{d}N_2(Z)}{\mathrm{d}Z} \tag{E.10}$$

where $\mathrm{d}N_2(Z)$ is the number concentration of all charged aerosol particles with the opposite polarity of the centre electrode of the DEMC in the mobility range from Z to $Z + \mathrm{d}Z$, then the total number concentration of particles $N_3(U^*)$ leaving the DEMC with the mobility selected aerosol flow q_3 is:

$$N_3\left(U^*\right) = \frac{q_2}{q_3} \int \Omega\left(Z, U^*\right) f(Z)\,\mathrm{d}Z \tag{E.11}$$

With Ω from Formulae (E.4) to (E.7), Formula (E.11) becomes:

$$N_3\left(U^*\right) = \frac{1}{q_3}\left\{\int_{Z_3}^{Z_a}\left[Z\frac{2\pi \cdot L \cdot U^*}{\ln\left(r_2/r_1\right)} - \left(q_1 - q_3\right)\right] f(Z)\,\mathrm{d}Z + \min\left(q_2, q_3\right)\int_{Z_a}^{Z_b} f(Z)\,\mathrm{d}Z + \int_{Z_b}^{Z_2}\left[q_1 + q_2 - Z\frac{2\pi \cdot L \cdot U^*}{\ln\left(r_2/r_1\right)}\right] f(Z)\,\mathrm{d}Z\right\} \tag{E.12}$$

where $Z_a = \min(Z_1, Z_4)$ and $Z_b = \max(Z_1, Z_4)$.

Once the flows are set, any one of the critical mobilities Z_1, Z_2, Z_3 and Z_4 in Formula (E.12) can be taken as an independent variable and is physically varied by changing the voltage, U^*.

If it is assumed that $f(Z)$ is nearly constant in the mobility intervals of (Z_3, Z_a) and (Z_b, Z_2), Formula (E.12) reduces to the approximation:

$$N_3\left(U^*\right) \cong \min\left(1, \frac{q_2}{q_3}\right)\cdot\left[\int_{Z_d}^{Z_a} f(Z)\,\mathrm{d}Z + \int_{Z_a}^{Z_b} f(Z)\,\mathrm{d}Z + \int_{Z_b}^{Z_c} f(Z)\,\mathrm{d}Z\right] \cong \min\left(1, \frac{q_2}{q_3}\right)\cdot\int_{Z_d}^{Z_c} f(Z)\,\mathrm{d}Z \tag{E.13}$$

where $Z_d = \frac{1}{2}\cdot\left[Z_3 + \min\left(Z_1, Z_4\right)\right]$ and $Z_c = \frac{1}{2}\cdot\left[Z_2 + \max\left(Z_1, Z_4\right)\right]$

If $q_1 = q_4$ (which forces $q_2 = q_3$), the mobility Z_1 equals Z_4. The transfer function becomes symmetrically triangular and Formula (E.13) further reduces to:

$$N_3\left(U^*\right) \cong \int_{Z_d}^{Z_c} f(Z)\,\mathrm{d}Z \cong \frac{1}{2}\int_{Z_3}^{Z_2} f(Z)\,\mathrm{d}Z \tag{E.14}$$

The above analysis is based on the assumptions that

a) particle inertia and Brownian motion may be neglected,

b) the flow is laminar, axi-symmetric and incompressible, and

c) the space charge and its image forces are negligible.

An analysis including the influence of Brownian motion can, for example, be found in Kousaka et al. (1986) [61], Stolzenburg (1988) [49], or Hagwood et al. (1999) [25]. Stolzenburg and McMurry (2008) [64] introduced a simple approximation with a lognormal function for the DEMC transfer function for the case when particle diffusion is significant.

E.3 Uncertainty calculation for Z^*

The influence parameters for the centre particle mobility follow [from Formula (E.8)]:

$$Z^* = \frac{2q_1 + q_2 - q_3}{4\pi LU} \ln\left(\frac{r_2}{r_1}\right) \tag{E.15}$$

This formula describes the static situation of the electrical mobility for the monodisperse aerosol and not the uncertainty in the scanning mode. The following assumptions allow the calculation of the uncertainty of Z^*. All uncertainties, u_x, in $(x \pm u_x)$ are given as standard uncertainties (coverage factor $k = 1$); the percentage contributions to the total uncertainty are given below.

— Sheath flow q_1 = (3,00 ± 0,06) l/min (volumetric flow, including fluctuation, and deviations due to atmospheric pressure and air temperature) contributes with 88 %.

— Voltage U (standard uncertainty of 0,5 %, negligible fluctuations) contributes with 6 %.

— Length L (standard uncertainty of 0,5 %) contributes with less than 1 %.

— Electrode diameters r_1 and r_2 (standard uncertainty of 0,1 % and 0,06 %) contribute with less than 1 %.

— Sample aerosol flow q_2 = (0,300 ± 0,006) l/min (volumetric flow, including fluctuation, and deviations due to atmospheric pressure and air temperature) contributes with less than 1 %.

— Mobility selected aerosol flow q_3 = (0,300 ± 0,006) l/min (volumetric flow, including fluctuation and deviations due to atmospheric pressure and air temperature, conservative assumption for the correlation between q_2 and q_3 is 0) contributes with less than 1 %.

— The roughness and the soiling of the electrode surface causes an inhomogeneity of the electrical field. This effect is assumed to be included in the uncertainty for U, r_1 and r_2.

— Inhomogeneities of the flow streamlines (due to surface effects) are neglected.

The uncertainty with the above assumptions is u_{Z^*} / Z^* = 2,2 % (slip correction factor $S_C = 1$).

Other uncertainty calculations can, for example, be found in Donnelly and Mulholland (2003) [16] and Mulholland et al. (2006) [42].

Annex F
(informative)

Example certificate for a DMAS particle size calibration

Name and Address of the Institution Issuing the Certificate
DMAS Model: **DMAS identification / serial number:** **DMAS configuration details:** **Order number:** **Description:** ☐ **Dynamic or static particle size calibration of a DMAS Model xxxx (according to ISO 15900:2020, 8.6.4)** ☐ **Static particle size calibration of a DMAS Model xxxx (according to ISO 15900:2020, 8.6.5)** **Date of calibration:** **(Certificate) Reference:** **Page 1 of 3** **Date of Issue:** **Signed:** **(Authorized signatory)** **Checked by:** **Signed:** **for Managing Director**

Date of instrument receipt in calibration room:
(Calibration institute's) instrument identification number:

DMAS model and serial number:
DEMC model and serial number:
DEMC voltage polarity:
Charge conditioner model and serial number:
Particle detector
type and serial number:
(optional) calibration certificate and date:

Result of initial instrument inspection:
Result of instrument functionality test:

DMAS software (system control):
DMAS software (data analysis):
DEMC sheath flow:
DEMC sample aerosol flow:
DMAS inlet impactor D_{50} value:
DEMC voltage range:
DEMC size range:
Number of size bins:
Total delay time:
DEMC Voltage scan rate[1]:
Total time between scans[1]:
Retrace time[1]:
Purge time[1]:
Total scan time[1]:

Length of tube between DEMC outlet and counting device inlet:
Diameter of tube between DEMC outlet and counting device inlet:

Sample gas properties during test
pressure:
temperature:
humidity:

[1] required for dynamic DMAS particle size calibration only

Reference: **Page 2 of 3**

Checked by:

Manufacturer(s), lot number(s) and/or certificate number(s) of particle size standard(s) used:

1

2

3

4

…

Table of results for dynamic particle size calibration:

numbering of particle size standards	1	2	3	4	…
certified diameter(s) of particle standard(s), d_c (nm)					
relative standard uncertainty of particle standard, $u_{r,cert}(d_c)$ (%)					
average of the median diameters, $\bar{d}$ (nm)					
relative error ε (d_c) (%)					

Table of results for static particle size calibration:

certified diameter of particle standard, d_c (nm)	
(optional) corresponding electrical mobility, Z_c ($m^2/V{\cdot}s$)	
standard uncertainty of particle standard, $u_{cert}(d_c)$ (nm)	
correction factor ζ (dimensionless)	
combined standard uncertainty $u_c(d_c)$ (nm)	

Observations/comments:

Reference:

Checked by:

Instrument return date:

Page 3 of 3